SCIREA Journal of Physics
ISSN: 2706-8862
http://www.scirea.org/journal/Physics
December 31, 2025
Volume 10, Issue 6, December, 2025
https://doi.org/10.54647/physics140706

# Resonance Absorption and Transverse Magnetization of a Ferromagnetic Spin System Interacting with a Phonon Reservoir in the Spin-Wave Region

Mizuhiko Saeki
Shimoasoushin-machi 859-40, Takaoka-shi, Toyama 939-1271, Japan

**Abstract**: The linear response of a ferromagnetic spin system interacting with a phonon reservoir in the spin-wave region, is discussed employing the TCLE method (a method in which the admittance of a physical system interacting with a heat reservoir is directly derived from time-convolutionless equations with external driving terms) in terms of the non-equilibrium thermo-field dynamics (NETFD). The power absorption and the amplitude of the expectation value of the transverse magnetization, which is referred as "the magnetization-amplitude", for the ferromagnetic system, are studied including not only the low-order parts but also the next higher-order parts in the spin-wave approximation. The approximate formulas of the resonance frequencies, peak-heights (heights of peak) and line half-widths in the resonance region of the power absorption and magnetization-amplitude, are derived for the ferromagnetic system interacting with the phonon reservoir in a transversely rotating magnetic-field. The power absorption and magnetization-amplitude are investigated numerically for a ferromagnetic system of one-dimensional infinite spins. The approximate formulas of the resonance frequencies, peak-heights and line half-widths, are shown to coincide well or nearly with the results investigated calculating numerically the analytic results of the power absorption and magnetization-amplitude in the resonance region, and also are shown to satisfy "the narrowing condition" that as the phonon reservoir is damped quickly, the peak-heights increase and the line half-widths decrease. Thus, the approximate formulas are verified numerically. The effects of the memory and initial correlation for the spin system and phonon reservoir, which are represented by the interference terms in the TCLE method and are referred as "the interference effects", are confirmed to increase the power absorption and magnetization-amplitude in the resonance region, and are shown to produce effects that cannot be disregarded for the high temperature, for the non-quickly damped reservoir or for the small wave-number.

*Keywords*: Ferromagnetic spin system; Spin-wave method; Transverse magnetic susceptibility; The TCLE methodof linear response; Resonance asorption; Non-equilibrium thermo-field dynamics

## 1 Introduction

The theories of ferromagnetic resonance were macroscopically treated by Kittel [1] and Van Vleck [2] on the basis of the equation of motion for the macroscopic magnetization, and were developed by Akhiezer et al. [3, 4] and Oguchi and Honma [5] from a microscopic point of view using the spin- wave theory of Holstein and Primakoff [6]. The ferromagnetic resonance was also discussed treating the collective motion of spins by Mori and Kawasaki [7] on the basis of the linear response theory of Kubo [8]. However, these theories for ferromagnetic resonances assume the damping of the spin, which is due to spin-spin interactions or spin- wave interactions, but do not deal with the effects of the phonon reservoir interacting with the spin system. Therefore, those theories cannot elucidate the damping mechanism of the spin for the case that the spin-spin interactions or the spin- wave interactions are small. In such a case, it is necessary to study the effects of the phonon reservoir interacting with the spin system in order to investigate the damping mechanism of the spin.

In the previous paper [9], the author derived a form of the transverse susceptibility for a ferromagnetic spin system interacting with the phonon reservoir in the spin-wave region, employing the TCLE method [10, 11, 12, 13, 14, 15, 16, 17] in terms of the non-equilibrium thermo-field dynamics (NETFD) [18, 19, 20, 21, 22] extended to the case of a non-bilinear unperturbed Hamiltonian [21, 22]. Here, the TCLE method is a method in which the admittance of a physical system interacting with a heat reservoir is directly derived from time-convolutionless equations with external driving terms in the problem of linear response. In Ref. [9], he discussed the temperature dependence and wave number dependence of the line shape for the transverse susceptibility in the resonance region of the ferromagnetic spin system, and found some interesting phenomena [9, 23]. In the previous papers [9, 23], the discussion of the linear response for the ferromagnetic spin system was approximately limited to the low-order parts in the spin-wave approximation, and effects of the higher-order parts on the line shapes were not discussed. It may be necessary to investigate effects of the higher-order parts in the spin-wave approximation.

In the present paper, we consider a ferromagnetic spin system with a uniaxial anisotropy energy and an anisotropic exchange interaction under an external static magnetic-field in the spin-wave region, interacting with a phonon reservoir and with an external driving magnetic-field which is a transversely rotating classical field. The interaction between the spin and phonon is assumed to include not only a bilinear part but also a non-bilinear part, which corresponds to the interaction between the $z$ components of the spin and phonon, as done in the previous paper [9]. We derive a form of the transverse magnetic susceptibility for such a ferromagnetic spin system employing the TCLE method in terms of the non-equilibrium thermo-field dynamics (NETFD) [18, 19, 20, 21, 22], including not only the low-order parts but also the next higher-order parts in the spin-wave approximation, and examine analytically the power

absorption and the amplitude of the expectation value of the transverse magnetization, which is referred as "the magnetization-amplitude" hereafter. We investigate numerically the power absorption and magnetization-amplitude for a ferromagnetic system of one-dimensional infinite spins interacting with a phonon reservoir, including not only the low-order parts but also the next higher-order parts in the spin-wave approximation.

Here, we mention the validity and usefulness of the TCLE method. In Refs. [13, 14, 24], the relation between the TCLE method and relaxation method in the problem of linear response was analytically examined in the second-order approximation for the interaction between the physical system and heat reservoir, where the relaxation method is the one in which the Kubo formula [8] is calculated for the physical system interacting with the heat reservoir. The admittances derived employing each method were shown to have the same second-order term and mutually different higher-order terms. The admittances derived employing each method were investigated numerically and were shown to agree well in the resonance region, for a quantum oscillator interacting with a heat reservoir [13] and for a quantum spin interacting with a heat reservoir [14, 25, 26]. This shows that the TCLE method is coincident with the relaxation method in the second-order approximation for the system-reservoir interaction, and that the TCLE method is valid in this approximation. In Refs. [15, 16, 17], the TCLE method and relaxation method were formulated in terms of the NETFD, and the relation between the admittances derived employing each method was analytically examined in the second-order approximation for the interaction between the physical system and heat reservoir [17]. When the relaxation method is employed in the van Hove limit [27] or in the narrowing limit [28], in which the heat reservoir is damped quickly, that is to say, the correlation time $\tau_c$ of the heat reservoir is much less than the relaxation time $\tau_r$ of the physical system, i.e., $\tau_c \ll \tau_r$, or $\tau_c \to 0$, as done in the formulation of the NETFD [18, 19, 20, 29], the obtained admittance is valid only in that limit and coincides with the one without the interference terms in the admittance derived employing the TCLE method [13, 14, 17]. In the TCLE method, the interference terms are included in the time-convolutionless (TCL) equations with external driving terms [10, 11, 12, 13, 14, 24, 15, 16, 17], represent the effects of the memory and initial correlation for the physical system and heat reservoir, and give the effects of the deviation from the van Hove limit [27] or in the narrowing limit [28]. When the TCLE method is employed, the complex admittance of the physical system can be calculated by inserting the interference terms into the results obtained in the van Hove limit [27] or in the narrowing limit [28], in which the NETFD has been formulated [18, 19, 20, 29]. Thus, by employing the NETFD and the TCLE method [15, 16, 17, 21, 22] as done in Refs. [9, 23, 30], the complex admittance of the physical system can be derived including the effects of the memory and initial correlation for the physical system and heat reservoir, i.e., the effects of the motion of the heat reservoir which influence the physical system. As discussed in Ref. [30], by employing the TCLE method, one can discuss theoretically variations of the peak-heights and line half-widths in the resonance regions of the power-absorption etc., because the admittance derived emloying the second-order TCLE method is valid even if the heat reservoir is damped slowly, in the region valid for the second-order perturbation approximation. We use the same symbols and notations as in Refs. [9, 23], and also provide the same basic requirements (axioms) as in Refs. [9, 23].

In Section 2, we model a ferromagnetic spin system interacting with a phonon reservoir in the spin-wave region. In Section 3, we derive a form of the transverse magnetic susceptibility for the ferromagnetic system employing the TCLE method in terms of the non-equilibrium thermo-field dynamics (NETFD), including not only the low-order parts but also the next higher-order parts in the spin-wave approximation, and also derive the approximate formulas of the resonance frequencies, peak-heights (heights of peak) and line half-widths in the resonance region of the power absorption and magnetization-amplitude for the ferromagnetic system in a transversely rotating magnetic-field. In Section 4, we investigate numerically the resonance frequencies, peak-heights (heights of peak) and line half-widths in the resonance region of the power absorption and magnetization-amplitude for a ferromagnetic system of one-dimensional infinite spins interacting with a phonon reservoir. In Section 5, we give a short summary and some concluding remarks.

## 2 Model of ferromagnetic spin system interacting with phonon reservoir

We consider a ferromagnetic spin system with a uniaxial anisotropy energy and an anisotropic exchange interaction under an external static magnetic-field $\vec{H}_z$ in the $z$ direction, where the ferromagnetic system is in the spin-wave region and is interacting with a phonon reservoir. We deal with the spin system of magnitude $S$ in the spin-wave approximation [6]. The spin operators $\vec{S}_j$ at site $j$ are expressed using the Bose operators $a_j$ and $a_j^\dagger$ of Holstein and Primakoff [6] as

$$S_j^+ = \sqrt{2\,S}\,p_j\,a_j\,, \qquad S_j^- = \sqrt{2\,S}\,a_j^\dagger\,p_j\,, \qquad S_j^z = S - a_j^\dagger\,a_j\,, \tag{2.1}$$

where the operator $p_j$ is defined by

$$p_j = \Big(1 - \frac{a_j^\dagger\,a_j}{2\,S}\Big)^{1/2} = \Big(1 - \frac{n_j}{2\,S}\Big)^{1/2} = 1 - \frac{n_j}{4\,S} - \frac{n_j^2}{32\,S^2} - \cdots\,, \qquad (n_j = a_j^\dagger\,a_j). \tag{2.2}$$

The Bose operators $a_j^\dagger$ and $a_j$ are the creation and annihilation operators of the spin deviation, respectively, and satisfy the commutation relations

$$[\, a_j \,,\, a_l^\dagger \,] = \delta_{jl} \,, \qquad\qquad [\, a_j \,,\, a_l \,] = [\, a_j^\dagger \,,\, a_l^\dagger \,] = 0. \tag{2.3}$$

We take the principal axis of the uniaxial anisotropy energy and anisotropic exchange interaction as the $z$ axis, and describe the Hamiltonian $\mathcal{H}_{\rm s}$ of the spin system under the external static magnetic-field $\vec{H}_z$ as

$$\mathcal{H}_{\rm s} = -\,\hbar\,\omega_z \sum_j^N S_j^z - \hbar \sum_{\langle jl \rangle} \{\, J_1\,(S_j^+ S_l^- + S_j^- S_l^+) + 2\,J_2\,S_j^z S_l^z \,\} - \hbar\,K \sum_j^N (S_j^z)^2, \tag{2.4}$$

where $\omega_z$ is the Zeeman frequency $\omega_z = \gamma H_z$ with the magnetomechanical ratio $\gamma$. In the above Hamiltonian $\mathcal{H}_{\rm s}$, $\hbar J_1$ and $\hbar J_2$ are the exchange energies, $\hbar K$ is the anisotropy energy, $N$ is the total number of spins and the summation $\sum_{\langle jl \rangle}$ is taken over all nearest-neighbor pairs. Performing the transformations (2.1) in the above Hamiltonian $\mathcal{H}_{\rm s}$ and expanding it according to (2.2), the Hamiltonian $\mathcal{H}_{\rm s}$ becomes

$$\begin{aligned}
\mathcal{H}_{\rm s} &= -\,\hbar\,\omega_z \sum_j (\, S - a_j^\dagger\, a_j \,) - \hbar\,J_1 \sum_{\langle jl \rangle} (2\,S)\,(\, p_j\, a_j\, a_l^\dagger\, p_l + a_j^\dagger\, p_j\, p_l\, a_l \,) \\
&\quad - 2\,\hbar\,J_2 \sum_{\langle jl \rangle} (\, S - a_j^\dagger\, a_j \,)\,(\, S - a_l^\dagger\, a_l \,) - \,\hbar\,K \sum_j (\, S - a_j^\dagger\, a_j \,)\,(\, S - a_j^\dagger\, a_j \,), \\
&= -\,\hbar\,\omega_z\,NS - \hbar\,z\,NJ_2\,S^2 - \hbar\,NKS^2 + \hbar\,\omega_z \sum_j a_j^\dagger\, a_j + 4\,\hbar\,S \sum_{\langle jl \rangle} \big(J_2\, a_j^\dagger\, a_j - J_1\, a_j^\dagger\, a_l\big) \\
&\quad + \hbar\,K(2S-1) \sum_j a_j^\dagger\, a_j + \hbar \sum_{\langle jl \rangle} \big\{ J_1\,(\, a_j^\dagger\, a_l^\dagger\, a_j\, a_j + a_j^\dagger\, a_j^\dagger\, a_j\, a_l \,) - 2\,J_2\, a_j^\dagger\, a_l^\dagger\, a_j\, a_l \big\} \\
&\quad - \hbar\,K \sum_j a_j^\dagger\, a_j^\dagger\, a_j\, a_j + \cdots \,,
\end{aligned} \tag{2.5}$$

where "$\cdots$" denotes the parts of higher order than the fourth power of $a_j$, $a_j^\dagger$. We perform the Fourier transformation of the Bose operator $a_j$ as

$$a_j = \frac{1}{\sqrt{N}} \sum_k \bar{a}_k \exp(i\,\vec{k}\cdot\vec{r}_j), \qquad\qquad \bar{a}_k = \frac{1}{\sqrt{N}} \sum_j a_j \exp(-\,i\,\vec{k}\cdot\vec{r}_j), \tag{2.6}$$

and their Hermite conjugates, where the transformed operator $\bar{a}_k$ is the Bose operator and satisfys the commutation relations

$$[\, \bar{a}_k \,,\, \bar{a}_{k'}^\dagger] = \delta_{kk'} \,, \qquad\qquad [\, \bar{a}_k \,,\, \bar{a}_{k'}] = [\, \bar{a}_k^\dagger \,,\, \bar{a}_{k'}^\dagger] = 0. \tag{2.7}$$

Hereafter, we mainly use the Fourier transformed variables and we omit "$^-$" unless the meaning is confusing. Then, the Hamiltonian $\mathcal{H}_{\rm s}$ can be written as [5]

$$\begin{aligned}
\mathcal{H}_{\rm s} &= -\,\hbar\,\omega_z NS - \hbar\,(zJ_2 + K)\,NS^2 + \hbar \sum_k \epsilon_1(k)\, a_k^\dagger\, a_k \\
&\quad + \frac{\hbar}{N} \sum_{k,\,k',\,k''} \big\{ \frac{z}{2}\, J_1 \cdot (\eta_k + \eta_{k'}) - z\,J_2\,\eta_{k-k'} - K \big\}\, a_{k'}^\dagger\, a_{k''}^\dagger\, a_k\, a_{k'+k''-k} + \cdots \,, \qquad (2.8a) \\
&= -\,\hbar\,\omega_z NS - \hbar\,(zJ_2 + K)\,NS^2 + \hbar \sum_k \epsilon_1(k)\, a_k^\dagger\, a_k + \frac{\hbar}{2} \sum_{k,\,k'} \epsilon_2(k,\,k')\, a_k^\dagger\, a_k\, a_{k'}^\dagger\, a_{k'} \\
&\quad + (\text{Non}-\text{Diagonal Terms}) + \cdots \,, \qquad (2.8b)
\end{aligned}$$

where $\epsilon_1(k)$ and $\epsilon_2(k,\,k')$ are defined by

$$\epsilon_1(k) = \omega_z + 2\,z\,S\,(J_2 - J_1\,\eta_k\,) + K\,(\,2\,S - 1), \tag{2.9a}$$

$$\epsilon_2(k,\,k') = \epsilon_2(k',\,k) = (4/N)\{(z/2)\,J_1 \cdot (\eta_k + \eta_{k'}) - (z/2)\,J_2 \cdot (1 + \eta_{k-k'}) - K\}, \tag{2.9b}$$

with $\eta_k$ defined by

$$\eta_k = \frac{1}{z} \sum_\sigma \exp(i\,\vec{k}\cdot\vec{\sigma}). \tag{2.10}$$

Here, $\vec{\sigma}$ denotes the vectors to the nearest-neighbour site from each site and $z$ is the number of the vectors. The Hamiltonian $\mathcal{H}_{\rm S}$ given by (2.8) can be divided as [5]

$$\mathcal{H}_{\rm S} = \mathcal{H}_{\rm S0} + \mathcal{H}_{\rm S1}, \qquad \mathcal{H}_{\rm S0} = -\hbar\,\omega_z NS - \hbar\,(zJ_2 + K)\,NS^2 + \hbar\sum_k \epsilon_k\, a_k^\dagger\, a_k, \tag{2.11}$$

$$\mathcal{H}_{\rm S1} = \hbar \sum_{k,\,k',\,k''} \epsilon_3(k,\,k')\, a_{k'}^\dagger\, a_{k''}^\dagger\, a_k\, a_{k'+k''-k} - \hbar \sum_{k,\,k'} \epsilon_2(k,\,k')\,\bar{n}(\epsilon_{k'})\, a_k^\dagger\, a_k + \cdots, \tag{2.12}$$

where $\epsilon_k$ and $\epsilon_3(k,\,k')$ are defined by

$$\epsilon_k = \epsilon_1(k) + \sum_{k'} \epsilon_2(k,\,k')\,\bar{n}(\epsilon_{k'}), \tag{2.13}$$

$$\epsilon_3(k,\,k') = \epsilon_3(k',\,k) = (1/N)\big\{(z/2)\,J_1{\cdot}(\eta_k + \eta_{k'}) - z\,J_2\,\eta_{k-k'} - K\big\}. \tag{2.14}$$

Here, $\mathcal{H}_{\rm S1}$ are the higher-order parts of $\mathcal{H}_{\rm S}$ in the spin-wave approximation and represent the interaction among the spin-waves, and $\bar{n}(\epsilon_k)$ is the thermal equilibrium value of the free boson number with energy $\hbar\epsilon_k$ at temperature $T = (k_{\rm B}\beta)^{-1}$, and is given by

$$\bar{n}(\epsilon_k) = 1/\{\exp(\beta\,\hbar\,\epsilon_k) - 1\} = 1/\{\exp(\hbar\,\epsilon_k/(k_{\rm B}T)) - 1\}. \tag{2.15}$$

The spin-wave energy $\hbar\epsilon_k$ includes not only the free spin-wave energy $\hbar\epsilon_1(k)$ but also the dominant parts of the higher-order parts [5], which represent the spin-wave interaction, in the spin-wave approximation. The spin-wave interaction $\mathcal{H}_{\rm S1}$ given by (2.12) represent the higher-order parts without the dominant parts of $\mathcal{H}_{\rm S}$ in the spin-wave approximation.

We next consider the interaction between the spin system and phonon reservoir. We assume that each spin interacts only with the reservoir field at the same site as the spin, and thus neglect the spin-reservoir interactions among the different sites. We take the interaction Hamiltonian $\mathcal{H}_{\rm SR}$ between the spin system and phonon reservoir as

$$\mathcal{H}_{\rm SR} = -\frac{\hbar}{2}\sum_j (S_j^+ R_j^- + S_j^- R_j^+) - \hbar\sum_j S_j^z R_j^z, \tag{2.16a}$$

$$= -\hbar\sqrt{S/2}\sum_j (a_j R_j^- + a_j^\dagger R_j^+) - \hbar\sum_j S_j^z R_j^z + \cdots, \tag{2.16b}$$

$$= -\hbar\sqrt{S/2}\sum_k (\bar{a}_k \bar{R}_k^- + \bar{a}_k^\dagger \bar{R}_k^+) - \hbar\sum_k \bar{S}_k^z \bar{R}_k^z + \cdots, \tag{2.16c}$$

with $R_j^\pm = R_j^x \pm i R_j^y$ and $\bar{R}_k^\pm = \bar{R}_k^x \pm i\bar{R}_k^y$, where $R_j^a$ $(a = x,\,y,\,z)$ are the reservoir operators which are Hermitian, $\bar{R}_k^a$ $(a = \pm,\,z)$ are the Fourier transformations of $R_j^a$ $(a = \pm,\,z)$, i.e.,

$$R_j^\pm = \frac{1}{\sqrt{N}}\sum_k \bar{R}_k^\pm \exp(\pm\, i\,\vec{k}{\cdot}\vec{r}_j), \qquad \bar{R}_k^\pm = \frac{1}{\sqrt{N}}\sum_j R_j^\pm \exp(\mp\, i\,\vec{k}{\cdot}\vec{r}_j), \tag{2.17a}$$

$$R_j^z = \frac{1}{\sqrt{N}}\sum_k \bar{R}_k^z \exp(-\,i\,\vec{k}{\cdot}\vec{r}_j), \qquad \bar{R}_k^z = \frac{1}{\sqrt{N}}\sum_j R_j^z \exp(i\,\vec{k}{\cdot}\vec{r}_j), \tag{2.17b}$$

and $\bar{S}_k^z$ is the Fourier transformation of the spin operator $S_j^z$, i.e.,

$$S_j^z = \frac{1}{\sqrt{N}}\sum_k \bar{S}_k^z \exp(i\,\vec{k}{\cdot}\vec{r}_j), \qquad \bar{S}_k^z = \frac{1}{\sqrt{N}}\sum_j S_j^z \exp(-\,i\,\vec{k}{\cdot}\vec{r}_j). \tag{2.18}$$

In Eqs. (2.16), "$\cdots$" denotes the higher-order parts in the spin-wave appoximation. Hereafter, we mainly use the Fourier transformed variables and we omit "$^-$" unless the meaning is confusing. By considering that the spin-wave of the wave number $k$ interacts with the phonon reservoir of the wave number $k$ as seen in (2.16c), we assume the form of the interaction $\mathcal{H}_{\rm SR}$ between the spin system and phonon reservoir as

$$\mathcal{H}_{\rm SR} = -\hbar\sqrt{S/2}\sum_k (a_k R_k^- + a_k^\dagger R_k^+) - \hbar\sum_k (S - a_k^\dagger\, a_k) R_k^z, \tag{2.19}$$

where we have neglected the higher-order parts in the spin-wave appoximation and the off-diagonal parts in the non-bilinear term. We also assume that the phonon reservoir is composed of many phonons and that the reservoir operators are expressed in terms of the phonon operators $B_{k\alpha}$ and $B_{k\alpha}^\dagger$ of the wave number $k$ and mode $\alpha$, which are Bose operators, as

$$R_k^+ = \sum_\alpha g_{1\alpha} B_{k\alpha}, \qquad R_k^- = \sum_\alpha g_{1\alpha}^* B_{k\alpha}^\dagger, \qquad R_k^z = \sum_\alpha g_{2\alpha} B_{k\alpha}^\dagger B_{k\alpha}, \tag{2.20}$$

where $g_{1\alpha}$ and $g_{2\alpha}$ are the coupling constants between the spin and the phonon of mode $\alpha$. Then, the spin-phonon interaction $\mathcal{H}_{\rm SR}$ given by (2.19) can be written as

$$\mathcal{H}_{\rm SR} = -\hbar\sqrt{S/2}\sum_{k,\,\alpha}(\,g^*_{1\alpha}a_kB^\dagger_{k\alpha}+g_{1\alpha}a^\dagger_kB_{k\alpha}\,)-\hbar\sum_{k,\,\alpha}g_{2\alpha}(S-a^\dagger_ka_k)B^\dagger_{k\alpha}B_{k\alpha}\,, \tag{2.21}$$

where the first term is the bilinear part and the second term is the non-bilinear part.

For the later convenience, we renormalize the spin-phonon interaction $\mathcal{H}_{\rm SR}$, the spin-wave Hamiltonian $\mathcal{H}_{\rm S0}$ and the spin-wave energy $\hbar\epsilon_k$, as

$$\mathcal{H}_{\rm SR} = -\hbar\sqrt{S/2}\sum_{k,\,\alpha}(\,g^*_{1\alpha}a_kB^\dagger_{k\alpha}+g_{1\alpha}a^\dagger_kB_{k\alpha}\,)-\hbar\sum_{k,\,\alpha}g_{2\alpha}(S-a^\dagger_ka_k)\,\Delta(B^\dagger_{k\alpha}B_{k\alpha}), \tag{2.22}$$

$$\mathcal{H}_{\rm S0} = -\hbar\,\omega_zNS-\hbar\,(zJ_2+K)NS^2+\sum_k\hbar\,\epsilon_k\,a^\dagger_ka_k-\hbar\,S\sum_{k,\,\alpha}g_{2\alpha}\,\langle 1_{\rm R}|B^\dagger_{k\alpha}B_{k\alpha}|\rho_{\rm R}\rangle, \tag{2.23}$$

$$\hbar\,\epsilon_k = \hbar\,\epsilon_1(k)+\hbar\sum_{k'}\epsilon_2(k,\,k')\,\bar{n}(\epsilon_{k'})+\hbar\sum_\alpha g_{2\alpha}\,\langle 1_{\rm R}|B^\dagger_{k\alpha}B_{k\alpha}|\rho_{\rm R}\rangle, \tag{2.24}$$

with the notation $\Delta(B^\dagger_{k\alpha}B_{k\alpha})=B^\dagger_{k\alpha}B_{k\alpha}-\langle 1_{\rm R}|B^\dagger_{k\alpha}B_{k\alpha}|\rho_{\rm R}\rangle$, where the renormalized spin-wave energy $\hbar\epsilon_k$ includes not only the free spin-wave energy $\hbar\epsilon_1(k)$ and the dominant parts of the higher-order parts in the spin-wave approximation, but also the thermal equilibrium value $\hbar\sum_\alpha g_{2\alpha}\langle 1_{\rm R}|B^\dagger_{k\alpha}B_{k\alpha}|\rho_{\rm R}\rangle$ of the phonon reservoir with the wave number $k$. Here, $\rho_{\rm R}$ is the thermal equilibrium density operator at temperature $T=1/(k_{\rm B}\beta)$ for the phonon reservoir with the Hamiltonian $\mathcal{H}_{\rm R}$, and is given by

$$\rho_{\rm R} = \exp(-\beta\,\mathcal{H}_{\rm R})/\langle 1_{\rm R}|\exp(-\beta\,\mathcal{H}_{\rm R})\rangle = \exp(-\beta\,\mathcal{H}_{\rm R})/{\rm tr}_{\rm R}\exp(-\beta\,\mathcal{H}_{\rm R}), \tag{2.25}$$

where the notation ${\rm tr}_{\rm R}$ denotes the trace operation in the space of the phonon reservoir. We do not specify the Hamiltonian $\mathcal{H}_{\rm R}$ of the phonon reservoir explicitly. Hereafter, we use $\mathcal{H}_{\rm SR}$, $\mathcal{H}_{\rm S0}$ and $\hbar\epsilon_k$ given by (2.22)−(2.24), respectively, for the spin-phonon interaction, the spin-wave Hamiltonian and the spin-wave energy. We assume that the thermal equilibrium values of the phonon operators $B_{k\alpha}$ and $B^\dagger_{k\alpha}$ vanish, i.e., $\langle 1_{\rm R}|B_{k\alpha}|\rho_{\rm R}\rangle=\langle 1_{\rm R}|B^\dagger_{k\alpha}|\rho_{\rm R}\rangle=0$. Then, we have

$$\langle 1_{\rm R}|\mathcal{H}_{\rm SR}|\rho_{\rm R}\rangle = 0, \qquad\qquad \langle 1_{\rm R}|\hat{\mathcal{H}}_{\rm SR}|\rho_{\rm R}\rangle = 0, \tag{2.26}$$

with the hat Hamiltonian $\hat{\mathcal{H}}_{\rm SR}=(\mathcal{H}_{\rm SR}-\tilde{\mathcal{H}}^\dagger_{\rm SR})/\hbar$ [17].

In the last of this section, we check the ground state of the ferromagnetic spin system. The ground state energy $E^{\rm G}_{\rm S0}$ in the spin-wave approximation is given by

$$E^{\rm G}_{\rm S0} = -\hbar\,\omega_zNS-\hbar\,(zJ_2+K)NS^2-\hbar\,S\sum_{k,\,\alpha}g_{2\alpha}\,\langle 1_{\rm R}|B^\dagger_{k\alpha}B_{k\alpha}|\rho_{\rm R}\rangle, \tag{2.27}$$

which is smaller than the energy $-\hbar\omega_zNS-\hbar(zJ_2+K)NS^2$ of the ferromagnetic ordered state with the anisotropy energy $\hbar K$ under external static magnetic-field $\vec{H}_z$ in the $z$ direction, where the ferromagnetic ordered state is the state that all of the spins are in the $z$ direction. Thus, the ground state of the spin system in the spin-wave approximation is lower than the ferromagnetic ordered state with the anisotropy energy under external static magnetic-field.

# 3 Resonance absorption and transverse magnetization

In this section, we derive a form of the transverse magnetic susceptibility for the ferromagnetic spin system modeled in the previous section, employing the TCLE method of linear response [15, 16, 17, 21, 22] in terms of NETFD, and discuss the resonance absorption and transverse magnetization for the ferromagnetic system interacting with the phonon reservoir and with an external driving magnetic-field.

We consider the case that the external driving magnetic-field is a transversely rotating classical-field $\vec{H}_j(t)$ given by

$$\vec{H}_j(t) = (H_j\cos\omega t\,,-H_j\sin\omega t\,,0), \qquad\qquad (H_j=H^*_j), \tag{3.1}$$

at site $j$. We assume that the external magnetic-field $\vec{H}_j(t)$ is turned on adiabatically at the initial time $t=0$, and that the ferromagnetic system and phonon reservoir are initially in the thermal equilibrium at temperature $T=1/(k_{\rm B}\beta)$, i.e., the initial state of the ferromagnetic system and phonon reservoir is given by the thermal equilibrium density operators at temperature $T=1/(k_{\rm B}\beta)$:

$$\rho_{\rm TE} = \exp(-\beta\,\mathcal{H})/\langle 1|\exp(-\beta\,\mathcal{H})\rangle = \exp(-\beta\,\mathcal{H})/\,{\rm Tr}\exp(-\beta\,\mathcal{H}), \tag{3.2}$$

with $\mathrm{Tr}=\mathrm{tr}\,\mathrm{tr}_{\mathtt{R}}$, where $\mathcal{H}$ is the Hamiltonian of the ferromagnetic system and phonon reservoir in external static magnetic-field $\vec{H}_z$, and is taken as

$$\mathcal{H}=\mathcal{H}_{\mathtt{S}}+\mathcal{H}_{\mathtt{R}}+\mathcal{H}_{\mathtt{SR}}=\mathcal{H}_0+\mathcal{H}_{\mathtt{SR}}, \qquad (\mathcal{H}_0=\mathcal{H}_{\mathtt{S}}+\mathcal{H}_{\mathtt{R}}). \tag{3.3}$$

Here, tr denotes the trace operation in the space of the ferromagnetic system. We take the interaction $\mathcal{H}_{\rm ed}(t)$ of the ferromagnetic system with the external driving magnetic-field given by (3.1) as

$$\begin{aligned}\mathcal{H}_{\rm ed}(t)&=-\hbar\,\gamma\sum_j\vec{H}_j(t)\cdot\vec{S}_j=-\frac{\hbar\,\gamma}{2}\sum_j H_j\big(S_j^+\exp(i\,\omega\,t)+S_j^-\exp(-i\,\omega\,t)\big),\\&=-\frac{\hbar\,\gamma}{2}\sum_k\big\{\bar{S}_k^+\,\bar{H}_k\exp(i\,\omega\,t)+\bar{S}_k^-\,\bar{H}_k^*\exp(-i\,\omega\,t)\big\},\end{aligned} \tag{3.4}$$

where $\bar{S}_k^\pm$ and $\bar{H}_k$ $[=\bar{H}_{-k}^*]$ are the Fourier transformations of the spin operators $S_j^\pm$ and magnetic-field amplitude $H_j$:

$$S_j^\pm=\frac{1}{\sqrt{N}}\sum_k\bar{S}_k^\pm\exp(\pm\,i\,\vec{k}\cdot\vec{r}_j), \qquad \bar{S}_k^\pm=\frac{1}{\sqrt{N}}\sum_j S_j^\pm\exp(\mp\,i\,\vec{k}\cdot\vec{r}_j), \tag{3.5}$$

$$H_j=\frac{1}{\sqrt{N}}\sum_k\bar{H}_k\exp(-\,i\,\vec{k}\cdot\vec{r}_j), \qquad \bar{H}_k=\frac{1}{\sqrt{N}}\sum_j H_j\exp(i\,\vec{k}\cdot\vec{r}_j). \tag{3.6}$$

Hereafter, we mainly use the Fourier transformed variables and we omit "$^-$" unless the meaning is confusing. The interaction $\mathcal{H}_{\rm ed}(t)$ given by (3.4) can be written, by performing the transformation (2.1) and the expansion (2.2), as

$$\mathcal{H}_{\rm ed}(t)=-\hbar\,\gamma\sqrt{S/2}\sum_k\big\{a_k\,H_k\exp(i\,\omega\,t)+a_k^\dagger\,H_k^*\exp(-i\,\omega\,t)\big\}+\cdots. \tag{3.7}$$

In Eq. (3.7), "$\cdots$" denotes the higher-order parts in the spin-wave approximation. When the external driving magnetic-field $\vec{H}_j(t)$ is uniform in space, i.e., $H_j=H$, we have $H_k=H_0\delta_{k0}$, $H_0=H_0^*=\sqrt{N}H$ and

$$\mathcal{H}_{\rm ed}(t)=-(\hbar\,\gamma/2)\big\{S_0^+H_0\exp(i\,\omega\,t)+S_0^-H_0\exp(-i\,\omega\,t)\big\}, \tag{3.8a}$$

$$=-\hbar\,\gamma\sqrt{SN/2}\,H\big\{a_0\exp(i\,\omega\,t)+a_0^\dagger\exp(-i\,\omega\,t)\big\}+\cdots. \tag{3.8b}$$

By putting $A_i=\gamma\hbar S_k^+/2$ and $A_j=\gamma\hbar S_k^-/2$ in the admittance $\chi_{ij}(\omega)$ derived employing the second-order TCLE method in terms of NETFD in Res. [15, 16, 17], the transverse magnetic susceptibility $\chi_{S_k^+S_k^-}(\omega)$ takes the form

$$\begin{aligned}\chi_{S_k^+S_k^-}(\omega)=\frac{\hbar\,\gamma^2}{4}\int_0^\infty dt\,\langle 1_{\mathtt{S}}|\,S_k^+\,U(t)\exp_{\leftarrow}\Big\{-i\int_0^t d\tau\,\hat{\mathcal{H}}_{\mathtt{S}1}(\tau)\Big\}\\ \times\big\{i\,(S_k^-\,-\tilde{S}_k^+)\,|\rho_0\rangle+|D^{(2)}_{S_k^-}[\omega]\rangle\big\}\exp(i\,\omega\,t),\end{aligned} \tag{3.9}$$

with $\rho_0=\mathrm{tr}_{\mathtt{R}}\rho_{\mathtt{TE}}$, where the evolution operator $U(t)$ and the hat-Hamiltonian $\hat{\mathcal{H}}(t)$ are defined by [17]

$$U(t)=\exp\{-\,(i\,\hat{\mathcal{H}}_{\mathtt{S}0}-C^{(2)})\,t\}=\exp\{-\,i\,(\hat{\mathcal{H}}_{\mathtt{S}0}+i\,C^{(2)})\,t\}, \tag{3.10}$$

$$\hat{\mathcal{H}}_{\mathtt{S}1}(t)=U^{-1}(t)\,\hat{\mathcal{H}}_{\mathtt{S}1}\,U(t), \qquad [\hat{\mathcal{H}}_{\mathtt{S}0(\mathtt{S}1)}=(\mathcal{H}_{\mathtt{S}0(\mathtt{S}1)}-\tilde{\mathcal{H}}^\dagger_{\mathtt{S}0(\mathtt{S}1)})/\hbar]. \tag{3.11}$$

Here, the second-order collision operator $C^{(2)}$ and the second-order interference thermal state $|D^{(2)}_{S_k^-}[\omega]\rangle$ are formally given in Ref. [16, 17], and for the model given in the previous section, take the forms [9]

$$\begin{aligned}C^{(2)}=-\sum_k\big\{S\{(a_k-\tilde{a}_k^\dagger)(a_k^\dagger\,\phi_k^{+-}(\epsilon_k)-\tilde{a}_k\,\phi_k^{-+}(\epsilon_k)^*)+(\tilde{a}_k-a_k^\dagger)(\tilde{a}_k^\dagger\,\phi_k^{+-}(\epsilon_k)^*-a_k\,\phi_k^{-+}(\epsilon_k))\}\\ -(a_k^\dagger\,a_k-\tilde{a}_k^\dagger\,\tilde{a}_k)\,\{(S-a_k^\dagger\,a_k)\,\phi_k^{zz}(0)-(S-\tilde{a}_k^\dagger\,\tilde{a}_k)\,\phi_k^{zz}(0)^*\}\big\},\end{aligned} \tag{3.12}$$

$$\begin{aligned}|D^{(2)}_{S_k^-}[\omega]\rangle=\sqrt{2\,S}\,\big\{S\{\phi_k^{-+}(\omega)-\phi_k^{-+}(\epsilon_k)-(\phi_k^{+-}(\omega)^*-\phi_k^{+-}(\epsilon_k)^*)\}\\ +\phi_k^{zz}(\omega-\epsilon_k)-\phi_k^{zz}(0)\big\}\,(a_k^\dagger-\tilde{a}_k)\,|\rho_0\rangle/(\omega-\epsilon_k),\end{aligned} \tag{3.13}$$

where $\phi_k^{+-}(\epsilon)$, $\phi_k^{-+}(\epsilon)$ and $\phi_k^{zz}(\epsilon)$ are defined by

$$\phi_k^{+-}(\epsilon)=\frac{1}{2}\sum_\alpha|\,g_{1\alpha}|^2\int_0^\infty d\tau\,\langle 1_{\mathtt{R}}|\,B_{k\alpha}^\dagger(\tau)B_{k\alpha}\,|\rho_{\mathtt{R}}\rangle\exp(-\,i\,\epsilon\,\tau), \tag{3.14a}$$

$$\phi_k^{-+}(\epsilon)=\frac{1}{2}\sum_\alpha|\,g_{1\alpha}|^2\int_0^\infty d\tau\,\langle 1_{\mathtt{R}}|\,B_{k\alpha}(\tau)B_{k\alpha}^\dagger\,|\rho_{\mathtt{R}}\rangle\exp(i\,\epsilon\,\tau), \tag{3.14b}$$

$$\phi_k^{zz}(\epsilon)=\sum_\alpha g_{2\alpha}^2\int_0^\infty d\tau\,\langle 1_{\mathtt{R}}|\,\Delta(B_{k\alpha}^\dagger(\tau)B_{k\alpha}(\tau))\,\Delta(B_{k\alpha}^\dagger B_{k\alpha})\,|\rho_{\mathtt{R}}\rangle\exp(i\,\epsilon\,\tau), \tag{3.14c}$$

with the notation $\Delta(B^\dagger_{k\alpha}(\tau)B_{k\alpha}(\tau)) = B^\dagger_{k\alpha}(\tau)B_{k\alpha}(\tau) - \langle 1_{\rm R}|B^\dagger_{k\alpha}B_{k\alpha}|\rho_{\rm R}\rangle$. The phonon operators $B_{k\alpha}(t)$ and $B^\dagger_{k\alpha}(t)$ are the Heisenberg operators $B_{k\alpha}(t) = \exp(i\mathcal{H}_{\rm R}t/\hbar)B_{k\alpha}\exp(-i\mathcal{H}_{\rm R}t/\hbar)$ and $B^\dagger_{k\alpha}(t) = \exp(i\mathcal{H}_{\rm R}t/\hbar)B^\dagger_{k\alpha}\exp(-i\mathcal{H}_{\rm R}t/\hbar)$ of the phonon reservoir, respectively. Here, the phonon operators for each wave number and each mode have been assumed to be mutually independent. The interference thermal state $|D^{(2)}_{S^-_k}[\omega]\rangle$ represents the effects of the memory and initial correlation for the spin system and phonon reservoir [17, 9], and can be written as [9]

$$|D^{(2)}_{S^-_k}[\omega]\rangle = \sqrt{2\,S}\,X_k(\omega)\,(a^\dagger_k - \tilde{a}_k)\,|\rho_0\rangle, \tag{3.15}$$

with the corresponding interference term $X_k(\omega)$ defined by

$$\begin{aligned} X_k(\omega) &= \big\{S\{(\phi^{-+}_k(\omega) - \phi^{+-}_k(\omega)^*) - (\phi^{-+}_k(\epsilon_k) - \phi^{+-}_k(\epsilon_k)^*)\} + (\phi^{zz}_k(\omega-\epsilon_k) - \phi^{zz}_k(0))\big\}/(\omega-\epsilon_k), \\ &= \frac{S}{2}\int_0^\infty d\tau \sum_\alpha |\,g_{1\alpha}|^2\,\langle 1_{\rm R}|\big[B_{k\alpha}(\tau), B^\dagger_{k\alpha}\big]\big|\rho_{\rm R}\rangle \frac{\exp(i\,\omega\,\tau) - \exp(i\,\epsilon_k\,\tau)}{\omega-\epsilon_k} \\ &\quad + \int_0^\infty d\tau \sum_\alpha g^2_{2\alpha}\,\langle 1_{\rm R}|\Delta(B^\dagger_{k\alpha}(\tau)B_{k\alpha}(\tau))\,\Delta(B^\dagger_{k\alpha}B_{k\alpha})\big|\rho_{\rm R}\rangle \frac{\exp\{i\,(\omega-\epsilon_k)\,\tau\} - 1}{\omega-\epsilon_k}. \end{aligned} \tag{3.16}$$

In the derivation of the collision operator $C^{(2)}$ and interference thermal state $|D^{(2)}_{S^-_k}[\omega]\rangle$, the higher-order parts except the dominant part in the spin-wave approximation was ignored [9]. The low-order part $\chi^{(0)}_{S^+_kS^-_k}(\omega)$ of the transverse susceptibility $\chi_{S^+_kS^-_k}(\omega)$, which includes the dominant parts of the higher-order parts in the spin-wave approximation, was derived as [9]

$$\chi^{(0)}_{S^+_kS^-_k}(\omega) = \frac{(S\,\hbar\,\gamma^2/\,2)\{i + X_k(\omega)\}}{-\,i\,(\omega - \epsilon_k - \Phi''_k) + \Phi'_k + \Psi_k}\,, \tag{3.17}$$

where $\Phi'_k\ [=\Phi'_k(\epsilon_k)]$ and $\Phi''_k\ [=\Phi''_k(\epsilon_k)]$ are, respectively, the real and imaginary parts of $\Phi_k(\epsilon_k)$ defined by [9]

$$\Phi_k(\epsilon_k) = S\{\phi^{-+}_k(\epsilon_k) - \phi^{+-}_k(\epsilon_k)^*\} = \frac{S}{2}\int_0^\infty d\tau \sum_\alpha |\,g_{1\alpha}\,|^2\,\langle 1_{\rm R}|[B_{k\alpha}(\tau), B^\dagger_{k\alpha}]|\rho_{\rm R}\rangle\exp(i\,\epsilon_k\,\tau), \tag{3.18}$$

and $\Psi_k$ is defined by [9]

$$\Psi_k = \phi^{zz}_k(0) = \sum_\alpha g^2_{2\alpha}\int_0^\infty d\tau\,\langle 1_{\rm R}|\,\Delta(B^\dagger_{k\alpha}(\tau)B_{k\alpha}(\tau))\,\Delta(B^\dagger_{k\alpha}B_{k\alpha})\,|\rho_{\rm R}\rangle. \tag{3.19}$$

In the above derivation, we have considered that $\Phi'_k\ [=\Phi'_k(\epsilon_k)]$ is non-negative for non-negative $\epsilon_k$ [16, 19] and that $\Psi_k\ [=\phi^{zz}_k(0)]$ is non-negative when $\Psi_k$ is real ($\Psi_k = \Psi^*_k$) as shown in [21, 22]. The corresponding interference term $X_k(\omega)$ defined by (3.16) can be written as

$$X_k(\omega) = \frac{\Phi_k(\omega) - \Phi_k(\epsilon_k)}{\omega-\epsilon_k} + \frac{\Psi_k(\omega-\epsilon_k) - \Psi_k}{\omega-\epsilon_k}, \tag{3.20}$$

where $\Psi_k(\epsilon)$ is defined by

$$\Psi_k(\epsilon) = \int_0^\infty d\tau \sum_\alpha g^2_{2\alpha}\langle 1_{\rm R}|\Delta(B^\dagger_{k\alpha}(\tau)B_{k\alpha}(\tau))\Delta(B^\dagger_{k\alpha}B_{k\alpha})|\rho_{\rm R}\rangle\exp(i\,\epsilon\,\tau), \tag{3.21}$$

with $\Psi_k(0) = \Psi_k$. The next higher-order parts $\chi^{(1)}_{S^+_kS^-_k}(\omega)$ of the transverse susceptibility $\chi_{S^+_kS^-_k}(\omega)$ in the spin-wave approximation, can be written as [23, 9]

$$\begin{aligned} \chi^{(1)}_{S^+_kS^-_k}(\omega) &= \frac{S\hbar\gamma^2}{2}\int_0^\infty dt\int_0^t d\tau\,\langle 1_{\rm S}|\,a_kU(t)\,\hat{\mathcal{H}}_{\rm S1}(\tau)(a^\dagger_k - \tilde{a}_k)\,|\rho_0\rangle\{1 - i\,X_k(\omega)\}\exp(i\,\omega\,t) \\ &\quad - \frac{\hbar\gamma^2}{8N}\sum_{k_1,\,k_2}\int_0^\infty dt\,\langle 1_{\rm S}|\,a^{\dagger\dagger}_{k_1+k_2-k}\,a_{k_1}a_{k_2}U(t)(a^\dagger_k - \tilde{a}_k)\,|\rho_0\rangle\{i + X_k(\omega)\}\exp(i\,\omega\,t) \\ &\quad - i\,\frac{\hbar\gamma^2}{8N}\sum_{k_1,\,k_2}\int_0^\infty dt\,\langle 1_{\rm S}|\,a_kU(t)(a^\dagger_{k_1}a^\dagger_{k_2}a_{k_1+k_2-k} - \tilde{a}^\dagger_{k_1+k_2-k}\tilde{a}_{k_1}\tilde{a}_{k_2})\,|\rho_0\rangle\exp(i\,\omega\,t). \end{aligned} \tag{3.22}$$

Taking the spin-wave interaction $\mathcal{H}_{\rm S1}$ given by (2.12) as

$$\mathcal{H}_{\rm S1} = \hbar\sum_{k,\,k',\,k''}\epsilon_3(k,\,k')\,a^\dagger_{k'}\,a^\dagger_{k''}\,a_k\,a_{k'+k''-k} - \hbar\sum_{k,\,k'}\epsilon_2(k,\,k')\,\bar{n}(\epsilon_{k'})\,a^\dagger_k\,a_k\,, \tag{3.23}$$

by neglecting the parts of higher order than the fourth power of $a_j$, $a_j^\dagger$ in the spin-wave approximation, the next higher-order parts $\chi^{(1)}_{S_k^+S_k^-}(\omega)$ of $\chi_{S_k^+S_k^-}(\omega)$ can be derived using the quasi-particle operators and takes the form [23, 9]

$$\begin{aligned}\chi^{(1)}_{S_k^+S_k^-}(\omega) &= \sum_{k_1}\frac{(\hbar\,\gamma^2 S/2)\,\epsilon_2(k,\,k_1)(n_{k_1}-\bar{n}(\epsilon_{k_1}))\,\{1-i\,X_k(\omega)\}}{\{-i\,(\omega-\epsilon_k-\Phi_k'')+\Phi_k'+\Psi_k\}\{-i\,(\omega-\epsilon_k-\Phi_k'')+\Phi_k'+\Psi_k+2\,\Phi_{k_1}'\}}\\ &-\frac{\hbar\,\gamma^2}{4\,N}\sum_{k_1}\Big\{\frac{(n_{k_1}-\bar{n}(\epsilon_{k_1}))\{i+X_k(\omega)\}}{-i\,(\omega-\epsilon_k-\Phi_k'')+\Phi_k'+\Psi_k+2\,\Phi_{k_1}'}+\frac{\bar{n}(\epsilon_{k_1})\{i+X_k(\omega)\}}{-i\,(\omega-\epsilon_k-\Phi_k'')+\Phi_k'+\Psi_k}\Big\}\\ &-i\,\frac{\hbar\,\gamma^2}{4\,N}\sum_{k_1}\frac{n_{k_1}}{-i\,(\omega-\epsilon_k-\Phi_k'')+\Phi_k'+\Psi_k},\end{aligned}\tag{3.24}$$

which is derived in Appendixes A and B, where $n_k$ is $n_k(0)$ given in Refs. [23, 9], i.e., $n_k=\langle 1_{\rm s}|a_k^\dagger a_k|\rho_0\rangle$. For the calculation of the physical quantities, we lead the real parts $\chi^{(0)}_{S_k^+S_k^-}(\omega)'$, $\chi^{(1)}_{S_k^+S_k^-}(\omega)'$ and imaginary parts $\chi^{(0)}_{S_k^+S_k^-}(\omega)''$, $\chi^{(1)}_{S_k^+S_k^-}(\omega)''$ of the low-order part $\chi^{(0)}_{S_k^+S_k^-}(\omega)$ and the next higher-order parts $\chi^{(1)}_{S_k^+S_k^-}(\omega)$ of the transverse susceptibility $\chi_{S_k^+S_k^-}(\omega)$, as follows

$$\chi^{(0)}_{S_k^+S_k^-}(\omega)'=\frac{S\,\hbar\,\gamma^2}{2}\cdot\frac{(\Phi_k'+\Psi_k)\,X_k'(\omega)-(\omega-\epsilon_k-\Phi_k'')\{1+X_k''(\omega)\}}{(\omega-\epsilon_k-\Phi_k'')^2+(\Phi_k'+\Psi_k)^2},\tag{3.25a}$$

$$\chi^{(0)}_{S_k^+S_k^-}(\omega)''=\frac{S\,\hbar\,\gamma^2}{2}\cdot\frac{(\Phi_k'+\Psi_k)\{1+X_k''(\omega)\}+(\omega-\epsilon_k-\Phi_k'')\,X_k'(\omega)}{(\omega-\epsilon_k-\Phi_k'')^2+(\Phi_k'+\Psi_k)^2},\tag{3.25b}$$

$$\begin{aligned}\chi^{(1)}_{S_k^+S_k^-}(\omega)' &= \frac{1}{2}\sum_{k_1}\hbar\,\gamma^2 S\,\epsilon_2(k,\,k_1)\{n_{k_1}-\bar{n}(\epsilon_{k_1})\}\\ &\times\Big\{\frac{2\,(\omega-\epsilon_k-\Phi_k'')(\Phi_k'+\Psi_k+\Phi_{k_1}')X_k'(\omega)}{\{(\omega-\epsilon_k-\Phi_k'')^2+(\Phi_k'+\Psi_k)^2\}\{(\omega-\epsilon_k-\Phi_k'')^2+(\Phi_k'+\Psi_k+2\,\Phi_{k_1}')^2\}}\\ &+\frac{\{(\Phi_k'+\Psi_k)(\Phi_k'+\Psi_k+2\,\Phi_{k_1}')-(\omega-\epsilon_k-\Phi_k'')^2\}\{1+X_k''(\omega)\}}{\{(\omega-\epsilon_k-\Phi_k'')^2+(\Phi_k'+\Psi_k)^2\}\{(\omega-\epsilon_k-\Phi_k'')^2+(\Phi_k'+\Psi_k+2\,\Phi_{k_1}')^2\}}\Big\}\\ &-\frac{\hbar\,\gamma^2}{4\,N}\sum_{k_1}\Big\{\{n_{k_1}-\bar{n}(\epsilon_{k_1})\}\frac{(\Phi_k'+\Psi_k+2\,\Phi_{k_1}')X_k'(\omega)-(\omega-\epsilon_k-\Phi_k'')\{1+X_k''(\omega)\}}{(\omega-\epsilon_k-\Phi_k'')^2+(\Phi_k'+\Psi_k+2\,\Phi_{k_1}')^2}\\ &+\frac{(\Phi_k'+\Psi_k)\,\bar{n}(\epsilon_{k_1})X_k'(\omega)-(\omega-\epsilon_k-\Phi_k'')\{\bar{n}(\epsilon_{k_1})\{1+X_k''(\omega)\}+n_{k_1}\}}{(\omega-\epsilon_k-\Phi_k'')^2+(\Phi_k'+\Psi_k)^2}\Big\},\end{aligned}\tag{3.26a}$$

$$\begin{aligned}\chi^{(1)}_{S_k^+S_k^-}(\omega)'' &= \frac{1}{2}\sum_{k_1}\hbar\,\gamma^2 S\,\epsilon_2(k,\,k_1)\{n_{k_1}-\bar{n}(\epsilon_{k_1})\}\\ &\times\Big\{\frac{2\,(\omega-\epsilon_k-\Phi_k'')(\Phi_k'+\Psi_k+\Phi_{k_1}')\{1+X_k''(\omega)\}}{\{(\omega-\epsilon_k-\Phi_k'')^2+(\Phi_k'+\Psi_k)^2\}\{(\omega-\epsilon_k-\Phi_k'')^2+(\Phi_k'+\Psi_k+2\,\Phi_{k_1}')^2\}}\\ &+\frac{\{(\omega-\epsilon_k-\Phi_k'')^2-(\Phi_k'+\Psi_k)(\Phi_k'+\Psi_k+2\,\Phi_{k_1}')\}X_k'(\omega)}{\{(\omega-\epsilon_k-\Phi_k'')^2+(\Phi_k'+\Psi_k)^2\}\{(\omega-\epsilon_k-\Phi_k'')^2+(\Phi_k'+\Psi_k+2\,\Phi_{k_1}')^2\}}\Big\}\\ &-\frac{\hbar\,\gamma^2}{4\,N}\sum_{k_1}\Big\{\{n_{k_1}-\bar{n}(\epsilon_{k_1})\}\frac{(\Phi_k'+\Psi_k+2\,\Phi_{k_1}')\{1+X_k''(\omega)\}+(\omega-\epsilon_k-\Phi_k'')X_k'(\omega)}{(\omega-\epsilon_k-\Phi_k'')^2+(\Phi_k'+\Psi_k+2\,\Phi_{k_1}')^2}\\ &+\frac{(\omega-\epsilon_k-\Phi_k'')\,\bar{n}(\epsilon_{k_1})X_k'(\omega)+(\Phi_k'+\Psi_k)\{\bar{n}(\epsilon_{k_1})\{1+X_k''(\omega)\}+n_{k_1}\}}{(\omega-\epsilon_k-\Phi_k'')^2+(\Phi_k'+\Psi_k)^2}\Big\},\end{aligned}\tag{3.26b}$$

where $X_k'(\omega)$ and $X_k''(\omega)$ are the real part and imaginary part of the corresponding interference term $X_k(\omega)$, and are given by

$$X_k'(\omega)=\frac{\Phi_k'(\omega)-\Phi_k'(\epsilon_k)}{\omega-\epsilon_k}+\frac{\Psi_k'(\omega-\epsilon_k)-\Psi_k}{\omega-\epsilon_k},\qquad X_k''(\omega)=\frac{\Phi_k''(\omega)-\Phi_k''(\epsilon_k)}{\omega-\epsilon_k}+\frac{\Psi_k''(\omega-\epsilon_k)-\Psi_k}{\omega-\epsilon_k},\tag{3.27}$$

with the real part $\Psi_k'(\omega-\epsilon_k)$ and imaginary part $\Psi_k''(\omega-\epsilon_k)$ of $\Psi_k(\omega-\epsilon_k)$, when $\Psi_k$ is real ($\Psi_k=\Psi_k^*$).

We consider the power absorption and transverse magnetization in the stationary state of the ferromagnetic spin system interacting with the transversely rotating magnetic-field given by (3.1). In the stationary state of the spin system, the linear response $\langle 1_{\rm s}|\hbar S_k^+|\rho_1(t)\rangle$ for spin operator $S_k^+$ with the wave-number $k$ have the form

$$\langle 1_{\rm s}|\hbar S_k^+|\rho_1(t)\rangle=(2/\gamma)\,\chi_{S_k^+S_k^-}(\omega)H_k^*\exp(-i\,\omega\,t),\qquad\qquad(t\to\infty),\tag{3.28}$$

with $|\rho_1(t)\rangle\rangle = \langle 1_{\rm R}|\rho_{\rm T1}(t)\rangle\rangle = |{\rm tr}_{\rm R}\rho_{\rm T1}(t)\rangle\rangle$, where $\rho_{\rm T1}(t)$ is the first-order part of the density operator $\rho_{\rm T}(t)$ for the total system in powers of the external driving magnetic-field given by (3.1). The power absorption of the ferromagnetic system is given by [16]

$$P(\omega) = \sum_k (\gamma/2)\big\{\big\langle (d\langle 1_{\rm S}|\hbar S_k^+|\rho_1(t)\rangle\rangle/dt) H_k \exp(i\,\omega\,t)\big\rangle + {\rm c.\,c.}\big\} = \sum_k P_k(\omega), \tag{3.29a}$$

$$P_k(\omega) = 2\,|H_k|^2\,\omega\,\chi''_{S_k^+ S_k^-}(\omega), \tag{3.29b}$$

with the power absorption $P_k(\omega)$ of the ferromagnetic system with the wave-number $k$, where the notation $\langle\cdots\rangle$ denotes the time average per one period of the external driving magnetic-field. According to (3.29b), (3.25b) and (3.26b), the line shape of the power absorption $P_k(\omega)$ of the ferromagnetic system with the wave-number $k$, has a peak at frequency $\omega \cong \epsilon_k + \Phi''_k$. The resonance frequency $\omega^{\rm P}_{{\rm R}k}$ and the peak-height (height of peak) $H^{\rm P}_{{\rm R}k}$ in the resonance region of the power absorption $P_k(\omega)$ approximate to

$$\omega^{\rm P}_{{\rm R}k} \cong \epsilon_k + \Phi''_k, \tag{3.30}$$

$$\begin{aligned} H^{\rm P}_{{\rm R}k} \cong{}& S\,\gamma^2\,|H_k|^2\,\hbar\,\omega^{\rm P}_{{\rm R}k}\,\{1 + X''_k(\omega^{\rm P}_{{\rm R}k})\}/(\Phi'_k + \Psi_k) \\ & - S\,\gamma^2\,|H_k|^2\,\hbar\,\omega^{\rm P}_{{\rm R}k} \sum_{k_1} \epsilon_2(k,\,k_1)\{n_{k_1} - \bar{n}(\epsilon_{k_1})\}\frac{X'_k(\omega^{\rm P}_{{\rm R}k})}{(\Phi'_k + \Psi_k)(\Phi'_k + \Psi_k + 2\,\Phi'_{k_1})} \\ & - \frac{\gamma^2\,|H_k|^2\,\hbar\,\omega^{\rm P}_{{\rm R}k}}{2\,N} \sum_{k_1} \Big\{ \frac{(n_{k_1} - \bar{n}(\epsilon_{k_1}))\{1 + X''_k(\omega^{\rm P}_{{\rm R}k})\}}{\Phi'_k + \Psi_k + 2\,\Phi'_{k_1}} + \frac{\bar{n}(\epsilon_{k_1})\{1 + X''_k(\omega^{\rm P}_{{\rm R}k})\} + n_{k_1}}{\Phi'_k + \Psi_k} \Big\}. \end{aligned} \tag{3.31}$$

The expectation value $M^x_k(t)$ of the $x$-component of the magnetization with the wave-number $k$, can be expressed as

$$M^x_k(t) = \{\langle 1_{\rm S}|\hbar S_k^+|\rho_1(t)\rangle\rangle + \langle 1_{\rm S}|\hbar S_k^-|\rho_1(t)\rangle\rangle\}/2 = {\rm Re}\,\langle 1_{\rm S}|\hbar S_k^+|\rho_1(t)\rangle\rangle, \tag{3.32a}$$

$$= (2/\gamma)\big\{(\chi_{S_k^+ S_k^-}(\omega)H_k^*)'\cos(\omega\,t) + (\chi_{S_k^+ S_k^-}(\omega)H_k^*)''\sin(\omega\,t)\big\}, \tag{3.32b}$$

$$= A^{\rm M}_k(\omega)\sin\{\omega\,t + \delta_k(\omega)\}, \tag{3.32c}$$

the expectation value $M^y_k(t)$ of the $y$-component of the magnetization with the wave-number $k$, can be expressed as

$$M^y_k(t) = \{\langle 1_{\rm S}|\hbar S_k^+|\rho_1(t)\rangle\rangle - \langle 1_{\rm S}|\hbar S_k^-|\rho_1(t)\rangle\rangle\}/(2\,i) = {\rm Im}\,\langle 1_{\rm S}|\hbar S_k^+|\rho_1(t)\rangle\rangle, \tag{3.33a}$$

$$= (2/\gamma)\big\{(\chi_{S_k^+ S_k^-}(\omega)H_k^*)''\cos(\omega\,t) - (\chi_{S_k^+ S_k^-}(\omega)H_k^*)'\sin(\omega\,t)\big\}, \tag{3.33b}$$

$$= A^{\rm M}_k(\omega)\cos\{\omega\,t + \delta_k(\omega)\}, \tag{3.33c}$$

where the amplitude $A^{\rm M}_k(\omega)$ is given by

$$A^{\rm M}_k(\omega) = (2/\gamma)\sqrt{\{(\chi_{S_k^+ S_k^-}(\omega)H_k^*)'\}^2 + \{(\chi_{S_k^+ S_k^-}(\omega)H_k^*)''\}^2}, \tag{3.34a}$$

$$= (2/\gamma)|H_k|\,|\chi_{S_k^+ S_k^-}(\omega)| = (2/\gamma)|H_k|\sqrt{(\chi_{S_k^+ S_k^-}(\omega)')^2 + (\chi_{S_k^+ S_k^-}(\omega)'')^2}, \tag{3.34b}$$

and the initial phase $\delta_k(\omega)$ is given by

$$\sin\delta_k(\omega) = (2/\gamma)(\chi_{S_k^+ S_k^-}(\omega)H_k^*)'/A^{\rm M}_k(\omega), \qquad \cos\delta_k(\omega) = (2/\gamma)(\chi_{S_k^+ S_k^-}(\omega)H_k^*)''/A^{\rm M}_k(\omega), \tag{3.35a}$$

$$\tan\delta_k(\omega) = (\chi_{S_k^+ S_k^-}(\omega)H_k^*)'/(\chi_{S_k^+ S_k^-}(\omega)H_k^*)''. \tag{3.35b}$$

Thus, the expectation values $M^x_k(t)$ and $M^y_k(t)$ of the $x$-component and $y$-component of the magnetization with the wave-number $k$ oscillate with the frequency $\omega$ and the amplitude $A^{\rm M}_k(\omega)$ given by (3.34). According to the (3.25) and (3.26), the amplitude $A^{\rm M}_k(\omega)$ of the expectation value of the transverse magnetization, which is referred as "the magnetization-amplitude", has a peak at frequency $\omega \cong \epsilon_k + \Phi''_k$. Thus, the expectation values $M^x_k(t)$ amd $M^y_k(t)$ of the $x$-component and $y$-component of the magnetization with the wave-number $k$ oscillate with the large amplitude $A^{\rm M}_k(\omega^{\rm M}_{{\rm R}k})$ at the resonance frequency $\omega^{\rm M}_{{\rm R}k}$, which coincides nearly with the resonance frequency $\omega^{\rm P}_{{\rm R}k}$ of the power absorption $P_k(\omega)$ of the ferromagnetic system with the wave-number $k$. The resonance frequency $\omega^{\rm M}_{{\rm R}k}$ and the peak-height (height of

peak) $H^{\mathtt{M}}_{\mathtt{R}k}$ of the magnetization-amplitude $A^{\mathtt{M}}_k(\omega)$ with the wave-number $k$ approximate to

$$\omega^{\mathtt{M}}_{\mathtt{R}k} \cong \epsilon_k + \Phi''_k, \tag{3.36}$$

$$\begin{aligned} H^{\mathtt{M}}_{\mathtt{R}k} \cong \hbar\gamma\,|H_k|\,\Big\{\Big\{ & S\,\frac{X'_k(\omega^{\mathtt{M}}_{\mathtt{R}k})}{\Phi'_k+\Psi_k} + S\sum_{k_1}\epsilon_2(k,\,k_1)\,\frac{\{n_{k_1}-\bar{n}(\epsilon_{k_1})\}\{1+X''_k(\omega^{\mathtt{M}}_{\mathtt{R}k})\}}{(\Phi'_k+\Psi_k)(\Phi'_k+\Psi_k+2\,\Phi'_{k_1})} \\ & - \frac{1}{2\,N}\sum_{k_1}\Big(\frac{n_{k_1}-\bar{n}(\epsilon_{k_1})}{\Phi'_k+\Psi_k+2\,\Phi'_{k_1}} + \frac{\bar{n}(\epsilon_{k_1})}{\Phi'_k+\Psi_k}\Big)X'_k(\omega^{\mathtt{M}}_{\mathtt{R}k})\Big\}^2 \\ & + \Big\{ S\,\frac{1+X''_k(\omega^{\mathtt{M}}_{\mathtt{R}k})}{\Phi'_k+\Psi_k} - S\sum_{k_1}\epsilon_2(k,\,k_1)\,\frac{\{n_{k_1}-\bar{n}(\epsilon_{k_1})\}X'_k(\omega^{\mathtt{M}}_{\mathtt{R}k})}{(\Phi'_k+\Psi_k)(\Phi'_k+\Psi_k+2\,\Phi'_{k_1})} \\ & - \frac{1}{2\,N}\sum_{k_1}\Big(\frac{\{n_{k_1}-\bar{n}(\epsilon_{k_1})\}\{1+X''_k(\omega^{\mathtt{M}}_{\mathtt{R}k})\}}{\Phi'_k+\Psi_k+2\,\Phi'_{k_1}} + \frac{\bar{n}(\epsilon_{k_1})\{1+X''_k(\omega^{\mathtt{M}}_{\mathtt{R}k})\}+n_{k_1}}{\Phi'_k+\Psi_k}\Big)\Big\}^2\Big\}^{1/2}. \end{aligned} \tag{3.37}$$

In the following section, we investigate numerically the resonanse frequencies and peak-heights in the resonance region of the power absorption $P_k(\omega)$ and magnetization-amplitude $A^{\mathtt{M}}_k(\omega)$ of the ferromagnetic spin system with the wave-number $k$.

If the relaxation method is employed [17] in the van Hove limit [27] or in the narrowing limit [28], in which the correlation time $\tau_c$ of the phonon reservoir is much less than the relaxation time $\tau_r$ of the spin system ($\tau_c \ll \tau_r$ or $\tau_c \to 0$), i.e., the Kubo formula [8] is calculated from the second-order TCL equations with no external driving terms in this limit, one obtains the transverse susceptibility [17]

$$\chi^{\mathrm{rv}}_{S^+_k S^-_k}(\omega) = i\,\frac{\hbar\,\gamma^2}{4}\int_0^\infty dt\,\langle 1_{\mathtt{S}}|\,S^+_k\,U(t)\exp_{\leftarrow}\Big\{-i\int_0^t d\tau\,\hat{\mathcal{H}}_{\mathtt{S}1}(\tau)\Big\}(S^-_k-\tilde{S}^+_k)\,|\rho_0\rangle\exp(i\,\omega\,t), \tag{3.38}$$

which coincides with the ones without the interference thermal state $|D^{(2)}_{S^-_k}[\omega]\rangle$ in the transverse susceptibility $\chi_{S^+_k S^-_k}(\omega)$ [(3.9)] derived employing the TCLE method. That limit neglects the effects of the memory and initial correlation for the spin system and phonon reservoir, and is valid for a quickly damped reservoir (the reservoir correlation time $\tau_c \to 0$), but not for a non-quickly damped reservoir, because the influence of motion of the phonon reservoir on the motoin of the spin system is neglected in that limit. The transverse susceptibility $\chi_{S^+_k S^-_k}(\omega)$ derived employing the TCLE method includes the interference thermal state $|D^{(2)}_{S^-_k}[\omega]\rangle$, which represents the effects of the memory and initial correlation for the spin system and phonon reservoir, i.e., the effects of deviation from the van Hove limit [27] or the narrowing limit [28], and is valid even if the spin system is interacting with a non-quickly damped phonon-reservoir in the region valid for the second-order perturbation approximation. The coincidence of the TCLE method and relaxation method in the second-order approximation for the system-reservoir interaction [17, 13, 14, 24, 25, 26], means that the interference effects, i.e., the effects of the interference terms or the interference thermal state in the TCLE method, are the effects of motion of the phonon reservoir which influence the motoin of the spin system. Therefore, the interference effects are considered to increase the power absorption and magnetization-amplitude in the resonance region to excite the phonon reservoir for a non-quickly damped reservoir, because the external driving field excites not only the spin system but also the phonon reservoir for a non-quickly damped reservoir. These are investigated numerically in the following section.

# 4 Numerical investigation

In the present section, we assume a damped phonon-reservoir model and investigate numerically the power absorption and the magnetization-amplitude (the amplitude of the expectation value of the transverse magnetization) for a ferromagnetic spin system, which is interacting with a phonon reservoir and with the transversely rotating magnetic-field given by (3.1) under an external static magnetic-field. We assume that the phonon reservoir consists of a phonon system coupled directly to the spin system and of a reservoir subsystem coupled to the phonon system, where the reservoir subsystem (R-subsystem) is damped very rapidly, as done in Refs. [9, 23]. Then, the correlation functions of the phonon operators can be derived using the relaxation theory for the phonon system [31, 32, 33], and are assumed to take the forms

$$\sum_\nu |\,g_{1\alpha}\,|^2\langle 1_{\mathtt{R}}|\,B^\dagger_{k\alpha}(t)B_{k\alpha}\,|\rho_{\mathtt{R}}\rangle = g_1^2\,\bar{n}(\omega_{\mathtt{R}k})\exp(i\,\omega_{\mathtt{R}k}\,t-\gamma_{\mathtt{R}k}\,t), \tag{4.1a}$$

$$\sum_\nu |\,g_{1\alpha}\,|^2\langle 1_{\mathtt{R}}|\,B_{k\alpha}(t)B^\dagger_{k\alpha}\,|\rho_{\mathtt{R}}\rangle = g_1^2\,\{\bar{n}(\omega_{\mathtt{R}k})+1\}\exp(-\,i\,\omega_{\mathtt{R}k}\,t-\gamma_{\mathtt{R}k}\,t), \tag{4.1b}$$

$$\begin{aligned} &\sum_\nu g^2_{2\alpha}\langle 1_{\mathtt{R}}|\Delta(B^\dagger_{k\alpha}(t)B_{k\alpha}(t))\Delta(B^\dagger_{k\alpha}B_{k\alpha})|\rho_{\mathtt{R}}\rangle = \sum_\nu g^2_{2\alpha}\langle 1_{\mathtt{R}}|\Delta(B^\dagger_{k\alpha}B_{k\alpha})\Delta(B^\dagger_{k\alpha}(t)B_{k\alpha}(t))|\rho_{\mathtt{R}}\rangle, \\ &= g_2^2\,\bar{n}(\omega_{\mathtt{R}k})\{\bar{n}(\omega_{\mathtt{R}k})+1\}\exp(-\,2\,\gamma_{\mathtt{R}k}\,t), \end{aligned} \tag{4.1c}$$

with the coupling constants $g_1$ and $g_2$ between the spin and phonon, where $\omega_{\mathrm{R}k}$ and $\gamma_{\mathrm{R}k}$ ($>0$) are, respectively, the characteristic frequency and damping constant of the phonon reservoir. Here, $\bar{n}(\omega_{\mathrm{R}k})$ is given by

$$\bar{n}(\omega_{\mathrm{R}k}) = \{\exp(\beta\,\hbar\,\omega_{\mathrm{R}k}) - 1\}^{-1} = \{\exp(\hbar\,\omega_{\mathrm{R}k}/(k_{\mathrm{B}}T) - 1\}^{-1}. \tag{4.2}$$

The phonon correlation function (4.1c) is real and non-negative, and therefore $\Psi_k$ [$=\phi_k^{zz}(0)$] defined by (3.19) is non-negative. The assumptions (4.1) establish when the phonon coupled to the spin system, which is moving periodically under the external driving field, is interacting with a reservoir subsystem damped very rapidly and undergoes damped oscillation. Using the above correlation functions, $\Phi_k(\epsilon)$ and $\Psi_k$ defined by (3.18) and (3.19), respectively, take the forms [29, 30]

$$\begin{aligned}\Phi_k(\epsilon) &= \frac{S}{2}\Big\{1 - \exp\Big(\frac{-\hbar\,\epsilon}{k_{\mathrm{B}}\,T}\Big)\Big\}\int_0^\infty d\tau \sum_\alpha |\,g_{1\alpha}\,|^2\langle 1_{\mathrm{R}}|B_{k\alpha}(\tau)B_{k\alpha}^\dagger\,|\rho_{\mathrm{R}}\rangle\exp(i\,\epsilon\,\tau),\\ &= \frac{1}{2}\,g_1^2\,S\Big\{1 - \exp\Big(\frac{-\hbar\,\epsilon}{k_{\mathrm{B}}\,T}\Big)\Big\}\,\frac{\bar{n}(\omega_{\mathrm{R}k}) + 1}{-\,i\,(\epsilon - \omega_{\mathrm{R}k}) + \gamma_{\mathrm{R}k}},\end{aligned} \tag{4.3}$$

$$\Psi_k = \int_0^\infty d\tau\, g_2^2\,\bar{n}(\omega_{\mathrm{R}k})\{\bar{n}(\omega_{\mathrm{R}k}) + 1\}\exp(-\,2\,\gamma_{\mathrm{R}k}\,\tau) = g_2^2\,\frac{\bar{n}(\omega_{\mathrm{R}k})\{\bar{n}(\omega_{\mathrm{R}k}) + 1\}}{2\,\gamma_{\mathrm{R}k}}. \tag{4.4}$$

The real part $\Phi_k'$ and imaginary part $\Phi_k''$ of $\Phi_{\mathrm{R}k}(\epsilon_k)$ can be expressed as

$$\Phi_k' = \Phi_k'(\epsilon_k) = \frac{1}{2}\,g_1^2\,S\Big\{1 - \exp\Big(\frac{-\hbar\,\epsilon_k}{k_{\mathrm{B}}\,T}\Big)\Big\}\,\frac{\gamma_{\mathrm{R}k}\,\{\bar{n}(\omega_{\mathrm{R}k}) + 1\}}{(\epsilon_k - \omega_{\mathrm{R}k})^2 + (\gamma_{\mathrm{R}k})^2}, \tag{4.5a}$$

$$\Phi_k'' = \Phi_k''(\epsilon_k) = \frac{1}{2}\,g_1^2\,S\Big\{1 - \exp\Big(\frac{-\hbar\,\epsilon_k}{k_{\mathrm{B}}\,T}\Big)\Big\}\,\frac{(\epsilon_k - \omega_{\mathrm{R}k})\,\{\bar{n}(\omega_{\mathrm{R}k}) + 1\}}{(\epsilon_k - \omega_{\mathrm{R}k})^2 + (\gamma_{\mathrm{R}k})^2}. \tag{4.5b}$$

The above expressions (4.4) and (4.5a) show that $\Psi_k$ [$=\phi_k^{zz}(0)$] is non-negative and that $\Phi_k'$ [$=\Phi_k'(\epsilon_k)$] is non-negative for non-negative $\epsilon_k$. We have for $\Psi_k(\epsilon)$ defined by (3.21), the form

$$\Psi_k(\epsilon) = \int_0^\infty d\tau\, g_2^2\,\bar{n}(\omega_{\mathrm{R}k})\{\bar{n}(\omega_{\mathrm{R}k}) + 1\}\exp(i\,\epsilon\,\tau - 2\,\gamma_{\mathrm{R}k}\,\tau) = g_2^2\,\frac{\bar{n}(\omega_{\mathrm{R}k})\{\bar{n}(\omega_{\mathrm{R}k}) + 1\}}{-\,i\,\epsilon + 2\,\gamma_{\mathrm{R}k}}, \tag{4.6}$$

which leads to the real part $\Psi_k'(\epsilon)$ and the imaginary part $\Psi_k''(\epsilon)$ of $\Psi_{\mathrm{R}k}(\epsilon)$ as

$$\Psi_k'(\epsilon) = g_2^2\,\frac{2\gamma_{\mathrm{R}k}\,\bar{n}(\omega_{\mathrm{R}k})\{\bar{n}(\omega_{\mathrm{R}k}) + 1\}}{\epsilon^2 + (2\,\gamma_{\mathrm{R}k})^2}, \qquad \Psi_k''(\epsilon) = g_2^2\,\frac{\epsilon\,\bar{n}(\omega_{\mathrm{R}k})\{\bar{n}(\omega_{\mathrm{R}k}) + 1\}}{\epsilon^2 + (2\,\gamma_{\mathrm{R}k})^2}. \tag{4.7}$$

In Appendix C, we derive the concrete forms of the the real part $X_k'(\omega)$ and the imaginary part $X_k''(\omega)$ of the corresponding interference term $X_k(\omega)$ given by (3.16) or (3.20). The form of $n_k = \langle 1_{\mathrm{S}}|a_k^\dagger a_k|\rho_0\rangle$, which is $n_k(0)$ given by in Refs. [23, 9], is derived in Appendix D and is given by (D.7) as

$$n_k = \bar{n}(\epsilon_k) + S\,g_1^2\,\{\bar{n}_k(\omega_{\mathrm{R}k}) - \bar{n}(\epsilon_k)\}\,\frac{(\epsilon_k - \omega_{\mathrm{R}k})^2 - (\gamma_{\mathrm{R}k})^2}{\{(\epsilon_k - \omega_{\mathrm{R}k})^2 + (\gamma_{\mathrm{R}k})^2\}^2}, \tag{4.8}$$

up to the second order in powers of the spin-phonon interactin $\mathcal{H}_{\mathrm{SR}}$. We assume for consistency with assumptions (4.1c) that

$$\sum_\alpha g_{2\alpha}\langle 1_{\mathrm{R}}|B_{k\alpha}^\dagger B_{k\alpha}|\rho_{\mathrm{R}}\rangle = g_2\,\bar{n}(\omega_{\mathrm{R}k}). \tag{4.9}$$

Then, for the renormalized energy $\hbar\epsilon_k$ of the spin-wave with the wave number $k$, which is given by (2.24), we have

$$\epsilon_k = \epsilon_1(k) + \sum_{k'}\epsilon_2(k,\,k')\,\bar{n}(\epsilon_{k'}) + g_2\,\bar{n}(\omega_{\mathrm{R}k}). \tag{4.10}$$

We consider the case that the phonon reservoir consists of a phonon system of lattice vibration, which has the frequency proportional to the magnitude $|k|$ of the wave number $k$, and of a reservoir subsystem coupled to the phonon system, where the reservoir subsystem (R-subsystem) is damped quickly. We assume that the characteristic frequency of the phonon reservoir is given by

$$\omega_{\mathrm{R}k} = V\,|k| + \omega_{\mathrm{R}0}, \tag{4.11}$$

where $\omega_{\mathrm{R}0}$ is the characteristic frequency of the phonon reservoir with the wave number $k=0$ and is the frequency shift of the phonon system, which is generated by the motion of the reservoir subsystem coupled to the phonon system.

We consider a ferromagnetic system of one-dimensional infinite spins interacting with the phonon reservoir, and investigate numerically the power absorption and the magnetization-amplitude (the amplitude of the expectation value

of the transverse magnetization) in the stationary state of the ferromagnetic system. For the case of a regular-interval ranked spin-chain, we have

$$z = 2, \qquad \eta_k = \cos k, \tag{4.12}$$

where $k$ is the wave number multiplied by the lattice constant and is referred to as "the wave number" hereafter. In the infinite limit of the total number $N$ of spins, the wave-number summation is replaced with the integral as

$$\frac{1}{N}\sum_k = \frac{1}{2\pi}\int_{-\pi}^{\pi} dk, \qquad (N \to \infty). \tag{4.13}$$

Then, by replacing $\bar{n}(\epsilon_{k'})$ in (4.10) with $\bar{n}(\epsilon_1(k'))$, we give $\epsilon_k$ approximately as

$$\epsilon_k \cong \epsilon_1(k) + \sum_{k'} \epsilon_2(k,\, k')\, \bar{n}_{k'}(\epsilon_1(k')) + g_2\, \bar{n}_k(\omega_{\mathrm{R}k}), \tag{4.14a}$$

$$\begin{aligned} &= \omega_z + (2\,S-1)\,K + 4\,S\,J\,(\zeta - \cos k) + g_2/\{\exp(\hbar\,\omega_{\mathrm{R}k}/(k_{\mathrm{B}}T)) - 1\} \\ &\quad + \frac{4}{\pi}\int_0^{\pi} dk'\, \frac{J\,(\cos k + \cos k') - \zeta\, J\,\{1 + \cos k\, \cos k'\} - K}{\exp\{[\,\hbar\,\omega_z + (2S-1)\,\hbar\,K + 4\,S\,\hbar\,J\,(\zeta - \cos k')\,]/(k_{\mathrm{B}}T)\} - 1}\,, \end{aligned} \tag{4.14b}$$

where we have put

$$J_1 = J\,, \qquad J_2 = \zeta\, J\,, \qquad \zeta = J_2/J_1\,. \tag{4.15}$$

We perform the numerical calculation for the case that $g_1/\omega_z = g_2/\omega_z = 0.25$ for the coupling constants $g_1$ and $g_2$ between the spin and phonon, and that $\zeta = 1.0$ and $J/\omega_z = 1.0$, i.e., $J_1 = J_2 = J = \omega_z$. We consider the case that $V_{\mathrm{R}}/\omega_z = 0.5$, $\omega_{\mathrm{R}0}/\omega_z = 0.5$ and $\gamma_{\mathrm{R}k}/\omega_z = 0.5$. In Appendix E, we investigate numerically the region valid for the low spin-wave approximation in the meaning that the expectation value $n/(4S)$ $[= \langle n_j \rangle/(4S)]$ of the second term in the expansion (2.2) is smaller than about 0.01. That approximation includes the dominant parts of the higher-order parts in the spin-wave approximation [5] and is referred as "the low spin-wave approximation" hereafter, in the ferromagnetic system of one-dimensional infinite spins. In Appendix E, the low spin-wave approximation is shown to be valid in the regions of the temperature $T$ and anisotropy energy $\hbar K$ given by $k_{\mathrm{B}}T/(\hbar\omega_z) \leq 1.1$ and $K/\omega_z \geq 1.0$, or $k_{\mathrm{B}}T/(\hbar\omega_z) \leq 1.5$ and $K/\omega_z \geq 2.0$, for the spin-magnitude $S \geq 1$.

We first investigate numerically the power absorption $P_k(\omega)$ given by (3.29b) for the ferromagnetic spin system with the wave-number $k$. In Fig. 1, the power absorption $P_k(\omega)$ given by (3.29b), scaled by $\hbar\gamma^2\,|H_k|^2$, are displayed varying the frequency $\omega$ scaled by $\omega_z$ from 1.0 to 7.0 for the cases of the wave-number $k = 0, \pi/6, \pi/4, \pi/3, \pi/2$ and for the spin-magnitude $S = 1$, the temperature $T$ and the anisotropy energy $\hbar K$ given by $k_{\mathrm{B}}T/(\hbar\omega_z) = 1.0$ and $K/\omega_z = 1.0$. Figure 1 shows that as the wave-number $k$ becomes large in the resonance region of the power absorption $P_k(\omega)$, the resonance frequency and the peak-height (height of peak) increase and the line half–width decreases. In Fig. 2, the power absorption $P_k(\omega)$ given by (3.29b), the results derived employing the relaxation method [17] in the van Hove limit [27] or in the narrowing limit [28], and the ones without the next higher-order parts $\chi^{(1)}_{S_k^+ S_k^-}(\omega)''$ in (3.29b), scaled by $\hbar\gamma^2\,|H_k|^2$, are displayed varying the frequency $\omega$ scaled by $\omega_z$ from 1.5 to 3.5 for the cases of the wave-number $k = 0, \pi/6$ and for the spin-magnitude $S = 1$, the temperature $T$ and the anisotropy energy $\hbar K$ given by $k_{\mathrm{B}}T/(\hbar\omega_z) = 1.0$ and $K/\omega_z = 1.0$. In Fig. 2, the power absorption $P_k(\omega)$ given by (3.29b) derived employing the TCLE method, are displayed by the solid lines, the results derived employing the relaxation method in the van Hove limit [27] or in the narrowing limit [28], are displayed by the dot lines, and the ones without the next higher-order parts $\chi^{(1)}_{S_k^+ S_k^-}(\omega)''$ in (3.29b) derived employing the TCLE method, are displayed by the short-dash lines. The power absorption $P_k(\omega)$ given by (3.29b), which have been derived employing the TCLE method, includes the effects of the interference terms in the TCLE method, which are referred as "the interference effects", represent the effects of the memory and initial correlation for the spin system and phonon reservoir [17], and are neglected in the results derived employing the relaxation method [17] in the van Hove limit [27] or in the narrowing limit [28]. Figure 2 shows that the interference effects produce the effects that increase the power absorption and cannot be disregarded for small wave-number $k$ in particular. Figure 2 also shows that the effects of the next higher-order parts $\chi^{(1)}_{S_k^+ S_k^-}(\omega)''$ are small in (3.29b). We derive the approximate formula of the line half-width $\Delta\omega^{\mathrm{P}}_{\mathrm{R}k}$ in the resonance region of the power absorption $P_k(\omega)$ given by (3.29b) for the ferromagnetic spin system with the wave-number $k$, neglecting the next higher-order parts in the spin-wave approximation, because the effects of the next higher-order parts $\chi^{(1)}_{S_k^+ S_k^-}(\omega)''$ are small in (3.29b) as seen in Fig. 2. Neglecting the next higher-order parts in the spin-wave approximation, the approximate formula of the peak-height (height of peak) $H^{\mathrm{P}}_{\mathrm{R}k}$ in the resonance region of the power absorption $P_k(\omega)$ becomes

$$H^{\mathrm{P}}_{\mathrm{R}k} \cong S\,\gamma^2\,|H_k|^2\,\hbar\,\omega^{\mathrm{P}}_{\mathrm{R}k}\,\{1 + X''_k(\omega^{\mathrm{P}}_{\mathrm{R}k})\}/(\Phi'_k + \Psi_k). \tag{4.16}$$

In order to obtain the approximate formula of the line half-width $\Delta\omega^{\rm P}_{{\rm R}k}$ in the resonance region of the power absorption $P_k(\omega)$, we put as $\Delta\omega^{\rm P}_{{\rm R}k}/2 = (\Phi'_k + \Psi_k)\, x_1$ for the first-step approximation of $\Delta\omega^{\rm P}_{{\rm R}k}$, which satisfies

$$\frac{1}{2}H^{\rm P}_{{\rm R}k} \cong S\,\gamma^2\,|H_k|^2\,\hbar\,\omega^{\rm P}_{{\rm R}k}\,\frac{1+X''_k(\omega^{\rm P}_{{\rm R}k})}{2\,(\Phi'_k+\Psi_k)} \cong S\,\hbar\,\gamma^2\,|H_k|^2\,\frac{\omega^{\rm P}_{{\rm R}k}+(\Phi'_k+\Psi_k)\,x_1}{(\Phi'_k+\Psi_k)(x_1^2+1)}\{1+X''_k(\omega^{\rm P}_{{\rm R}k})+x_1X'_k(\omega^{\rm P}_{{\rm R}k})\}, \tag{4.17}$$

where we have approximated $X_k(\omega^{\rm P}_{{\rm R}k}+(\Phi'_k+\Psi_k)\,x_1)$ with $X_k(\omega^{\rm P}_{{\rm R}k})$ in the right-hand side of the above equation. Equation (4.17) can be rewritten as

$$\begin{aligned}&\big\{\omega^{\rm P}_{{\rm R}k}\{1+X''_k(\omega^{\rm P}_{{\rm R}k})\}-2\,(\Phi'_k+\Psi_k)X'_k(\omega^{\rm P}_{{\rm R}k})\big\}\,x_1^2\\ &\quad-2\,\big\{\omega^{\rm P}_{{\rm R}k}X'_k(\omega^{\rm P}_{{\rm R}k})+(\Phi'_k+\Psi_k)\{1+X''_k(\omega^{\rm P}_{{\rm R}k})\}\big\}\,x_1-\omega^{\rm P}_{{\rm R}k}\{1+X''_k(\omega^{\rm P}_{{\rm R}k})\}\cong 0.\end{aligned} \tag{4.18}$$

By obtaining the positive solution of the above second-order equation for $x_1$, the first-step approximation of the line half-width $\Delta\omega^{\rm P}_{{\rm R}k}$ can be derived as

$$\begin{aligned}2\,(\Phi'_k+\Psi_k)\,x_1 \cong\ & 2\,(\Phi'_k+\Psi_k)\big\{\omega^{\rm P}_{{\rm R}k}X'_k(\omega^{\rm P}_{{\rm R}k})+(\Phi'_k+\Psi_k)\{1+X''_k(\omega^{\rm P}_{{\rm R}k})\}\\ &+\big\{(\omega^{\rm P}_{{\rm R}k})^2\{X'_k(\omega^{\rm P}_{{\rm R}k})^2+\{1+X''_k(\omega^{\rm P}_{{\rm R}k})\}^2\}+(\Phi'_k+\Psi_k)^2\{1+X''_k(\omega^{\rm P}_{{\rm R}k})\}^2\big\}^{1/2}\big\}\\ &/\big\{\omega^{\rm P}_{{\rm R}k}\{1+X''_k(\omega^{\rm P}_{{\rm R}k})\}-2\,(\Phi'_k+\Psi_k)X'_k(\omega^{\rm P}_{{\rm R}k})\big\}.\end{aligned} \tag{4.19}$$

Then, by putting as $\Delta\omega^{\rm P}_{{\rm R}k}/2 = (\Phi'_k+\Psi_k)\,x$, the approximate formula of the line half-width $\Delta\omega^{\rm P}_{{\rm R}k}$ in the resonance region of the power absorption $P_k(\omega)$, can be derived from the equation

$$\begin{aligned}S\,\gamma^2\,|H_k|^2\,\hbar\,\omega^{\rm P}_{{\rm R}k}\,\frac{1+X''_k(\omega^{\rm P}_{{\rm R}k})}{2\,(\Phi'_k+\Psi_k)} \cong\ & S\,\hbar\,\gamma^2\,|H_k|^2\,\frac{\omega^{\rm P}_{{\rm R}k}+(\Phi'_k+\Psi_k)\,x}{(\Phi'_k+\Psi_k)(x^2+1)}\\ &\times\big\{1+X''_k(\omega^{\rm P}_{{\rm R}k}+(\Phi'_k+\Psi_k)\,x_1)+xX'_k(\omega^{\rm P}_{{\rm R}k}+(\Phi'_k+\Psi_k)\,x_1)\big\},\end{aligned} \tag{4.20}$$

which can be rewritten as

$$\begin{aligned}&\big\{\omega^{\rm P}_{{\rm R}k}\{1+X''_k(\omega^{\rm P}_{{\rm R}k})\}-2\,(\Phi'_k+\Psi_k)X'_k(\omega^{\rm P}_{{\rm R}k}+(\Phi'_k+\Psi_k)\,x_1)\big\}\,x^2\\ &\quad-2\,\big\{\omega^{\rm P}_{{\rm R}k}\,X'_k(\omega^{\rm P}_{{\rm R}k}+(\Phi'_k+\Psi_k)\,x_1)+(\Phi'_k+\Psi_k)\{1+X''_k(\omega^{\rm P}_{{\rm R}k}+(\Phi'_k+\Psi_k)\,x_1)\}\big\}\,x\\ &\quad-\omega^{\rm P}_{{\rm R}k}\big\{2\,\{1+X''_k(\omega^{\rm P}_{{\rm R}k}+(\Phi'_k+\Psi_k)\,x_1)\}-\{1+X''_k(\omega^{\rm P}_{{\rm R}k})\}\big\}\cong 0.\end{aligned} \tag{4.21}$$

By obtaining the positive solution of the above second-order equation for $x$, the approximate formula of the line half–width $\Delta\omega^{\rm P}_{{\rm R}k}$ in the resonance region of the power absorption $P_k(\omega)$ can be obtained as

$$\begin{aligned}\Delta\omega^{\rm P}_{{\rm R}k} \cong\ & 2\,(\Phi'_k+\Psi_k)\big\{\omega^{\rm P}_{{\rm R}k}\,X'_k(\omega^{\rm P}_{{\rm R}k}+(\Phi'_k+\Psi_k)\,x_1)+(\Phi'_k+\Psi_k)\{1+X''_k(\omega^{\rm P}_{{\rm R}k}+(\Phi'_k+\Psi_k)\,x_1)\}\\ &+\big\{(\omega^{\rm P}_{{\rm R}k})^2\,X'_k(\omega^{\rm P}_{{\rm R}k}+(\Phi'_k+\Psi_k)\,x_1)^2+(\Phi'_k+\Psi_k)^2\,\{1+X''_k(\omega^{\rm P}_{{\rm R}k}+(\Phi'_k+\Psi_k)\,x_1)\}^2\\ &\quad+2\,\omega^{\rm P}_{{\rm R}k}\{1+X''_k(\omega^{\rm P}_{{\rm R}k})\}\{(\Phi'_k+\Psi_k)X'_k(\omega^{\rm P}_{{\rm R}k}+(\Phi'_k+\Psi_k)\,x_1)+\omega^{\rm P}_{{\rm R}k}\{1+X''_k(\omega^{\rm P}_{{\rm R}k}+(\Phi'_k+\Psi_k)\,x_1)\}\}\\ &\quad-2\,\omega^{\rm P}_{{\rm R}k}\,(\Phi'_k+\Psi_k)\,X'_k(\omega^{\rm P}_{{\rm R}k}+(\Phi'_k+\Psi_k)\,x_1)\,\{1+X''_k(\omega^{\rm P}_{{\rm R}k}+(\Phi'_k+\Psi_k)\,x_1)\}\\ &\quad-(\omega^{\rm P}_{{\rm R}k})^2\{1+X''_k(\omega^{\rm P}_{{\rm R}k})\}^2\big\}^{1/2}\big\}/\big\{\omega^{\rm P}_{{\rm R}k}\{1+X''_k(\omega^{\rm P}_{{\rm R}k})\}-2\,(\Phi'_k+\Psi_k)X'_k(\omega^{\rm P}_{{\rm R}k}+(\Phi'_k+\Psi_k)\,x_1)\big\}.\end{aligned} \tag{4.22}$$

In Fig. 3, the approximate formula given by (3.30) for the resonance frequency $\omega^{\rm P}_{{\rm R}k}$ of the power absorption $P_k(\omega)$ with the wave-number $k$, and the resonance frequency $\omega^{\rm P}_{{\rm R}k}$ investigated calculating numerically the power absorption $P_k(\omega)$ without the next higher-order parts $\chi^{(1)}_{S_k^+S_k^-}(\omega)''$ in (3.29b), scaled by $\omega_z$, are displayed varying the wave-number $k$ from 0 to 2.0 for the cases of the spin-magnitude $S = 1, 3/2, 2, 5/2, 3$ and for the temperature $T$ and the anisotropy energy $\hbar K$ given by $k_{\rm B}T/(\hbar\omega_z) = 1.0$ and $K/\omega_z = 1.0$. In Fig. 3, the approximate formula given by (3.30) are displayed by the solid lines, and the results investigated calculating numerically the power absorption $P_k(\omega)$ are displayed by the dots. Figure 3 shows that the numerical results of the approximate formula given by (3.30) coincide well with the ones investigated calculating numerically the power absorption $P_k(\omega)$, and that the resonance frequency $\omega^{\rm P}_{{\rm R}k}$ becomes large as the spin-magnitude $S$ becomes large or the wave-number $k$ becomes large. In Fig. 4, the approximate formula given by (4.16) for the peak-height $H^{\rm P}_{{\rm R}k}$ of the power absorption $P_k(\omega)$ with the wave-number $k$, and the peak-height $H^{\rm P}_{{\rm R}k}$ investigated calculating numerically the power absorption $P_k(\omega)$ without the next higher-order parts $\chi^{(1)}_{S_k^+S_k^-}(\omega)''$ in (3.29b), scaled by $\hbar\gamma^2\,|H_k|^2$, are displayed varying the wave-number $k$ from 0 to 2.0 for the cases of the spin-magnitude $S = 1, 3/2, 2, 5/2, 3$ and for the temperature $T$ and the anisotropy energy $\hbar K$ given by $k_{\rm B}T/(\hbar\omega_z) = 1.0$ and $K/\omega_z = 1.0$. In Fig. 4, the approximate formula given by (4.16) are displayed by the solid lines, and the results investigated calculating numerically the power absorption $P_k(\omega)$ are displayed by the dots. Figure 4 shows that the numerical results of the approximate formula given by (4.16) coincide well with the ones investigated calculating numerically the power absorption $P_k(\omega)$, and that the peak-height $H^{\rm P}_{{\rm R}k}$ becomes large as the spin-magnitude $S$ becomes large or the wave-number $k$ becomes large. In Fig. 5, the approximate formula given by (4.22) for the line half-width $\Delta\omega^{\rm P}_{{\rm R}k}$ in the

resonance region of the power absorption $P_k(\omega)$ with the wave-number $k$, and the line half-width $\Delta\omega^{\mathtt{P}}_{\mathtt{R}k}$ investigated calculating numerically the power absorption $P_k(\omega)$ without the next higher-order parts $\chi^{(1)}_{S^+_k S^-_k}(\omega)''$ in (3.29b), scaled by $\omega_z$, are displayed varying the wave-number $k$ from 0 to 2.0 for the case of the spin-magnitude $S=1$ and for the temperature $T$ and the anisotropy energy $\hbar K$ given by $k_{\mathtt{B}}T/(\hbar\omega_z)=1.0$ and $K/\omega_z=1.0$. In Fig. 5, the approximate formula given by (4.22) are displayed by the solid lines, and the results investigated calculating numerically the power absorption $P_k(\omega)$ are displayed by the dots. Figure 5 shows that the numerical results of the approximate formula given by (4.22) coincide well with the ones investigated calculating numerically the power absorption $P_k(\omega)$, except the slight deviations in the small wave-number region, and deviate slightly from the results investigated calculating numerically the power absorption $P_k(\omega)$ in the small wave-number region. In Fig. 6, the approximate formula given by (4.22) for the line half-width $\Delta\omega^{\mathtt{P}}_{\mathtt{R}k}$, and the line half-width $\Delta\omega^{\mathtt{P}}_{\mathtt{R}k}$ investigated calculating numerically the power absorption $P_k(\omega)$ without the next higher-order parts $\chi^{(1)}_{S^+_k S^-_k}(\omega)''$ in (3.29b), scaled by $\omega_z$, are displayed varying the wave-number $k$ from 0 to 2.0 for the case of the spin-magnitude $S=3$ and for the temperature $T$ and the anisotropy energy $\hbar K$ given by $k_{\mathtt{B}}T/(\hbar\omega_z)=1.0$ and $K/\omega_z=1.0$. In Fig. 6, the approximate formula given by (4.22) are displayed by the solid lines, and the results investigated calculating numerically the power absorption $P_k(\omega)$ are displayed by the dots. Figure 6 shows that the numerical results of the approximate formula given by (4.22) coincide well with the ones investigated calculating numerically the power absorption $P_k(\omega)$. Figures 5 and 6 show that the line half-width $\Delta\omega^{\mathtt{P}}_{\mathtt{R}k}$ in the resonance region of the power absorption $P_k(\omega)$ decreases as the wave-number $k$ becomes large, and decreases slightly as the spin-magnitude $S$ becomes large. In Fig. 7, the approximate formula given by (3.30) for the resonance frequency $\omega^{\mathtt{P}}_{\mathtt{R}k}$ of the power absorption $P_k(\omega)$ with the wave-number $k$, and the resonance frequency $\omega^{\mathtt{P}}_{\mathtt{R}k}$ investigated calculating numerically the power absorption $P_k(\omega)$ without the next higher-order parts $\chi^{(1)}_{S^+_k S^-_k}(\omega)''$ in (3.29b), scaled by $\omega_z$, are displayed varying the temperature $T$ scaled by $(\hbar\omega_z)/k_{\mathtt{B}}$ from 0.1 to 1.1 for the cases of the anisotropy energy $\hbar K$ given by $K/\omega_z=1.0, 1.5, 2.0, 2.5, 3.0$, and for the spin-magnitude $S=1$ and the wave-number $k=\pi/6$. The anisotropy energy is denoted as "$A$" $[=K/\omega_z]$ in the figures. In Fig. 7, the approximate formula given by (3.30) are displayed by the solid lines, and the results investigated calculating numerically the power absorption $P_k(\omega)$ are displayed by the dots. Figure 7 shows that the numerical results of the approximate formula given by (3.30) coincide well with the ones investigated calculating numerically the power absorption $P_k(\omega)$, and that the resonance frequency $\omega^{\mathtt{P}}_{\mathtt{R}k}$ becomes large as the anisotropy energy $\hbar K$ becomes large, and becomes large slightly as the temperature $T$ becomes high. In Fig. 8, the approximate formula given by (4.16) for the peak-height $H^{\mathtt{P}}_{\mathtt{R}k}$ of the power absorption $P_k(\omega)$ with the wave-number $k$, and the peak-height $H^{\mathtt{P}}_{\mathtt{R}k}$ investigated calculating numerically the power absorption $P_k(\omega)$ without the next higher-order parts $\chi^{(1)}_{S^+_k S^-_k}(\omega)''$ in (3.29b), scaled by $\hbar\gamma^2\,|H_k|^2$, are displayed varying the temperature $T$ scaled by $(\hbar\omega_z)/k_{\mathtt{B}}$ from 0.1 to 1.1 for the cases of the anisotropy energy $\hbar K$ given by $K/\omega_z=1.0, 1.5, 2.0, 2.5, 3.0$, and for the spin-magnitude $S=1$ and the wave-number $k=\pi/6$. The anisotropy energy is denoted as "$A$" $[=K/\omega_z]$ in the figures. In Fig. 8, the approximate formula given by (4.16) are displayed by the solid lines, and the results investigated calculating numerically the power absorption $P_k(\omega)$ are displayed by the dots. Figure 8 shows that the numerical results of the approximate formula given by (4.16) coincide well with the ones investigated calculating numerically the power absorption $P_k(\omega)$, and that the peak-height $H^{\mathtt{P}}_{\mathtt{R}k}$ becomes large as the anisotropy energy $\hbar K$ becomes large, and becomes small as the temperature $T$ becomes high. In Fig. 9, the approximate formula given by (4.22) for the line half-width $\Delta\omega^{\mathtt{P}}_{\mathtt{R}k}$ in the resonance region of the power absorption $P_k(\omega)$ with the wave-number $k$, and the line half-width $\Delta\omega^{\mathtt{P}}_{\mathtt{R}k}$ investigated calculating numerically the power absorption $P_k(\omega)$ without the next higher-order parts $\chi^{(1)}_{S^+_k S^-_k}(\omega)''$ in (3.29b), scaled by $\omega_z$, are displayed varying the temperature $T$ scaled by $(\hbar\omega_z)/k_{\mathtt{B}}$ from 0.1 to 1.1 for the cases of the anisotropy energies $\hbar K$ given by $K/\omega_z=1.0, 3.0$, and for the spin-magnitude $S=1$ and the wave-number $k=\pi/6$. The anisotropy energy is denoted as "$A$" $[=K/\omega_z]$ in the figures. In Fig. 9, the approximate formula given by (4.22) are displayed by the solid lines, and the results investigated calculating numerically the power absorption $P_k(\omega)$ are displayed by the dots. Figure 9 shows that the numerical results of the approximate formula given by (4.22) coincide well with the ones investigated calculating numerically the power absorption $P_k(\omega)$, except the slight deviations in the high temperature region for the anisotropy energy $\hbar K$ given by $K/\omega_z=1.0$, and deviate slightly from the results investigated calculating numerically the power absorption $P_k(\omega)$ in the high temperature region for the anisotropy energy $\hbar K$ given by $K/\omega_z=1.0$, and that the line half-width $\Delta\omega^{\mathtt{P}}_{\mathtt{R}k}$ increases as the temperature $T$ becomes high, and decreases slightly as the anisotropy energy $\hbar K$ becomes large.

We next investigate numerically the magnetiation-amplitude $A^{\mathtt{M}}_k(\omega)$ given by (3.34b) for the ferromagnetic spin system with the wave-number $k$. In Fig. 10, the magnetiation-amplitude $A^{\mathtt{M}}_k(\omega)$ given by (3.34b), scaled by $\hbar\gamma\,|H_k|/\omega_z$, are displayed varying the frequency $\omega$ scaled by $\omega_z$ from 1.0 to 7.0 for the cases of the wave-number $k=0, \pi/6, \pi/4, \pi/3, \pi/2$ and for the spin-magnitude $S=1$, the temperature $T$ and the anisotropy energy $\hbar K$ given by $k_{\mathtt{B}}T/(\hbar\omega_z)=1.0$ and $K/\omega_z=1.0$. Figure 10 shows that as the wave-number $k$ becomes large in the resonance region of the magnetiation-amplitude $A^{\mathtt{M}}_k(\omega)$, the resonance frequency and the peak-height (height of peak) increase and the line half–width decreases. In Fig. 11, the magnetiation-amplitude $A^{\mathtt{M}}_k(\omega)$ given by (3.34b), the results derived employing the relaxation method [17] in the van Hove limit [27] or in the narrowing limit [28], and the ones without the next higher-order parts $\chi^{(1)}_{S^+_k S^-_k}(\omega)$ in (3.34b), scaled by $\hbar\gamma\,|H_k|/\omega_z$, are displayed varying the frequency $\omega$ scaled by $\omega_z$ from 1.5 to 3.5

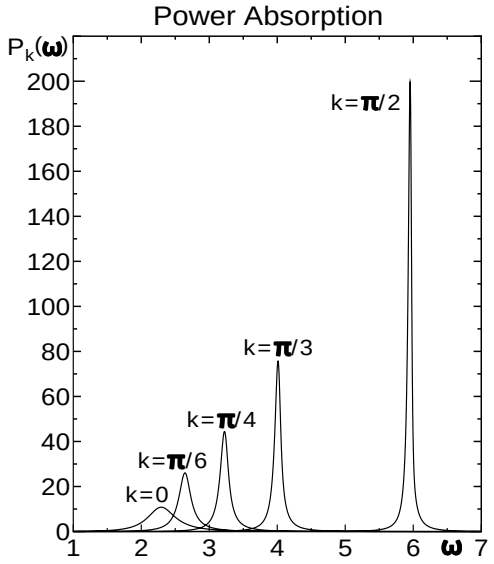


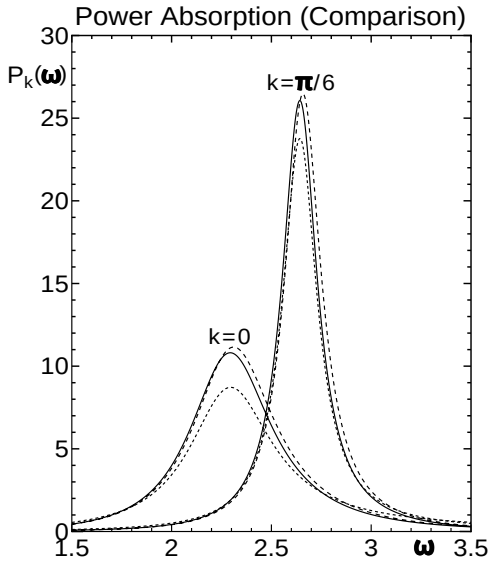


Figure 1: The power absorption $P_k(\omega)$ given by (3.29b) for the ferromagnetic spin system with the wave-number $k$, scaled by $\hbar\gamma^2\,|H_k|^2$, are displayed varying the frequency $\omega$ scaled by $\omega_z$ from 1.0 to 7.0 for the cases of the wave-number $k=0,\pi/6,\pi/4,\pi/3,\pi/2$ and for the spin-magnitude $S=1$, the temperature $T$ and the anisotropy energy $\hbar K$ given by $k_{\rm B}T/(\hbar\omega_z)=1.0$ and $K/\omega_z=1.0$. As the wave-number $k$ becomes large, the resonance frequency and the peak-height (height of peak) of the power absorption $P_k(\omega)$ increase and the line half–width decreases.

Figure 2: The power absorption $P_k(\omega)$ given by (3.29b) for the ferromagnetic spin system with the wave-number $k$, the results calculated by the relaxation method [17] in the van Hove limit [27] or in the narrowing limit [28], and the ones without the next higher-order parts $\chi^{(1)}_{S_k^+S_k^-}(\omega)''$ in (3.29b), scaled by $\hbar\gamma^2\,|H_k|^2$, are displayed varying the frequency $\omega$ scaled by $\omega_z$ from 1.5 to 3.5 for the cases of the wave-number $k=0,\pi/6$ and for the spin-magnitude $S=1$, the temperature $T$ and the anisotropy energy $\hbar K$ given by $k_{\rm B}T/(\hbar\omega_z)=1.0$ and $K/\omega_z=1.0$. The power absorption $P_k(\omega)$ given by (3.29b) are displayed by the solid lines, the results calculated by the relaxation method in the van Hove limit [27] or in the narrowing limit [28], are displayed by the dot lines, and the ones without the next higher-order parts $\chi^{(1)}_{S_k^+S_k^-}(\omega)''$ in (3.29b), are displayed by the short-dash lines.

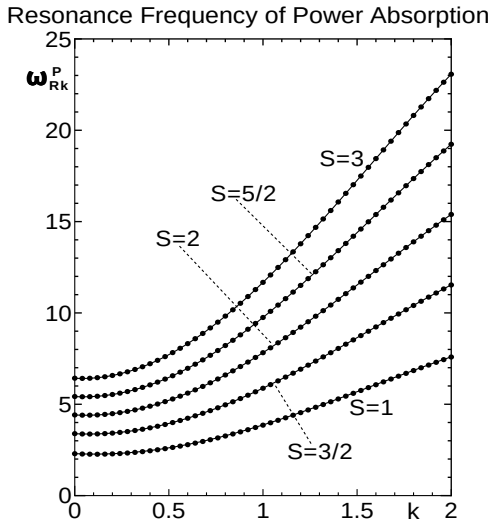


Figure 3: The approximate formula given by (3.30) for the resonance frequency $\omega^{\rm P}_{{\rm R}k}$ of the power absorption $P_k(\omega)$ with the wave-number $k$, and the resonance frequency $\omega^{\rm P}_{{\rm R}k}$ investigated calculating numerically the power absorption $P_k(\omega)$ without the next higher-order parts $\chi^{(1)}_{S_k^+S_k^-}(\omega)''$ in (3.29b), scaled by $\omega_z$, are displayed varying the wave-number $k$ from 0 to 2.0 for the cases of the spin-magnitude $S=1,3/2,2,5/2,3$ and for the temperature $T$ and the anisotropy energy $\hbar K$ given by $k_{\rm B}T/(\hbar\omega_z)=1.0$ and $K/\omega_z=1.0$. The approximate formula given by (3.30) are displayed by the solid lines, and the results investigated calculating numerically the power absorption $P_k(\omega)$ are displayed by the dots.

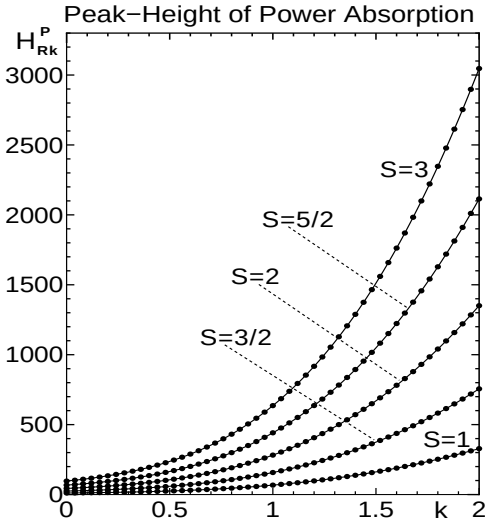


Figure 4: The approximate formula given by (4.16) for the peak-height $H^{\mathrm{P}}_{\mathrm{R}k}$ of the power absorption $P_k(\omega)$ with the wave-number $k$, and the peak-height $H^{\mathrm{P}}_{\mathrm{R}k}$ investigated calculating numerically the power absorption $P_k(\omega)$ without the next higher-order parts $\chi^{(1)}_{S^+_k S^-_k}(\omega)''$ in (3.29b), scaled by $\hbar\gamma^2\,|H_k|^2$, are displayed varying the wave-number $k$ from 0 to 2.0 for the cases of the spin-magnitude $S = 1, 3/2, 2, 5/2, 3$ and for the temperature $T$ and the anisotropy energy $\hbar K$ given by $k_{\mathrm{B}}T/(\hbar\omega_z) = 1.0$ and $K/\omega_z = 1.0$. The approximate formula given by (4.16) are displayed by the solid lines, and the results investigated calculating numerically the power absorption $P_k(\omega)$ are displayed by the dots.

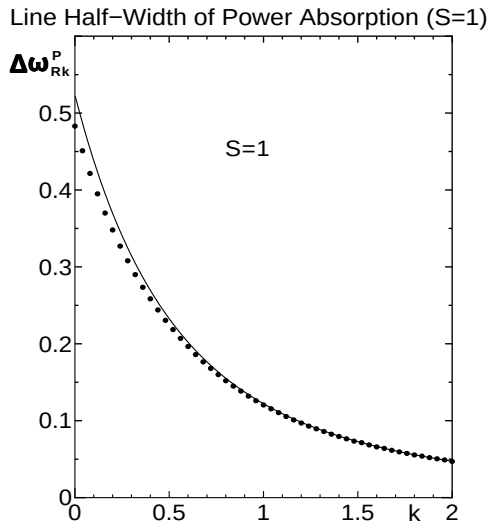


Figure 5: The approximate formula given by (4.22) for the line half-width $\Delta\omega^{\mathrm{P}}_{\mathrm{R}k}$ in the resonance region of the power absorption $P_k(\omega)$ with the wave-number $k$, and the line half-width $\Delta\omega^{\mathrm{P}}_{\mathrm{R}k}$ investigated calculating numerically the power absorption $P_k(\omega)$ without the next higher-order parts $\chi^{(1)}_{S^+_k S^-_k}(\omega)''$ in (3.29b), scaled by $\omega_z$, are displayed varying the wave-number $k$ from 0 to 2.0 for the case of the spin-magnitude $S = 1$ and for the temperature $T$ and the anisotropy energy $\hbar K$ given by $k_{\mathrm{B}}T/(\hbar\omega_z) = 1.0$ and $K/\omega_z = 1.0$. The approximate formula given by (4.22) are displayed by the solid lines, and the results investigated calculating numerically the power absorption $P_k(\omega)$ are displayed by the dots.

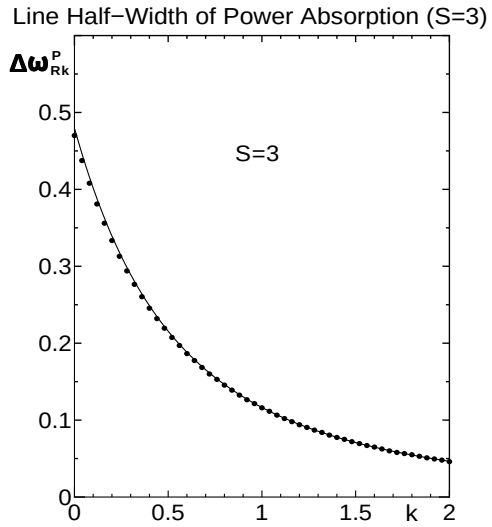


Figure 6: The approximate formula given by (4.22) for the line half-width $\Delta\omega^{\mathrm{P}}_{\mathrm{R}k}$ in the resonance region of the power absorption $P_k(\omega)$ with the wave-number $k$, and the line half-width $\Delta\omega^{\mathrm{P}}_{\mathrm{R}k}$ investigated calculating numerically the power absorption $P_k(\omega)$ without the next higher-order parts $\chi^{(1)}_{S^+_k S^-_k}(\omega)''$ in (3.29b), scaled by $\omega_z$, are displayed varying the wave-number $k$ from 0 to 2.0 for the case of the spin-magnitude $S = 3$ and for the temperature $T$ and the anisotropy energy $\hbar K$ given by $k_{\mathrm{B}}T/(\hbar\omega_z) = 1.0$ and $K/\omega_z = 1.0$. The approximate formula given by (4.22) are displayed by the solid lines, and the results investigated calculating numerically the power absorption $P_k(\omega)$ are displayed by the dots.

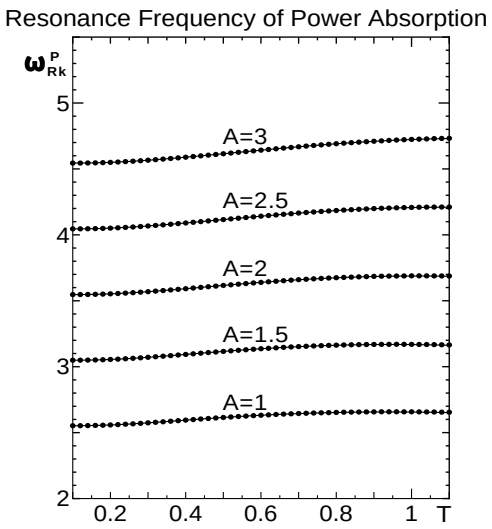


Figure 7: The approximate formula given by (3.30) for the resonance frequency $\omega^{\mathrm{P}}_{\mathrm{R}k}$ of the power absorption $P_k(\omega)$ with the wave-number $k$, and the resonance frequency $\omega^{\mathrm{P}}_{\mathrm{R}k}$ investigated calculating numerically the power absorption $P_k(\omega)$ without the next higher-order parts $\chi^{(1)}_{S^+_k S^-_k}(\omega)''$ in (3.29b), scaled by $\omega_z$, are displayed varying the temperature $T$ scaled by $(\hbar\omega_z)/k_{\mathrm{B}}$ from 0.1 to 1.1 for the cases of the anisotropy energy $\hbar K$ given by $K/\omega_z = 1.0, 1.5, 2.0, 2.5, 3.0$, and for the spin-magnitude $S=1$ and the wave-number $k=\pi/6$. The anisotropy energy is denoted as "$A$" $[=K/\omega_z]$ in the figures. The approximate formula given by (3.30) are displayed by the solid lines, and the results investigated calculating numerically the power absorption $P_k(\omega)$ are displayed by the dots.

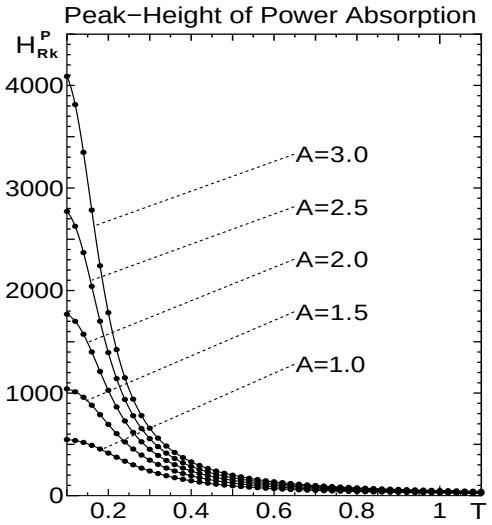


Figure 8: The approximate formula given by (4.16) for the peak-height $H^{\mathrm{P}}_{\mathrm{R}k}$ of the power absorption $P_k(\omega)$ with the wave-number $k$, and the peak-height $H^{\mathrm{P}}_{\mathrm{R}k}$ investigated calculating numerically the power absorption $P_k(\omega)$ without the next higher-order parts $\chi^{(1)}_{S^+_k S^-_k}(\omega)''$ in (3.29b), scaled by $\hbar\gamma^2\,|H_k|^2$, are displayed varying the temperature $T$ scaled by $(\hbar\omega_z)/k_{\mathrm{B}}$ from 0.1 to 1.1 for the cases of the anisotropy energy $\hbar K$ given by $K/\omega_z = 1.0, 1.5, 2.0, 2.5, 3.0$, and for the spin-magnitude $S=1$ and the wave-number $k=\pi/6$. The anisotropy energy is denoted as "$A$" $[=K/\omega_z]$ in the figures. The approximate formula given by (4.16) are displayed by the solid lines, and the results investigated calculating numerically the power absorption $P_k(\omega)$ are displayed by the dots.

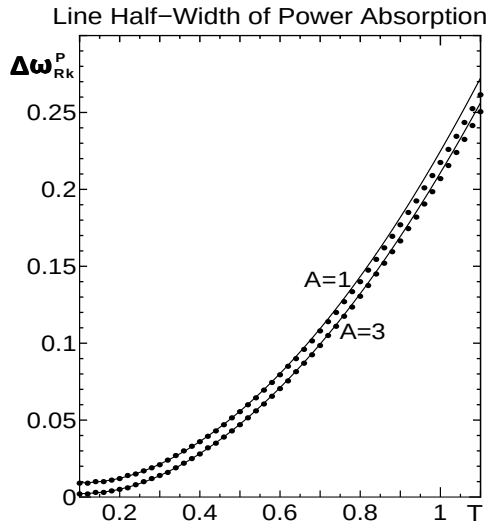


Figure 9: The approximate formula given by (4.22) for the line half-width $\Delta\omega^{\mathrm{P}}_{\mathrm{R}k}$ in the resonance region of the power absorption $P_k(\omega)$ with the wave-number $k$, and the line half-width $\Delta\omega^{\mathrm{P}}_{\mathrm{R}k}$ investigated calculating numerically the power absorption $P_k(\omega)$ without the next higher-order parts $\chi^{(1)}_{S^+_k S^-_k}(\omega)''$ in (3.29b), scaled by $\omega_z$, are displayed varying the temperature $T$ scaled by $(\hbar\omega_z)/k_{\mathrm{B}}$ from 0.1 to 1.1 for the cases of the anisotropy energy $\hbar K$ given by $K/\omega_z = 1.0, 3.0$, and for the spin-magnitude $S=1$ and the wave-number $k=\pi/6$. The anisotropy energy is denoted as "$A$" $[=K/\omega_z]$ in the figures. The approximate formula given by (4.22) are displayed by the solid lines, and the results investigated calculating numerically the power absorption $P_k(\omega)$ are displayed by the dots.

for the cases of the wave-number $k=0,\pi/6$ and for the spin-magnitude $S=1$, the temperature $T$ and the anisotropy energy $\hbar K$ given by $k_{\rm B}T/(\hbar\omega_z)=1.0$ and $K/\omega_z=1.0$. In Fig. 11, the magnetiation-amplitude $A_k^{\rm M}(\omega)$ given by (3.34b) are displayed by the solid lines, the results derived employing the relaxation method in the van Hove limit [27] or in the narrowing limit [28], are displayed by the dot lines, and the ones without the next higher-order parts $\chi^{(1)}_{S_k^+S_k^-}(\omega)$ in (3.34b), are displayed by the short-dash lines. The magnetiation-amplitude $A_k^{\rm M}(\omega)$ given by (3.34b), which have been derived employing the TCLE method, includes the effects of the interference terms in the TCLE method, i.e., "the interference effects", which represent the effects of the memory and initial correlation for the spin system and phonon reservoir [17], and are neglected in the results derived employing the relaxation method [17] in the van Hove limit [27] or in the narrowing limit [28]. Figure 11 shows that the interference effects produce the effects that increase the magnetiation-amplitude and cannot be disregarded for small wave-number $k$ in particular. Figure 11 also shows that the effects of the next higher-order parts $\chi^{(1)}_{S_k^+S_k^-}(\omega)''$ are small in (3.34b). We derive the approximate formula of the line half-width $\Delta\omega_{{\rm R}k}^{\rm M}$ in the resonance region of the magnetization-amplitude $A_k^{\rm M}(\omega)$ given by (3.34b) for the ferromagnetic spin system with the wave-number $k$, neglecting the next higher-order parts $\chi^{(1)}_{S_k^+S_k^-}(\omega)$ in the spin-wave approximation, because the effects of the next higher-order parts $\chi^{(1)}_{S_k^+S_k^-}(\omega)$ are small in (3.34b) as seen in Fig. 11. Neglecting the next higher-order parts in the spin-wave approximation, the approximate formula of the peak-height (height of peak) $H_{{\rm R}k}^{\rm M}$ in the resonance region of the magnetization-amplitude $A_k^{\rm M}(\omega)$ given by (3.34b) becomes

$$H_{{\rm R}k}^{\rm M} \cong S\,\hbar\,\gamma\,|H_k|\,\sqrt{(X_k'(\omega_{{\rm R}k}^{\rm M}))^2+(1+X_k''(\omega_{{\rm R}k}^{\rm M}))^2}\,/(\Phi_k'+\Psi_k). \tag{4.23}$$

In order to obtain the approximate formula of the line half-width $\Delta\omega_{{\rm R}k}^{\rm M}$ in the resonance region of the magnetization-amplitude $A_k^{\rm M}(\omega)$, we put as $\Delta\omega_{{\rm R}k}^{\rm M}/2=(\Phi_k'+\Psi_k)\,y_1$ for the first-step approximation of $\Delta\omega_{{\rm R}k}^{\rm M}$, which satisfies

$$\frac{1}{2}H_{{\rm R}k}^{\rm M} \cong S\,\hbar\,\gamma\,|H_k|\,\frac{\sqrt{(X_k'(\omega_{{\rm R}k}^{\rm M}))^2+(1+X_k''(\omega_{{\rm R}k}^{\rm M}))^2}}{2\,(\Phi_k'+\Psi_k)} \cong S\,\hbar\,\gamma\,|H_k|\,\sqrt{\frac{(X_k'(\omega_{{\rm R}k}^{\rm M}))^2+(1+X_k''(\omega_{{\rm R}k}^{\rm M}))^2}{(\Phi_k'+\Psi_k)^2\,(y_1^2+1)}}, \tag{4.24}$$

where we have approximated $X_k(\omega_{{\rm R}k}^{\rm M}+(\Phi_k'+\Psi_k)\,y_1)$ with $X_k(\omega_{{\rm R}k}^{\rm M})$ in the right-hand side of the above equation. Equation (4.24) gives the positive solution as

$$y_1^2+1\cong 4, \qquad\qquad y_1\cong\sqrt{3}, \tag{4.25}$$

which leads the first-step approximation of $\Delta\omega_{{\rm R}k}^{\rm M}$ as

$$2\,(\Phi_k'+\Psi_k)\,y_1 \cong 2\,\sqrt{3}\,(\Phi_k'+\Psi_k). \tag{4.26}$$

Then, by putting as $\Delta\omega_{{\rm R}k}^{\rm M}/2=(\Phi_k'+\Psi_k)\,y$, the approximate formula of the line half-width $\Delta\omega_{{\rm R}k}^{\rm M}$ in the resonance region of the magnetization-amplitude $A_k^{\rm M}(\omega)$, can be derived from the equation

$$\begin{aligned} &S\,\hbar\,\gamma\,|H_k|\,\frac{\sqrt{(X_k'(\omega_{{\rm R}k}^{\rm M}))^2+(1+X_k''(\omega_{{\rm R}k}^{\rm M}))^2}}{2\,(\Phi_k'+\Psi_k)} \\ &\qquad\cong S\,\hbar\,\gamma\,|H_k|\,\sqrt{\frac{(X_k'(\omega_{{\rm R}k}^{\rm M}+\sqrt{3}\,(\Phi_k'+\Psi_k)))^2+(1+X_k''(\omega_{{\rm R}k}^{\rm M}+\sqrt{3}\,(\Phi_k'+\Psi_k)))^2}{(\Phi_k'+\Psi_k)^2\,(y^2+1)}}\,, \end{aligned} \tag{4.27}$$

which can be rewritten as

$$y^2+1\cong 4\,\frac{(X_k'(\omega_{{\rm R}k}^{\rm M}+\sqrt{3}\,(\Phi_k'+\Psi_k)))^2+(1+X_k''(\omega_{{\rm R}k}^{\rm M}+\sqrt{3}\,(\Phi_k'+\Psi_k)))^2}{(X_k'(\omega_{{\rm R}k}^{\rm M}))^2+(1+X_k''(\omega_{{\rm R}k}^{\rm M}))^2}. \tag{4.28}$$

By obtaining the positive solution of the above second-order equation for $y$, the approximate formula of the line half–width $\Delta\omega_{{\rm R}k}^{\rm M}$ in the resonance region of the magnetization-amplitude $A_k^{\rm M}(\omega)$ can be obtained as

$$\Delta\omega_{{\rm R}k}^{\rm M} \cong 2\,(\Phi_k'+\Psi_k)\,\sqrt{4\,\frac{\{X_k'(\omega_{{\rm R}k}^{\rm M}+\sqrt{3}\,(\Phi_k'+\Psi_k))\}^2+\{1+X_k''(\omega_{{\rm R}k}^{\rm M}+\sqrt{3}\,(\Phi_k'+\Psi_k))\}^2}{\{X_k'(\omega_{{\rm R}k}^{\rm M})\}^2+\{1+X_k''(\omega_{{\rm R}k}^{\rm M})\}^2}-1}\,. \tag{4.29}$$

In Fig. 12, the approximate formula given by (3.36) for the resonance frequency $\omega_{{\rm R}k}^{\rm M}$ of the magnetization-amplitude $A_k^{\rm M}(\omega)$ with the wave-number $k$, and the resonance frequency $\omega_{{\rm R}k}^{\rm M}$ investigated calculating numerically the magnetization-amplitude $A_k^{\rm M}(\omega)$ without the next higher-order parts $\chi^{(1)}_{S_k^+S_k^-}(\omega)$ in (3.34b), scaled by $\omega_z$, are displayed varying the wave-number $k$ from 0 to 2.0 for the cases of the spin-magnitude $S=1,3/2,2,5/2,3$ and for the temperature $T$ and the anisotropy energy $\hbar K$ given by $k_{\rm B}T/(\hbar\omega_z)=1.0$ and $K/\omega_z=1.0$. In Fig. 12, the approximate formula given by (3.36) are displayed by the solid lines, and the results investigated calculating numerically the magnetization-amplitude

$A_k^{\mathtt{M}}(\omega)$ are displayed by the dots. Figure 12 shows that the numerical results of the approximate formula given by (3.36) coincide well with the ones investigated calculating numerically the magnetization-amplitude $A_k^{\mathtt{M}}(\omega)$, and that the resonance frequency $\omega_{\mathtt{R}k}^{\mathtt{M}}$ becomes large as the spin-magnitude $S$ becomes large or the wave-number $k$ becomes large. In Fig. 13, the approximate formula given by (4.23) for the peak-height $H_{\mathtt{R}k}^{\mathtt{M}}$ of the magnetization-amplitude $A_k^{\mathtt{M}}(\omega)$ with the wave-number $k$, and the peak-height $H_{\mathtt{R}k}^{\mathtt{M}}$ investigated calculating numerically the magnetization-amplitude $A_k^{\mathtt{M}}(\omega)$ without the next higher-order parts $\chi^{(1)}_{S_k^+S_k^-}(\omega)$ in (3.34b), scaled by $\hbar\gamma\,|H_k|/\omega_z$, are displayed varying the wave-number $k$ from 0 to 2.0 for the cases of the spin-magnitude $S=1, 3/2, 2, 5/2, 3$ and for the temperature $T$ and the anisotropy energy $\hbar K$ given by $k_{\mathtt{B}}T/(\hbar\omega_z)=1.0$ and $K/\omega_z=1.0$. In Fig. 13, the approximate formula given by (4.23) are displayed by the solid lines, and the results investigated calculating numerically the magnetization-amplitude $A_k^{\mathtt{M}}(\omega)$ are displayed by the dots. Figure 13 shows that the numerical results of the approximate formula given by (4.23) coincide well with the ones investigated calculating numerically the magnetization-amplitude $A_k^{\mathtt{M}}(\omega)$, and that the peak-height $H_{\mathtt{R}k}^{\mathtt{M}}$ becomes large as the spin-magnitude $S$ becomes large or the wave-number $k$ becomes large. In Fig. 14, the approximate formula given by (4.29) for the line half-width $\Delta\omega_{\mathtt{R}k}^{\mathtt{M}}$ in the resonance region of the magnetization-amplitude $A_k^{\mathtt{M}}(\omega)$ with the wave-number $k$, and the line half-width $\Delta\omega_{\mathtt{R}k}^{\mathtt{M}}$ investigated calculating numerically the magnetization-amplitude $A_k^{\mathtt{M}}(\omega)$ without the next higher-order parts $\chi^{(1)}_{S_k^+S_k^-}(\omega)$ in (3.34b), scaled by $\omega_z$, are displayed varying the wave-number $k$ from 0 to 2.0 for the case of the spin-magnitudes $S=1, 3$ and for the temperature $T$ and the anisotropy energy $\hbar K$ given by $k_{\mathtt{B}}T/(\hbar\omega_z)=1.0$ and $K/\omega_z=1.0$. In Fig. 14, the approximate formula given by (4.29) are displayed by the solid lines, and the results investigated calculating numerically the magnetization-amplitude $A_k^{\mathtt{M}}(\omega)$ are displayed by the dots. Figure 14 shows that the numerical results of the approximate formula given by (4.29) coincide well with the ones investigated calculating numerically the magnetization-amplitude $A_k^{\mathtt{M}}(\omega)$, and that the line half-width $\Delta\omega_{\mathtt{R}k}^{\mathtt{M}}$ in the resonance region of the magnetization-amplitude $A_k^{\mathtt{M}}(\omega)$ with the wave-number $k$ decreases as the wave-number $k$ becomes large, and decreases slightly as the spin-magnitude $S$ becomes large. In Fig.15, the approximate formula given by (3.36) for the resonance frequency $\omega_{\mathtt{R}k}^{\mathtt{M}}$ of the magnetization-amplitude $A_k^{\mathtt{M}}(\omega)$ with the wave-number $k$, and the resonance frequency $\omega_{\mathtt{R}k}^{\mathtt{M}}$ investigated calculating numerically the magnetization-amplitude $A_k^{\mathtt{M}}(\omega)$ without the next higher-order parts $\chi^{(1)}_{S_k^+S_k^-}(\omega)$ in (3.34b), scaled by $\omega_z$, are displayed varying the temperature $T$ scaled by $(\hbar\omega_z)/k_{\mathtt{B}}$ from 0.1 to 1.1 for the cases of the anisotropy energy $\hbar K$ given by $K/\omega_z=1.0, 2.0, 3.0, 4.0, 5.0$, and for the spin-magnitude $S=1$ and the wave-number $k=\pi/6$. The anisotropy energy is denoted as "$A$" $[=K/\omega_z]$ in the figures. In Fig.15, the approximate formula given by (3.36) are displayed by the solid lines, and the results investigated calculating numerically the magnetization-amplitude $A_k^{\mathtt{M}}(\omega)$ are displayed by the dots. Figure 15 shows that the numerical results of the approximate formula given by (3.36) coincide well with the ones investigated calculating numerically the magnetization-amplitude $A_k^{\mathtt{M}}(\omega)$, and that the resonance frequency $\omega_{\mathtt{R}k}^{\mathtt{M}}$ becomes large as the anisotropy energy $\hbar K$ becomes large, and becomes large slightly as the temperature $T$ becomes high. In Fig.16, the approximate formula given by (4.23) for the peak-height $H_{\mathtt{R}k}^{\mathtt{M}}$ of the magnetization-amplitude $A_k^{\mathtt{M}}(\omega)$ with the wave-number $k$, and the peak-height $H_{\mathtt{R}k}^{\mathtt{P}}$ investigated calculating numerically the magnetization-amplitude $A_k^{\mathtt{M}}(\omega)$ without the next higher-order parts $\chi^{(1)}_{S_k^+S_k^-}(\omega)$ in (3.34b), scaled by $\hbar\gamma\,|H_k|/\omega_z$, are displayed varying the temperature $T$ scaled by $(\hbar\omega_z)/k_{\mathtt{B}}$ from 0.1 to 1.1 for the cases of the anisotropy energy $\hbar K$ given by $K/\omega_z=1.0, 2.0, 3.0, 4.0, 5.0$, and for the spin-magnitude $S=1$ and the wave-number $k=\pi/6$. The anisotropy energy is denoted as "$A$" $[=K/\omega_z]$ in the figures. In Fig.16, the approximate formula given by (4.23) are displayed by the solid lines, and the results investigated calculating numerically the magnetization-amplitude $A_k^{\mathtt{M}}(\omega)$ are displayed by the dots. Figure 16 shows that the numerical results of the approximate formula given by (4.23) coincide well with the ones investigated calculating numerically the magnetization-amplitude $A_k^{\mathtt{M}}(\omega)$, and that the peak-height $H_{\mathtt{R}k}^{\mathtt{M}}$ becomes large as the anisotropy energy $\hbar K$ becomes large, and becomes small as the temperature $T$ becomes high. In Fig.17, the approximate formula given by (4.29) for the line half-width $\Delta\omega_{\mathtt{R}k}^{\mathtt{M}}$ in the resonance region of the magnetization-amplitude $A_k^{\mathtt{M}}(\omega)$ with the wave-number $k$, and the line half-width $\Delta\omega_{\mathtt{R}k}^{\mathtt{M}}$ investigated calculating numerically the magnetization-amplitude $A_k^{\mathtt{M}}(\omega)$ without the next higher-order parts $\chi^{(1)}_{S_k^+S_k^-}(\omega)$ in (3.34b), scaled by $\omega_z$, are displayed varying the temperature $T$ scaled by $(\hbar\omega_z)/k_{\mathtt{B}}$ from 0.1 to 1.1 for the cases of the anisotropy energy $\hbar K$ given by $K/\omega_z=1.0, 5.0$, and for the spin-magnitude $S=1$ and the wave-number $k=\pi/6$. The anisotropy energy is denoted as "$A$" $[=K/\omega_z]$ in the figures. In Fig.17, the approximate formula given by (4.29) are displayed by the solid lines, and the results investigated calculating numerically the magnetization-amplitude $A_k^{\mathtt{M}}(\omega)$ are displayed by the dots. Figure 17 shows that the numerical results of the approximate formula given by (4.29) coincide well with the ones investigated calculating numerically the magnetization-amplitude $A_k^{\mathtt{M}}(\omega)$, and that the line half-width $\Delta\omega_{\mathtt{R}k}^{\mathtt{M}}$ in the resonance region of the magnetization-amplitude $A_k^{\mathtt{M}}(\omega)$ with the wave-number $k$ increases as the temperature $T$ becomes high, and decreases slightly as the anisotropy energy $\hbar K$ becomes large. Each peak of the line shapes of magnetization-amplitude has the hemline longer than those of the power absorption as seen in Figs. 1, 2, 10 and 11. Also, the line half-widths in the resonance region of the magnetization-amplitude are larger than those of the power absorption as seen in Figs. 5, 6, 9, 14 and 17.

In the last of this section, we investigate numerically the interference effects, i.e., the effects of the memory and initial correlation for the ferromagnetic spin system and phonon reservoir, in further detail. Those effects are represented by the interference terms in the TCLE method [17], are the effects of deviation from the van Hove limit [27] or the

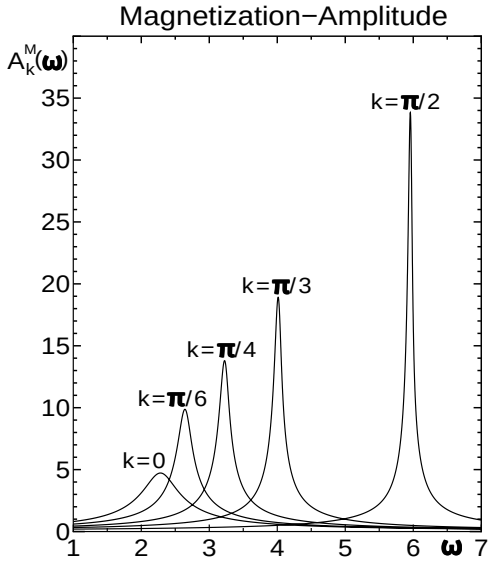


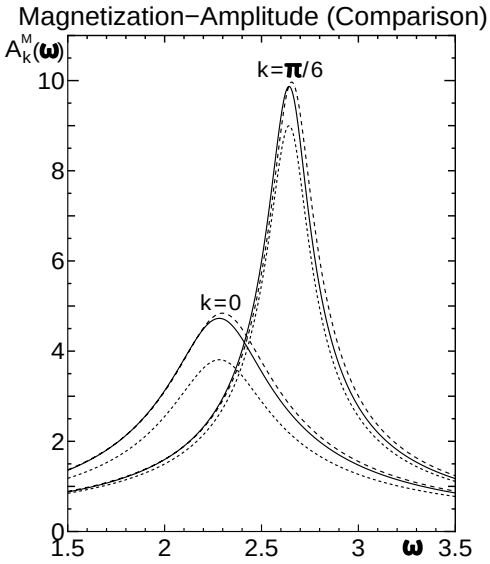


Figure 10: The magnetization-amplitude $A^{\mathtt{M}}_{k}(\omega)$ given by (3.34b) for the ferromagnetic spin system with the wave-number $k$, scaled by $\hbar\gamma\,|H_k|/\omega_z$, are displayed varying the frequency $\omega$ scaled by $\omega_z$ from 1.0 to 7.0 for the cases of the wave-number $k=0,\pi/6,\pi/4,\pi/3,\pi/2$ and for the spin-magnitude $S=1$, the temperature $T$ and the anisotropy energy $\hbar K$ given by $k_{\mathtt{B}}T/(\hbar\omega_z)=1.0$ and $K/\omega_z=1.0$. As the wave-number $k$ becomes large, the resonance frequency and the peak-height (height of peak) of the magnetization-amplitude $A^{\mathtt{M}}_{k}(\omega)$ increase and the line half–width decreases.

Figure 11: The magnetization-amplitude $A^{\mathtt{M}}_{k}(\omega)$ given by (3.34b) for the ferromagnetic spin system with the wave-number $k$, the results calculated by the relaxation method [17] in the van Hove limit [27] or in the narrowing limit [28], and the ones without the next higher-order parts $\chi^{(1)}_{S^+_k S^-_k}(\omega)$ in (3.34b), scaled by $\hbar\gamma\,|H_k|/\omega_z$, are displayed varying the frequency $\omega$ scaled by $\omega_z$ from 1.5 to 3.5 for the cases of the wave-number $k=0,\pi/6$ and for the spin-magnitude $S=1$, the temperature $T$ and the anisotropy energy $\hbar K$ given by $k_{\mathtt{B}}T/(\hbar\omega_z)=1.0$ and $K/\omega_z=1.0$. The magnetization-amplitude $A^{\mathtt{M}}_{k}(\omega)$ given by (3.34b) are displayed by the solid lines, the results calculated by the relaxation method in the van Hove limit [27] or in the narrowing limit [28], are displayed by the dot lines, and the ones without the next higher-order parts $\chi^{(1)}_{S^+_k S^-_k}(\omega)$ in (3.34b), are displayed by the short-dash lines.

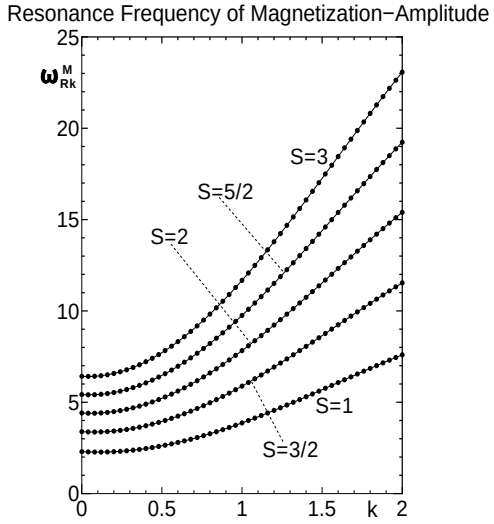


Figure 12: The approximate formula given by (3.36) for the resonance frequency $\omega^{\mathtt{M}}_{\mathtt{R}k}$ of the magnetization-amplitude $A^{\mathtt{M}}_{k}(\omega)$ with the wave-number $k$, and the resonance frequency $\omega^{\mathtt{M}}_{\mathtt{R}k}$ investigated calculating numerically the magnetization-amplitude $A^{\mathtt{M}}_{k}(\omega)$ without the next higher-order parts $\chi^{(1)}_{S^+_k S^-_k}(\omega)$ in (3.34b), scaled by $\omega_z$, are displayed varying the wave-number $k$ from 0 to 2.0 for the cases of the spin-magnitude $S=1,3/2,2,5/2,3$ and for the temperature $T$ and the anisotropy energy $\hbar K$ given by $k_{\mathtt{B}}T/(\hbar\omega_z)=1.0$ and $K/\omega_z=1.0$. The approximate formula given by (3.36) are displayed by the solid lines, and the results investigated calculating numerically the magnetization-amplitude $A^{\mathtt{M}}_{k}(\omega)$ are displayed by the dots.

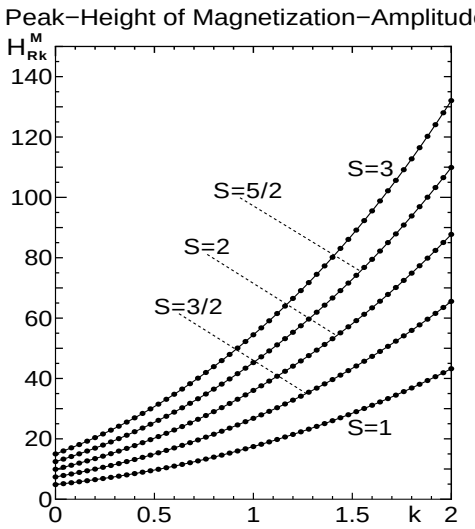


Figure 13: The approximate formula given by (4.23) for the peak-height $H^{\mathtt{M}}_{\mathtt{R}k}$ of the magnetization-amplitude $A^{\mathtt{M}}_{k}(\omega)$ with the wave-number $k$, and the peak-height $H^{\mathtt{M}}_{\mathtt{R}k}$ investigated calculating numerically the magnetization-amplitude $A^{\mathtt{M}}_{k}(\omega)$ without the next higher-order parts $\chi^{(1)}_{S^+_k S^-_k}(\omega)$ in (3.34b), scaled by $\hbar\gamma\,|H_k|/\omega_z$, are displayed varying the wave-number $k$ from 0 to 2.0 for the cases of the spin-magnitude $S = 1, 3/2, 2, 5/2, 3$ and for the temperature $T$ and the anisotropy energy $\hbar K$ given by $k_{\mathtt{B}}T/(\hbar\omega_z) = 1.0$ and $K/\omega_z = 1.0$. The approximate formula given by (4.23) are displayed by the solid lines, and the results investigated calculating numerically the magnetization-amplitude $A^{\mathtt{M}}_{k}(\omega)$ are displayed by the dots.

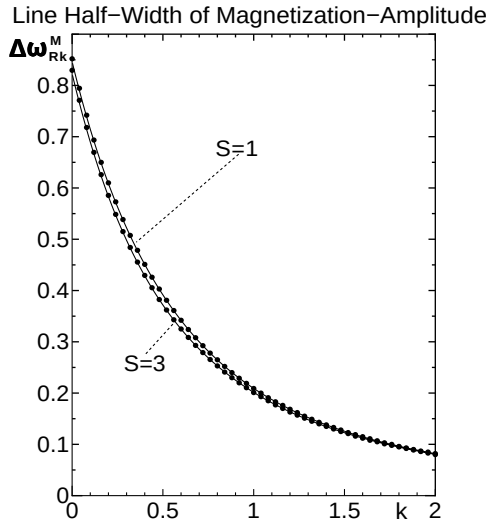


Figure 14: The approximate formula given by (4.29) for the line half-width $\Delta\omega^{\mathtt{M}}_{\mathtt{R}k}$ in the resonance region of the magnetization-amplitude $A^{\mathtt{M}}_{k}(\omega)$ with the wave-number $k$, and the line half-width $\Delta\omega^{\mathtt{M}}_{\mathtt{R}k}$ investigated calculating numerically the magnetization-amplitude $A^{\mathtt{M}}_{k}(\omega)$ without the next higher-order parts $\chi^{(1)}_{S^+_k S^-_k}(\omega)$ in (3.34b), scaled by $\omega_z$, are displayed varying the wave-number $k$ from 0 to 2.0 for the case of the spin-magnitudes $S = 1, 3$ and for the temperature $T$ and the anisotropy energy $\hbar K$ given by $k_{\mathtt{B}}T/(\hbar\omega_z) = 1.0$ and $K/\omega_z = 1.0$. The approximate formula given by (4.29) are displayed by the solid lines, and the results investigated calculating numerically the magnetization-amplitude $A^{\mathtt{M}}_{k}(\omega)$ are displayed by the dots.

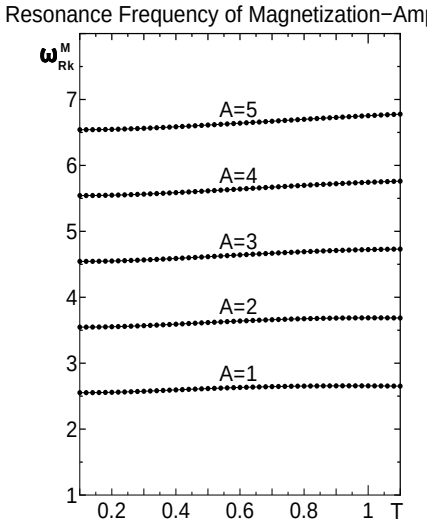


Figure 15: The approximate formula given by (3.36) for the resonance frequency $\omega^{\mathtt{M}}_{\mathtt{R}k}$ of the magnetization-amplitude $A^{\mathtt{M}}_{k}(\omega)$ with the wave-number $k$, and the resonance frequency $\omega^{\mathtt{M}}_{\mathtt{R}k}$ investigated calculating numerically the magnetization-amplitude $A^{\mathtt{M}}_{k}(\omega)$ without the next higher-order parts $\chi^{(1)}_{S^+_k S^-_k}(\omega)$ in (3.34b), scaled by $\omega_z$, are displayed varying the temperature $T$ scaled by $(\hbar\omega_z)/k_{\mathtt{B}}$ from 0.1 to 1.1 for the cases of the anisotropy energy $\hbar K$ given by $K/\omega_z = 1.0, 2.0, 3.0, 4.0, 5.0$, and for the spin-magnitude $S = 1$ and the wave-number $k = \pi/6$. The anisotropy energy is denoted as "$A$" $[= K/\omega_z]$ in the figures. The approximate formula given by (3.36) are displayed by the solid lines, and the results investigated calculating numerically the magnetization-amplitude $A^{\mathtt{M}}_{k}(\omega)$ are displayed by the dots.

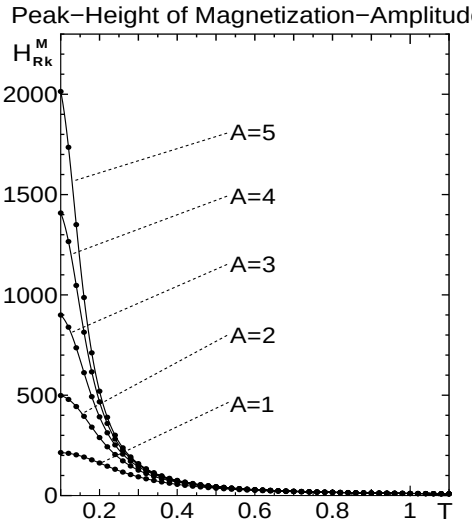


Figure 16: The approximate formula given by (4.23) for the peak-height $H^{\mathtt{M}}_{\mathtt{R}k}$ of the magnetization-amplitude $A^{\mathtt{M}}_k(\omega)$ with the wave-number $k$, and the peak-height $H^{\mathtt{P}}_{\mathtt{R}k}$ investigated calculating numerically the magnetization-amplitude $A^{\mathtt{M}}_k(\omega)$ without the next higher-order parts $\chi^{(1)}_{S^+_k S^-_k}(\omega)$ in (3.34b), scaled by $\hbar\gamma\,|H_k|/\omega_z$, are displayed varying the temperature $T$ scaled by $(\hbar\omega_z)/k_{\mathtt{B}}$ from 0.1 to 1.1 for the cases of the anisotropy energy $\hbar K$ given by $K/\omega_z = 1.0, 2.0, 3.0, 4.0, 5.0$, and for the spin-magnitude $S=1$ and the wave-number $k=\pi/6$. The anisotropy energy is denoted as "$A$" $[=K/\omega_z]$ in the figures. The approximate formula given by (4.23) are displayed by the solid lines, and the results investigated calculating numerically the magnetization-amplitude $A^{\mathtt{M}}_k(\omega)$ are displayed by the dots.

narrowing limit [28], and produce the effects that increase the the power absorption and magnetization-amplitude in the resonance region and cannot be disregarded, as seen in Figs. 2 and 11. In Fig. 18, the approximation of the rate $(H^{\mathtt{P}}_{\mathtt{R}k} - H^{\mathtt{Prv}}_{\mathtt{R}k})/H^{\mathtt{P}}_{\mathtt{R}k}$ of the interference effects $(H^{\mathtt{P}}_{\mathtt{R}k} - H^{\mathtt{Prv}}_{\mathtt{R}k})$ for the peak-height $H^{\mathtt{P}}_{\mathtt{R}k}$ of the power absorption $P_k(\omega)$ with the wave-number $k$, are displayed varying the temperature $T$ scaled by $\hbar\omega_z/k_{\mathtt{B}}$ from 0.2 to 1.5 for the cases of spin-magnitudes $S=1,3$, and for the anisotropy energy $\hbar K$ given by $K/\omega_z = 2.0$, the wave-number $k=0$ and the daming constant $\gamma_{\mathtt{R}k}$ given by $\gamma_{\mathtt{R}k}/\omega_z = 0.5$. Here, the approximation for the peak-height $H^{\mathtt{P}}_{\mathtt{R}k}$ is the approximate formula given by (4.16), and the approximation formula for the peak-height $H^{\mathtt{Prv}}_{\mathtt{R}k}$, which is the one without the interference terms in the peak-height $H^{\mathtt{P}}_{\mathtt{R}k}$ of the power absorption $P_k(\omega)$ with the wave-number $k$, is given by

$$H^{\mathtt{Prv}}_{\mathtt{R}k} \cong S\,\gamma^2\,|H_k|^2\,\hbar\,\omega^{\mathtt{P}}_{\mathtt{R}k}\,/(\Phi'_k + \Psi_k). \tag{4.30}$$

In Fig. 19, the approximation of the rate $(H^{\mathtt{M}}_{\mathtt{R}k} - H^{\mathtt{Mrv}}_{\mathtt{R}k})/H^{\mathtt{M}}_{\mathtt{R}k}$ of the interference effects $(H^{\mathtt{M}}_{\mathtt{R}k} - H^{\mathtt{Mrv}}_{\mathtt{R}k})$ for the peak-height $H^{\mathtt{M}}_{\mathtt{R}k}$ of the magnetization-amplitudes $A^{\mathtt{M}}_k(\omega)$ with the wave-number $k$, are displayed varying the temperature $T$ scaled by $\hbar\omega_z/k_{\mathtt{B}}$ from 0.2 to 1.5 for the cases of spin-magnitudes $S=1,3$, and for the anisotropy energy $\hbar K$ given by $K/\omega_z = 2.0$, the wave-number $k=0$ and the daming constant $\gamma_{\mathtt{R}k}$ given by $\gamma_{\mathtt{R}k}/\omega_z = 0.5$. Here, the approximation for the peak-height $H^{\mathtt{M}}_{\mathtt{R}k}$ is the approximate formula given by (4.23), and the approximation formula for the peak-height $H^{\mathtt{Mrv}}_{\mathtt{R}k}$, which is the one without the interference terms in the peak-height $H^{\mathtt{M}}_{\mathtt{R}k}$ of the magnetization-amplitudes $A^{\mathtt{M}}_k(\omega)$ with the wave-number $k$, is given by

$$H^{\mathtt{Mrv}}_{\mathtt{R}k} \cong S\,\hbar\,\gamma\,|H_k|\,/(\Phi'_k + \Psi_k). \tag{4.31}$$

Figures 18 and 19 show in the resonance region that as the temperature $T$ becomes high, the interference effects for

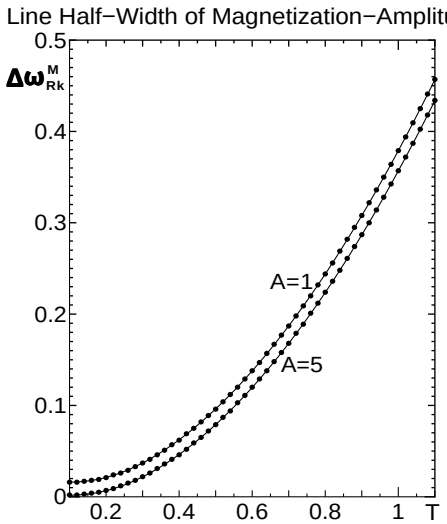


Figure 17: The approximate formula given by (4.29) for the line half-width $\Delta\omega^{\mathtt{M}}_{\mathtt{R}k}$ in the resonance region of the magnetization-amplitude $A^{\mathtt{M}}_k(\omega)$ with the wave-number $k$, and the line half-width $\Delta\omega^{\mathtt{M}}_{\mathtt{R}k}$ investigated calculating the magnetization-amplitude $A^{\mathtt{M}}_k(\omega)$ without the next higher-order parts $\chi^{(1)}_{S^+_k S^-_k}(\omega)$ in (3.34b) numerically, scaled by $\omega_z$, are displayed varying the temperature $T$ scaled by $(\hbar\omega_z)/k_{\mathtt{B}}$ from 0.1 to 1.1 for the cases of the anisotropy energy $\hbar K$ given by $K/\omega_z = 1.0, 5.0$, and for the spin-magnitude $S=1$ and the wave-number $k=\pi/6$. The anisotropy energy is denoted as "$A$" $[=K/\omega_z]$ in the figures. The approximate formula given by (4.29) are displayed by the solid lines, and the results investigated calculating the magnetization-amplitude $A^{\mathtt{M}}_k(\omega)$ numerically are displayed by the dots.

the power absorption $P_k(\omega)$ and the magnetization-amplitudes $A^{\mathtt{M}}_k(\omega)$ become large, and that as the spin-magnitude $S$ becomes large, those effects become large slightly in the in the low temperature region. In Fig. 20, the approximation of the rate $(H^{\mathtt{P}}_{\mathtt{R}k} - H^{\mathtt{Prv}}_{\mathtt{R}k})/H^{\mathtt{P}}_{\mathtt{R}k}$ of the interference effects $(H^{\mathtt{P}}_{\mathtt{R}k} - H^{\mathtt{Prv}}_{\mathtt{R}k})$ for the peak-height $H^{\mathtt{P}}_{\mathtt{R}k}$ of the power absorption $P_k(\omega)$ with the wave-number $k$, are displayed varying the daming constant $\gamma_{\mathtt{R}k}$ of the phonon reservoir, scaled by

$\omega_z$, from 0.5 to 3.5 for the cases of the wave numbers $k=0,\pi/6,\pi/4,\pi/3,\pi/2$, and for the spin-magnitude $S=1$, the temperature $T$ given by $k_{\rm B}T/(\hbar\omega_z)=1.0$ and the anisotropy energy $\hbar K$ given by $K/\omega_z=1.0$. Here, the approximation for the peak-height $H^{\rm P}_{{\rm R}k}$ is the approximate formula given by (4.16), and the approximation formula for the peak-height $H^{\rm Prv}_{{\rm R}k}$, which is the one without the interference terms in the peak-height $H^{\rm P}_{{\rm R}k}$ of the power absorption $P_k(\omega)$, is given by (4.30). In Fig. 21, the approximation of the rate $(H^{\rm M}_{{\rm R}k}-H^{\rm Mrv}_{{\rm R}k})/H^{\rm M}_{{\rm R}k}$ of the interference effects $(H^{\rm M}_{{\rm R}k}-H^{\rm Mrv}_{{\rm R}k})$ for the peak-height $H^{\rm M}_{{\rm R}k}$ of the magnetization-amplitudes $A^{\rm M}_k(\omega)$ with the wave-number $k$, are displayed varying the daming constant $\gamma_{{\rm R}k}$ of the phonon reservoir, scaled by $\omega_z$, from 0.5 to 3.5 for the cases of wave numbers $k=0,\pi/6,\pi/4,\pi/3,\pi/2$, and for the spin-magnitudes $S=1$, the temperature $T$ given by $k_{\rm B}T/(\hbar\omega_z)=1.0$ and the anisotropy energy $\hbar K$ given by $K/\omega_z=1.0$. Here, the approximation for the peak-height $H^{\rm M}_{{\rm R}k}$ is the approximate formula given by (4.23), and the approximation formula for the peak-height $H^{\rm Mrv}_{{\rm R}k}$, which is the one without the interference terms in the peak-height $H^{\rm M}_{{\rm R}k}$ of the magnetization-amplitudes $A^{\rm M}_k(\omega)$, is given by (4.31). Figures 20 and 21 show in the resonance region that as the damping constant $\gamma_{{\rm R}k}$ of the phonon reservoir becomes small, the interference effects for the power absorption $P_k(\omega)$ and the magnetization-amplitudes $A^{\rm M}_k(\omega)$ become large, and also that as the wave number $k$ becomes small, those effects become large in the small damping-constant region. As the damping constant $\gamma_{{\rm R}k}$, which is equal to the inverse of the correlation time $\tau_c$ of the phonon reservoir, become small, the phonon reservoir is damped slowly, and the interference effects become large as the phonon reservoir is damped slowly. Thus, the interference effects produce effects that cannot be disregarded for the high temperature, for the non-quickly damped reservoir or for the small wave-number.

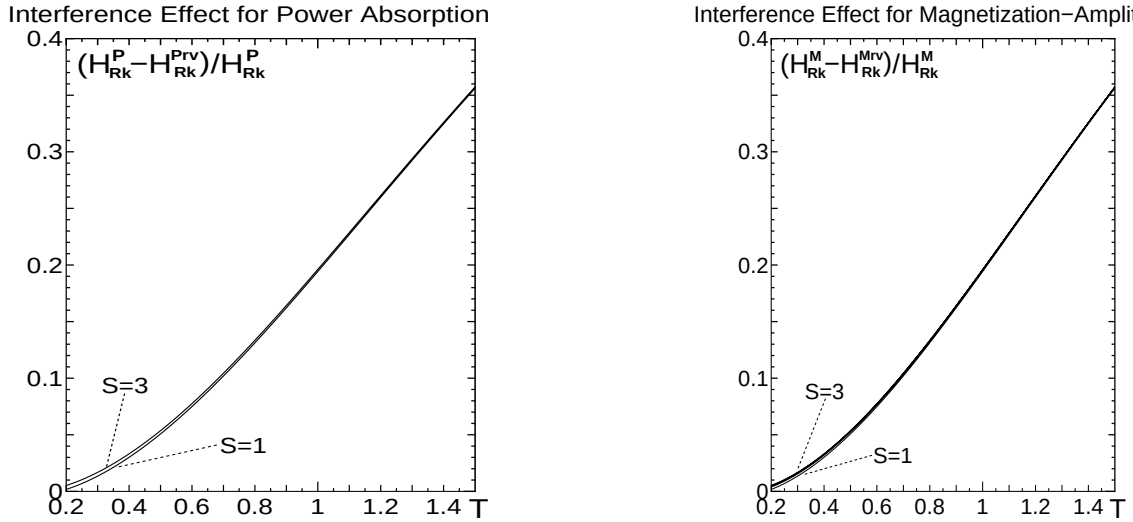


Figure 18: The approximation of the rate $(H^{\rm P}_{{\rm R}k}-H^{\rm Prv}_{{\rm R}k})/H^{\rm P}_{{\rm R}k}$ of the interference effects $(H^{\rm P}_{{\rm R}k}-H^{\rm Prv}_{{\rm R}k})$ for the peak-height $H^{\rm P}_{{\rm R}k}$ of the power absorption $P_k(\omega)$, are displayed varying the temperature $T$ scaled by $\hbar\omega_z/k_{\rm B}$ from 0.2 to 1.5 for the cases of spin-magnitudes $S=1,3$, and for the anisotropy energy $\hbar K$ given by $K/\omega_z=2.0$, the wave-number $k=0$ and the daming constant $\gamma_{{\rm R}k}$ given by $\gamma_{{\rm R}k}/\omega_z=0.5$. Here, the peak-height $H^{\rm P}_{{\rm R}k}$ is the approximate formula given by (4.16), and the peak-height $H^{\rm Prv}_{{\rm R}k}$ is the approximate formula given by (4.30), which is the one without the interference terms in the peak-height $H^{\rm P}_{{\rm R}k}$ of the power absorption $P_k(\omega)$.

Figure 19: The approximation of the rate $(H^{\rm M}_{{\rm R}k}-H^{\rm Mrv}_{{\rm R}k})/H^{\rm M}_{{\rm R}k}$ of the interference effects $(H^{\rm M}_{{\rm R}k}-H^{\rm Mrv}_{{\rm R}k})$ for the peak-height $H^{\rm M}_{{\rm R}k}$ of the magnetization-amplitudes $A^{\rm M}_k(\omega)$, are displayed varying the temperature $T$ scaled by $\hbar\omega_z/k_{\rm B}$ from 0.2 to 1.5 for the cases of spin-magnitudes $S=1,3$, and for the anisotropy energy $\hbar K$ given by $K/\omega_z=2.0$ and the wave-number $k=0$ and the daming constant $\gamma_{{\rm R}k}$ given by $\gamma_{{\rm R}k}/\omega_z=0.5$. Here, the peak-height $H^{\rm M}_{{\rm R}k}$ is the approximate formula given by (4.23), and the peak-height $H^{\rm Mrv}_{{\rm R}k}$ is the approximate formula given by (4.31), which is the one without the interference terms in the peak-height $H^{\rm M}_{{\rm R}k}$ of the magnetization-amplitudes $A^{\rm M}_k(\omega)$.

# 5 Summary and concluding remarks

We have considered a ferromagnetic spin system with a uniaxial anisotropy energy and an anisotropic exchange interaction under an external static magnetic-field in the spin-wave region, interacting with a phonon reservoir, and have studied the resonance absorption and transverse magnetization for such a spin system interacting with an external driving magnetic-field, which is a transversely rotating classical-field, in the spin-wave approximation by employing the TCLE method of linear response in terms of the non-equilibrium thermo-field dynamics (NETFD). The expectation values of the $x$-component and $y$-component of the magnetization with the wave-number $k$ have been shown to oscillate with the frequency $\omega$ of the external driving magnetic-field and with the amplitude $A^{\rm M}_k(\omega)$ given by (3.34). We have analytically examined the power absorption and the amplitude of the expectation value of the transverse

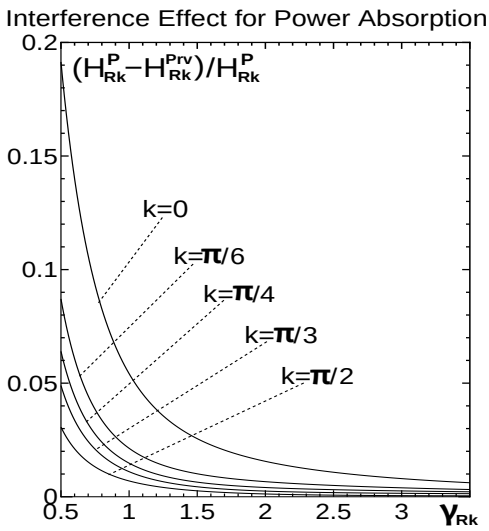


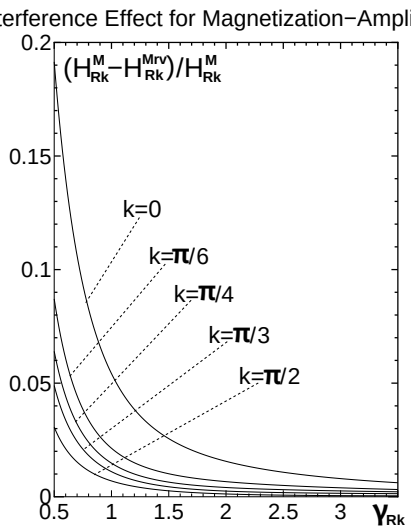


Figure 20: The approximation of the rate $(H^{\mathrm{P}}_{\mathrm{R}k}-H^{\mathrm{Prv}}_{\mathrm{R}k})/H^{\mathrm{P}}_{\mathrm{R}k}$ of the interference effects $(H^{\mathrm{P}}_{\mathrm{R}k}-H^{\mathrm{Prv}}_{\mathrm{R}k})$ for the peak-height $H^{\mathrm{P}}_{\mathrm{R}k}$ of of the power absorption $P_k(\omega)$, are displayed varying the daming constant $\gamma_{\mathrm{R}k}$ scaled by $\omega_z$ from 0.5 to 3.5, for the cases of wave numbers $k=0,\pi/6,\pi/4,\pi/3,\pi/2$, and for the spin-magnitude $S=1$, the temperature $T$ given by $k_{\mathrm{B}}T/(\hbar\omega_z)=1.0$ and the anisotropy energy $\hbar K$ given by $K/\omega_z=1.0$. Here, the peak-height $H^{\mathrm{P}}_{\mathrm{R}k}$ is the approximate formula given by (4.16), and the peak-height $H^{\mathrm{Prv}}_{\mathrm{R}k}$ is the approximate formula given by (4.30), which is the one without the interference terms in the peak-height $H^{\mathrm{P}}_{\mathrm{R}k}$ of the power absorption $P_k(\omega)$.

Figure 21: The approximation of the rate $(H^{\mathrm{M}}_{\mathrm{R}k}-H^{\mathrm{Mrv}}_{\mathrm{R}k})/H^{\mathrm{M}}_{\mathrm{R}k}$ of the interference effects $(H^{\mathrm{M}}_{\mathrm{R}k}-H^{\mathrm{Mrv}}_{\mathrm{R}k})$ for the peak-height $H^{\mathrm{M}}_{\mathrm{R}k}$ of the magnetization-amplitudes $A^{\mathrm{M}}_{k}(\omega)$, are displayed varying the daming constant $\gamma_{\mathrm{R}k}$ scaled by $\omega_z$ from 0.5 to 3.5, for the cases of wave numbers $k=0,\pi/6,\pi/4,\pi/3,\pi/2$, and for the spin-magnitude $S=1$, the temperature $T$ given by $k_{\mathrm{B}}T/(\hbar\omega_z)=1.0$ and the anisotropy energy $\hbar K$ given by $K/\omega_z=1.0$. Here, the peak-height $H^{\mathrm{M}}_{\mathrm{R}k}$ is the approximate formula given by (4.23), and the peak-height $H^{\mathrm{Mrv}}_{\mathrm{R}k}$ is the approximate formula given by (4.31), which is the one without the interference terms in the peak-height $H^{\mathrm{M}}_{\mathrm{R}k}$ of the magnetization-amplitudes $A^{\mathrm{M}}_{k}(\omega)$.

magnetization, which is referred as "the magnetization-amplitude", for the ferromagnetic spin system, and have derived the approximate formulas of the resonance frequencies, peak-heights (heights of peak) and line half-widths in the resonance region of the power absorption and magnetization-amplitude. We have numerically investigated the power absorption and magnetization-amplitude for an ferromagnetic system of one-dimensional infinite spins by assuming a damped phonon-reservoir model in the region valid for the low spin-wave approximation, which includes the dominant parts of the higher-order parts in the spin-wave approximation [5] and is referred as "the low spin-wave approximation". Here, the valid region means that $n(t)/(4S)$, which corresponds to the expectation value of the second term in the expansion given by Eq. (2.2), is smaller than about 0.01 in that region, where $n(t)$ is the expectation value of the spin deviation number. We have mainly obtained the following results by the numerical investigations.

1. The power absorption $P_k(\omega)$ and magnetization-amplitude $A^{\mathrm{M}}_{k}(\omega)$ for the ferromagnetic system with the wave number $k$ have a peak for each wave-number. As the wave number $k$ becomes large, the resonance frequencies and peak-heights (heights of peak) increase, and the line half-widths in the resonance region decrease. Thus, as the wave number $k$ becomes large, the line shapes of the power absorption and magnetization-amplitude show "the narrowing" in the resonance region.

2. In the resonance region of the power absorption and magnetization-amplitude, as the spin-magnitude $S$ becomes large, the resonance frequencies become large, the peak-heights increase and the line half-widths decrease slightly, and also as the anisotropy energy $\hbar K$ becomes large, the resonance frequencies become large, the peak-heights increase in the low temperature region and the line half-widths decrease slightly.

3. In the resonance region of the power absorption and magnetization-amplitude, as the temperature $T$ becomes high, the resonance frequencies become large slightly, the peak-heights decrease and the line half-widths increase.

4. The approximate formulas of the resonance frequency and peak-height for the power absorption $P_k(\omega)$ coincide well with the results investigated calculating numerically the power absorption $P_k(\omega)$. The approximate formula of the line half-width in the resonance region of the power absorption $P_k(\omega)$ coincides well or nearly with the results investigated calculating numerically the power absorption $P_k(\omega)$. The approximate formula of the line half-width deviates slightly from the results investigated calculating numerically the power absorption $P_k(\omega)$ in small wave-number region for the spin-magnitude $S=1$ and in high temperature region for the anisotropy energy $\hbar K$ given by $K/\omega_z=1.0$, and coincides well with the results investigated calculating numerically the power absorption $P_k(\omega)$ except those region.

5. The approximate formulas of the resonance frequency, peak-height and line half-width in the resonance region of the magnetization-amplitude $A^{\mathrm{M}}_{k}(\omega)$ coincide well with the results investigated calculating numerically the magnetization-

amplitude $A_k^{\mathtt{M}}(\omega)$.
6. The effects of the memory and initial correlation for the spin system and phonon reservoir, i.e., the interference effects, which are represented by the interference terms or the interference thermal states in the TCLE method, are confirmed to increase the power absorption and magnetization-amplitude in the resonance region, and become large as the temperature $T$ becomes high, as the phonon reservoir is damped slowly or as the wave number becomes small. Thus, the interference effects produce effects that cannot be neglected for the high temperature, for the non-quickly damped reservoir or for the small wave-number.
7. Each peak of the line shapes of magnetization-amplitude has the hemline longer than that of the power absorption. Also, the line half-widths in the resonance region of the magnetization-amplitude are larger than those of the power absorption.

We have analytically examined the power absorption $P_k(\omega)$ and the magnetization-amplitude $A_k^{\mathtt{M}}(\omega)$ (the amplitude of the expectation value of the transverse magnetization) for the ferromagnetic spin system with the wave number $k$, and have derived the approximate formulas of the resonance frequencies, peak-heights (heights of peak) and line half-widths in the resonance region of the power absorption and magnetization-amplitude. The approximate formulas of the resonance frequencies $\omega_{\mathtt{R}k}^{\mathtt{P}}$ and $\omega_{\mathtt{R}k}^{\mathtt{M}}$ for the power absorption and magnetization-amplitude are given by (3.30) and (3.36), respectively, i.e.

$$\omega_{\mathtt{R}k}^{\mathtt{P}} \cong \epsilon_k + \Phi_k'', \qquad\qquad \omega_{\mathtt{R}k}^{\mathtt{M}} \cong \epsilon_k + \Phi_k'', \tag{5.1}$$

with the imaginary part $\Phi_k''$ of the $\Phi_k(\epsilon_k)$ given by (3.18) or (4.3). The approximate formulas of the peak-heights (heights of peak) $H_{\mathtt{R}k}^{\mathtt{P}}$ and $H_{\mathtt{R}k}^{\mathtt{M}}$ for the power absorption and magnetization-amplitude are given by (4.16) and (4.23), respectively, i.e.

$$H_{\mathtt{R}k}^{\mathtt{P}} \cong S\,\gamma^2\,|H_k|^2\,\hbar\,\omega_{\mathtt{R}k}^{\mathtt{P}}\,\{1+X_k''(\omega_{\mathtt{R}k}^{\mathtt{P}})\}/(\Phi_k'+\Psi_k), \tag{5.2}$$

$$H_{\mathtt{R}k}^{\mathtt{M}} \cong S\,\hbar\,\gamma\,|H_k|\,\sqrt{\{X_k'(\omega_{\mathtt{R}k}^{\mathtt{M}})\}^2+\{1+X_k''(\omega_{\mathtt{R}k}^{\mathtt{M}})\}^2}\,/(\Phi_k'+\Psi_k), \tag{5.3}$$

with $\Psi_k$ given by (3.19) or (4.4) and the real part $\Phi_k'$ of the $\Phi_k(\epsilon_k)$, where $X_k'(\omega)$ and $X_k''(\omega)$ are the real and imaginary parts of the corresponding interference term $X_k(\omega)$ given by (3.16) or (C.2), and take the forms given by (C.3a) and (C.3b), respectively. As shown in Figs. 3, 4, 7, 8, 12, 13, 15 and 16, the approximate formulas of the resonance frequencies $\omega_{\mathtt{R}k}^{\mathtt{P}}$, $\omega_{\mathtt{R}k}^{\mathtt{M}}$ and the peak-heights $H_{\mathtt{R}k}^{\mathtt{P}}$, $H_{\mathtt{R}k}^{\mathtt{M}}$ coincide well with the results investigated calculating numerically the power absorption $P_k(\omega)$ and the magnetization-amplitude $A_k^{\mathtt{M}}(\omega)$ for the spin-magnitudes $S \geq 1$ and for the temperature $T$ and anisotropy energy $\hbar K$ given by $k_{\mathtt{B}}T/(\hbar\omega_z) \leq 1.1$ and $K/\omega_z \geq 1.0$. The approximate formulas of the line half-widths $\Delta\omega_{\mathtt{R}k}^{\mathtt{P}}$ and $\Delta\omega_{\mathtt{R}k}^{\mathtt{M}}$ in the resonance region of the power absorption and magnetization-amplitude are given by (4.22) and (4.29), respectively, i.e.

$$\begin{aligned}
\Delta\omega_{\mathtt{R}k}^{\mathtt{P}} \cong\; & 2\,(\Phi_k'+\Psi_k)\big\{\omega_{\mathtt{R}k}^{\mathtt{P}}\,X_k'(\omega_{\mathtt{R}k}^{\mathtt{P}}+(\Phi_k'+\Psi_k)\,x_1)+(\Phi_k'+\Psi_k)\{1+X_k''(\omega_{\mathtt{R}k}^{\mathtt{P}}+(\Phi_k'+\Psi_k)\,x_1)\} \\
& +\big\{(\omega_{\mathtt{R}k}^{\mathtt{P}})^2\,X_k'(\omega_{\mathtt{R}k}^{\mathtt{P}}+(\Phi_k'+\Psi_k)\,x_1)^2+(\Phi_k'+\Psi_k)^2\,\{1+X_k''(\omega_{\mathtt{R}k}^{\mathtt{P}}+(\Phi_k'+\Psi_k)\,x_1)\}^2 \\
& \quad +2\,\omega_{\mathtt{R}k}^{\mathtt{P}}\{1+X_k''(\omega_{\mathtt{R}k}^{\mathtt{P}})\}\{(\Phi_k'+\Psi_k)X_k'(\omega_{\mathtt{R}k}^{\mathtt{P}}+(\Phi_k'+\Psi_k)\,x_1)+\omega_{\mathtt{R}k}^{\mathtt{P}}\{1+X_k''(\omega_{\mathtt{R}k}^{\mathtt{P}}+(\Phi_k'+\Psi_k)\,x_1)\}\} \\
& \quad -2\,\omega_{\mathtt{R}k}^{\mathtt{P}}\,(\Phi_k'+\Psi_k)\,X_k'(\omega_{\mathtt{R}k}^{\mathtt{P}}+(\Phi_k'+\Psi_k)\,x_1)\,\{1+X_k''(\omega_{\mathtt{R}k}^{\mathtt{P}}+(\Phi_k'+\Psi_k)\,x_1)\} \\
& \quad -(\omega_{\mathtt{R}k}^{\mathtt{P}})^2\{1+X_k''(\omega_{\mathtt{R}k}^{\mathtt{P}})\}^2\big\}^{1/2}\big\}/\big\{\omega_{\mathtt{R}k}^{\mathtt{P}}\{1+X_k''(\omega_{\mathtt{R}k}^{\mathtt{P}})\}-2\,(\Phi_k'+\Psi_k)X_k'(\omega_{\mathtt{R}k}^{\mathtt{P}}+(\Phi_k'+\Psi_k)\,x_1)\big\},
\end{aligned} \tag{5.4}$$

$$\Delta\omega_{\mathtt{R}k}^{\mathtt{M}} \cong 2\,(\Phi_k'+\Psi_k)\,\sqrt{4\,\frac{\{X_k'(\omega_{\mathtt{R}k}^{\mathtt{M}}+\sqrt{3}\,(\Phi_k'+\Psi_k))\}^2+\{1+X_k''(\omega_{\mathtt{R}k}^{\mathtt{M}}+\sqrt{3}\,(\Phi_k'+\Psi_k))\}^2}{\{X_k'(\omega_{\mathtt{R}k}^{\mathtt{M}})\}^2+\{1+X_k''(\omega_{\mathtt{R}k}^{\mathtt{M}})\}^2}-1}\,, \tag{5.5}$$

where $x_1$ is given by

$$\begin{aligned}
x_1 \cong\; & \big\{\omega_{\mathtt{R}k}^{\mathtt{P}}X_k'(\omega_{\mathtt{R}k}^{\mathtt{P}})+(\Phi_k'+\Psi_k)\{1+X_k''(\omega_{\mathtt{R}k}^{\mathtt{P}})\} \\
& +\big\{(\omega_{\mathtt{R}k}^{\mathtt{P}})^2\{X_k'(\omega_{\mathtt{R}k}^{\mathtt{P}})^2+\{1+X_k''(\omega_{\mathtt{R}k}^{\mathtt{P}})\}^2\}+(\Phi_k'+\Psi_k)^2\{1+X_k''(\omega_{\mathtt{R}k}^{\mathtt{P}})\}^2\big\}^{1/2}\big\} \\
& \quad /\big\{\omega_{\mathtt{R}k}^{\mathtt{P}}\{1+X_k''(\omega_{\mathtt{R}k}^{\mathtt{P}})\}-2\,(\Phi_k'+\Psi_k)X_k'(\omega_{\mathtt{R}k}^{\mathtt{P}})\big\}.
\end{aligned} \tag{5.6}$$

As shown in Figs. 5, 6, 9, 14 and 17, the approximate formulas of the line half-widths $\Delta\omega_{\mathtt{R}k}^{\mathtt{P}}$ and $\Delta\omega_{\mathtt{R}k}^{\mathtt{M}}$ in the resonance region of the power absorption and magnetization-amplitude coincide well with the results investigated calculating numerically the power absorption $P_k(\omega)$ and the magnetization-amplitude $A_k^{\mathtt{M}}(\omega)$ for the spin-magnitudes $S \geq 1$ and for the temperature $T$ and anisotropy energy $\hbar K$ given by $k_{\mathtt{B}}T/(\hbar\omega_z) \leq 1.1$ and $K/\omega_z \geq 1.0$, except the slight deviations for the line half-width $\Delta\omega_{\mathtt{R}k}^{\mathtt{P}}$ of the power absorption $P_k(\omega)$ in the small wave-number region of the case that the spin-magnitudes $S=1$, the temperature $T$ and anisotropy energy $\hbar K$ given by $k_{\mathtt{B}}T/(\hbar\omega_z)=1.0$ and $K/\omega_z=1.0$, and in the high temperature region of the case that the spin-magnitudes $S=1$, the wave-number $k=\pi/6$ and the anisotropy energy $\hbar K$ given by $K/\omega_z=1.0$.

The above approximate formulas obtained for the resonance frequencies, peak-heights and line half-widths in the resonance region of the power absorption $P_k(\omega)$ and magnetization-amplitude $A_k^{\mathtt{M}}(\omega)$, are useful for investigating

dependence of the line shapes on variation of various physical quantities. As examples, we investigate dependence of the peak-heights and line half-widths on the anisotropy energy $\hbar K$ in the resonance region of the ferromagnetic spin system with the wave number $k$ and the damping constant $\gamma_{\mathrm{R}k}$ of the phonon reservoir. In Fig. 22, the approximate formula of the peak-height $H^{\mathrm{P}}_{\mathrm{R}k}$ in the resonance region of the power absorption, scaled by $\hbar\gamma^2\,|H_k|^2$, is displayed varying the daming constant $\gamma_{\mathrm{R}k}$ of the phonon reservoir, scaled by $\omega_z$, from 0.5 to 5.5 for the cases of anisotropy energies $\hbar K$ given by $A = K/\omega_z = 1.0, 1.5, 2.0, 2.5, 3.0$, and for the spin-magnitude $S = 1$, the temperature $T$ given by $k_{\mathrm{B}}T/(\hbar\omega_z) = 1.0$ and the wave-number $k = 0$. In Fig. 23, the approximate formula of the peak-height $H^{\mathrm{M}}_{\mathrm{R}k}$ in the resonance region of the magnetization-amplitude, scaled by $\hbar\gamma\,|H_k|/\omega_z$, is displayed varying the daming constant $\gamma_{\mathrm{R}k}$ of the phonon reservoir, scaled by $\omega_z$, from 0.5 to 5.5 for the cases of anisotropy energies $\hbar K$ given by $A = K/\omega_z = 1.0, 2.0, 3.0, 4.0, 5.0$, and for the spin-magnitude $S = 1$, the temperature $T$ given by $k_{\mathrm{B}}T/(\hbar\omega_z) = 1.0$ and the wave-number $k = 0$. Figures 22 and 23 show in the resonance region of the power absorption and magnetization-amplitude that as the damping constant $\gamma_{\mathrm{R}k}$ of the phonon reservoir becomes large, the peak-heights $H^{\mathrm{P}}_{\mathrm{R}k}$ and $H^{\mathrm{M}}_{\mathrm{R}k}$ increase, and that as the anisotropy energy $\hbar K$ increases, the peak-heights $H^{\mathrm{P}}_{\mathrm{R}k}$ and $H^{\mathrm{M}}_{\mathrm{R}k}$ increase. In Fig. 24, the approximate formula of the line half-width $\Delta\omega^{\mathrm{P}}_{\mathrm{R}k}$ in the resonance region of the power absorption, scaled by $\omega_z$, is displayed varying the daming constant $\gamma_{\mathrm{R}k}$ of the phonon reservoir, scaled by $\omega_z$, from 0.5 to 5.5 for the cases of anisotropy energies $\hbar K$ given by $A = K/\omega_z = 1.0, 1.5, 2.0, 3.0$, and for the spin-magnitude $S = 1$, the temperature $T$ given by $k_{\mathrm{B}}T/(\hbar\omega_z) = 1.0$ and the wave-number $k = 0$. In Fig. 25, the approximate formula of the line half-width $\Delta\omega^{\mathrm{M}}_{\mathrm{R}k}$ in the resonance region of the magnetization-amplitude, scaled by $\omega_z$, is displayed varying the daming constant $\gamma_{\mathrm{R}k}$ of the phonon reservoir, scaled by $\omega_z$, from 0.5 to 5.5 for the cases of anisotropy energies $\hbar K$ given by $A = K/\omega_z = 1.0, 2.0, 3.0, 5.0$, and for the spin-magnitude $S = 1$, the temperature $T$ given by $k_{\mathrm{B}}T/(\hbar\omega_z) = 1.0$ and the wave-number $k = 0$. Figures 24 and 25 show in the resonance region of the power absorption and magnetization-amplitude that as the damping constant $\gamma_{\mathrm{R}k}$ of the phonon reservoir becomes large, the line half-widths $\Delta\omega^{\mathrm{P}}_{\mathrm{R}k}$ and $\Delta\omega^{\mathrm{M}}_{\mathrm{R}k}$ decrease, and that as the anisotropy energy $\hbar K$ increases, the line half-widths $\Delta\omega^{\mathrm{P}}_{\mathrm{R}k}$ and $\Delta\omega^{\mathrm{M}}_{\mathrm{R}k}$ decrease slightly. Figures $22-25$ show in the resonance region of the power absorption and magnetization-amplitude that as the damping constant $\gamma_{\mathrm{R}k}$ of the phonon reservoir becomes large, the peak-heights $H^{\mathrm{P}}_{\mathrm{R}k}$ and $H^{\mathrm{M}}_{\mathrm{R}k}$ increase and the line half-widths $\Delta\omega^{\mathrm{P}}_{\mathrm{R}k}$ and $\Delta\omega^{\mathrm{M}}_{\mathrm{R}k}$ decrease. As the damping constant $\gamma_{\mathrm{R}k}$ of the phonon reservoir, which is equal to the inverse of its correlation time $\tau_c$, become large, the phonon reservoir is damped quickly. Thus, as the phonon reservoir is damped quickly, the line shapes of the power absorption and magnetization-amplitude show "the narrowing" in the resonance region.

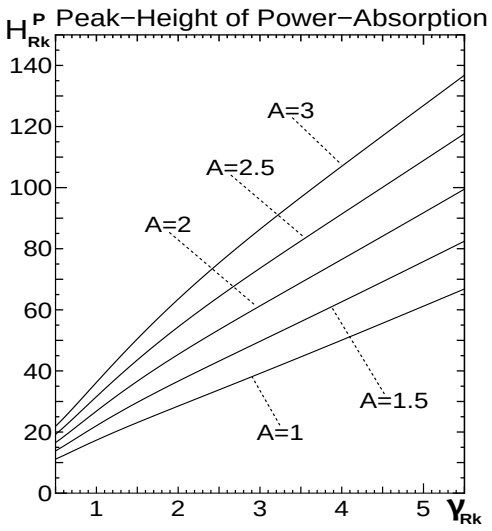


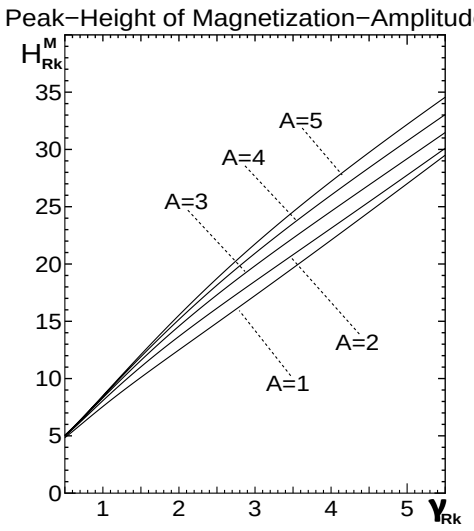


Figure 22: The approximate formula of the peak-height $H^{\mathrm{P}}_{\mathrm{R}k}$ in the resonance region of the power absorption, scaled by $\hbar\gamma^2\,|H_k|^2$, is displayed varying the daming constant $\gamma_{\mathrm{R}k}$ of the phonon reservoir, scaled by $\omega_z$, from 0.5 to 5.5 for the cases of anisotropy energies $\hbar K$ given by $A = K/\omega_z = 1.0, 1.5, 2.0, 2.5, 3.0$, and for the spin-magnitude $S = 1$, the temperature $T$ given by $k_{\mathrm{B}}T/(\hbar\omega_z) = 1.0$ and the wave-number $k = 0$.

Figure 23: The approximate formula of the peak-height $H^{\mathrm{M}}_{\mathrm{R}k}$ in the resonance region of the magnetization-amplitude, scaled by $\hbar\gamma\,|H_k|/\omega_z$, is displayed varying the daming constant $\gamma_{\mathrm{R}k}$ of the phonon reservoir, scaled by $\omega_z$, from 0.5 to 5.5 for the cases of anisotropy energies $\hbar K$ given by $A = K/\omega_z = 1.0, 2.0, 3.0, 4.0, 5.0$, and for the spin-magnitude $S = 1$, the temperature $T$ given by $k_{\mathrm{B}}T/(\hbar\omega_z) = 1.0$ and the wave-number $k = 0$.

We have discussed the linear response of a ferromagnetic spin system interacting with a phonon reservoir to an external driving magnetic-field, which is a transversely rotating classical field, by employing the TCLE method in the second-order approximation for the system-reservoir interaction, including the effects of the memory and initial correlation for the spin system and phonon reservoir, i.e., the interference effects (the effects of interference between the external driving field and the phonon reservoir), which are represented by the interference terms or the interference

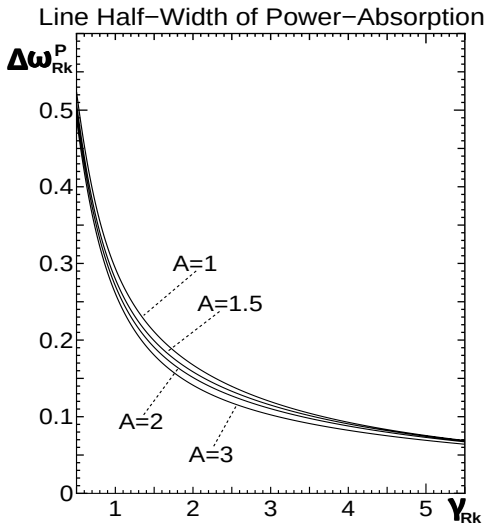


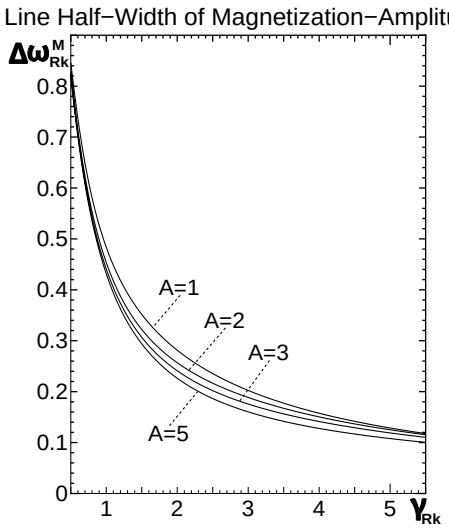


Figure 24: The approximate formula of the line half-width $\Delta\omega^{\mathrm{P}}_{\mathrm{R}k}$ in the resonance region of the power absorption, scaled by $\omega_z$, is displayed varying the daming constant $\gamma_{\mathrm{R}k}$ of the phonon reservoir, scaled by $\omega_z$, from 0.5 to 5.5 for the cases of anisotropy energies $\hbar K$ given by $A = K/\omega_z = 1.0, 1.5, 2.0, 3.0$, and for the spin-magnitude $S = 1$, the temperature $T$ given by $k_{\mathrm{B}}T/(\hbar\omega_z) = 1.0$ and the wave-number $k = 0$.

Figure 25: The approximate formula of the line half-width $\Delta\omega^{\mathrm{M}}_{\mathrm{R}k}$ in the resonance region of the magnetization-amplitude, scaled by $\omega_z$, is displayed varying the daming constant $\gamma_{\mathrm{R}k}$ of the phonon reservoir, scaled by $\omega_z$, from 0.5 to 5.5 for the cases of anisotropy energies $\hbar K$ given by $A = K/\omega_z = 1.0, 2.0, 3.0, 5.0$, and for the spin-magnitude $S = 1$, the temperature $T$ given by $k_{\mathrm{B}}T/(\hbar\omega_z) = 1.0$ and the wave-number $k = 0$.

thermal state in the TCLE method, give the effects of the deviation from the van Hove limit [27] or the narrowing limit [28]. The interference effects are the effects of collision of the spin system excited by the external driving field with the phonon reservoir, and influence the motoin of the spin system according to the motion of the phonon reservoir, and therefore those effects increases the power absorption and magnetization-amplitude in the resonance region for a non-quickly damped phonon-reservoir as seen in Figs. 2 and 11, because the external driving field excites not only the spin system but also the phonon reservoir in that region. The interference effects become large as the temperature becomes high as seen in Figs. 18 and 19, and also become large as the phonon reservoir is damped slowly or as the wave number $k$ becomes small as seen in Figs. 20 and 21, and thus those effects produce effects that cannot be neglected for the high temperature, for the non-quickly damped reservoir or for the small wave number $k$. If the phonon reservoir is damped quickly, that is to say, the relaxation time $\tau_r$ of the spin system is much greater than the correlation time $\tau_c$ of the phonon reservoir, i.e., $\tau_r \gg \tau_c$, as being discussed in Ref. [17], one obtains the transverse susceptibility $\chi^{\mathrm{rv}}_{S^+_k S^-_k}(\omega)$ given by (3.38) without the interference thermal state $|D^{(2)}_{S^-_k}[\omega]\rangle$ in the transverse susceptibility $\chi_{S^+_k S^-_k}(\omega)$ [(3.9)] derived employing the TCLE method [17]. The susceptibility $\chi^{\mathrm{rv}}_{S^+_k S^-_k}(\omega)$ is derived employing the relaxation method [17] in the van Hove limit [27] or in the narrowing limit [28], and is valid only in the limit in which the phonon reservoir is damped quickly [17]. Since the transverse relaxation times of the ferromagnetic spin system are equal to $(\Phi'_k + \Psi_k)^{-1}$ according to (3.36) and (3.37) in Ref. [9], where $\Phi'_k$ and $\Psi_k$ are given by (4.5a) and (4.4), and the transverse correlation time of the phonon reservoir is equal to $(\gamma_{\mathrm{R}k})^{-1}$ according to (4.1a) or (4.1b), we have $(\Phi'_k + \Psi_k)^{-1} \gg (\gamma_{\mathrm{R}k})^{-1}$, i.e., $(\Phi'_k + \Psi_k) \ll \gamma_{\mathrm{R}k}$, or (the transverse correlation time $(\gamma_{\mathrm{R}k})^{-1} = \tau^{\mathrm{T}}_c$ of the phonon reservoir) $\to 0$ in the van Hove limit [27] or in the narrowing limit [28]. In this limit, since the corresponding interference terms $X_k(\omega)$ vanish according to (C.2), (C.3a) and (C.3b) as seen in Figs. 20 and 21, the transverse susceptibility becomes $\chi^{\mathrm{rv}}_{S^+_k S^-_k}(\omega)$ given by (3.38), and therefore one cannot discuss theoretically variations of the peak-heights and line half-widths in the resonance region of the power-absorption and magnetization-amplitude, because the peak-heights approach to $\infty$ and the line half-widths approach to 0 in that limit as seen in Figs. $22-25$. The transverse magnetic susceptibility $\chi_{S^+_k S^-_k}(\omega)$ derived employing the second-order TCLE method is valid even if the phonon reservoir is damped slowly, in the region valid for the second-order perturbation approximation. Thus, the TCLE method is available for a spin system interacting with a non-quickly damped phonon-reservoir as well, and one can discuss theoretically variations of the peak-heights and line half-widths in the resonance region of the power-absorption and magnetization-amplitude derived employing the TCLE method, whereas one cannot discuss theoretically variations of the peak-heights and line half-widths employing the relaxation method [17] in the van Hove limit [27] or in the narrowing limit [28], in which the phonon reservoir is damped quickly [17].

We have analytically examined the power absorption and magnetization-amplitude in the resonance region of a ferromagnetic spin system interacting with a phonon reservoir in the spin-wave region [6], including not only the low-

order parts but also the next higher-order parts in the spin-wave approximation, and have derived the approximate formulas of the resonance frequencies, peak-heights (heights of peak) and line half-widths in the low spin-wave approximation. We have numerically investigated a ferromagnetic system of one-dimensional ininite spins in the region valid for the low spin-wave approximation, and have shown that the approximate formulas of the resonance frequencies, peak-heights and line half-widths, coincide well or nearly with the results investigated calculating numerically the analytic results of the power absorption and magnetization-amplitude in the resonance region, and satisfy "the narrowing condition" that as phonon reservoir is damped quickly, the peak-heights increase and the line half-widths decrease, and thus we have numerically verified the approximate formulas. The approximate formulas obtained for the resonance frequencies, peak-heights and line half-widths in the resonance region, may have to be verified for the various cases both experimentally and by the other theoretical method, e.g. the simulation method. We have also investigated numerically the effects of the memory and initial correlation for the spin system and phonon reservoir, i.e., the interference effects (the effects of interference between the external driving field and the phonon reservoir), and have shown to produce effects that cannot be neglected for the high temperature, for the non-quickly damped reservoir or for the small wave-number. Although the numerical investigation have been performed for a ferromagnetic system of one-dimensional infinite spins, the analytic results obtained in the present paper are available for the two- and three-dimensional spin systems as well.

# A Derivation of formulas useful for the perturbation calculations

In this Appendix, formulas useful for the perturbation calculations are derived. Taking the perturbed part $\mathcal{H}_{\mathtt{s}1}$ given by (2.12) in the Hamiltonian $\mathcal{H}_{\mathtt{s}}$ of the spin system by neglecting the parts of higher order than the fourth power of $a_j$, $a_j^\dagger$ in the spin-wave approximation, as (3.23), the hat-Hamiltonian $\hat{\mathcal{H}}_{\mathtt{s}1}(t)$ defined by (3.11) takes the form

$$\hat{\mathcal{H}}_{\mathtt{s}1}(t) = \sum_{k,\,k',\,k''} \epsilon_3(k,\,k')\big\{a_{k'}^{\dagger\dagger}(t)\,a_{k+k''}^{\dagger\dagger}(t)\,a_k(t)\,a_{k'+k''}(t) - \tilde{a}_k^{\dagger\dagger}(t)\,\tilde{a}_{k'+k''}^{\dagger\dagger}(t)\,\tilde{a}_{k'}(t)\,\tilde{a}_{k+k''}(t)\big\}$$
$$- \sum_{k,\,k'} \epsilon_2(k,\,k')\,\bar{n}(\epsilon_{k'})\{a_k^{\dagger\dagger}(t)\,a_k(t) - \tilde{a}_k^{\dagger\dagger}(t)\,\tilde{a}_k(t)\}\,, \tag{A.1}$$

where we have defined the Heisenberg operators as [19, 20, 23, 9]

$$a_k(t) = U^{-1}(t)\,a_k\,U(t), \qquad\qquad a_k^{\dagger\dagger}(t) = U^{-1}(t)\,a_k^\dagger\,U(t), \tag{A.2}$$

and their tilde conjugates. By using the axioms and transformations provided in Refs. [20, 23, 9] and the forms of the quasi-particle operators [9] in the NETFD, we can derive the forms of $\langle 1_{\mathtt{s}}|a_k(t)\hat{\mathcal{H}}_{\mathtt{s}1}(\tau)$ and $\langle 1_{\mathtt{s}}|a_k^{\dagger\dagger}(t)\hat{\mathcal{H}}_{\mathtt{s}1}(\tau)$ for $\mathcal{H}_{\mathtt{s}1}$ given by (3.23) as follows,

$$\langle 1_{\mathtt{s}}|\,a_k\,U(t)\,\hat{\mathcal{H}}_{\mathtt{s}1}(\tau) = \langle 1_{\mathtt{s}}|\,a_k(t)\,\hat{\mathcal{H}}_{\mathtt{s}1}(\tau) = Z_k^{1/2}(t)\langle 1_{\mathtt{s}}|\,\alpha_k(t)\,\hat{\mathcal{H}}_{\mathtt{s}1}(\tau), \tag{A.3a}$$

$$= Z_k^{1/2}(\tau)\langle 1_{\mathtt{s}}|\,\alpha_k(\tau)\,\hat{\mathcal{H}}_{\mathtt{s}1}(\tau)\exp\{(-\,i\,(\epsilon_k+\Phi_k'') - \Phi_k' - \Psi_k)(t-\tau)\}, \tag{A.3b}$$

$$= Z_k(\tau)\langle 1_{\mathtt{s}}|\,[\,a_k(\tau) - h_k(\tau)\,\tilde{a}_k^{\dagger\dagger}(\tau)\,,\hat{\mathcal{H}}_{\mathtt{s}1}(\tau)\,]\exp\{(-\,i\,(\epsilon_k+\Phi_k'') - \Phi_k' - \Psi_k)(t-\tau)\}, \tag{A.3c}$$

$$= \Big\{\sum_{k',\,k''}\big\{\epsilon_3(k',k)\langle 1_{\mathtt{s}}|\,a_{k'+k''}^{\dagger\dagger}(\tau)\,a_{k'}(\tau)\,a_{k+k''}(\tau) + \epsilon_3(k'',k')\langle 1_{\mathtt{s}}|\,a_{k'}^{\dagger\dagger}(\tau)\,a_{k''}(\tau)\,a_{k'+k-k''}(\tau)\big\}$$
$$- \sum_{k'}\epsilon_2(k,\,k')\,\bar{n}(\epsilon_{k'})\langle 1_{\mathtt{s}}|\,a_k(\tau)\Big\}\,Z_k(\tau)(1-h_k(\tau))\exp\{(-\,i\,(\epsilon_k+\Phi_k'') - \Phi_k' - \Psi_k)(t-\tau)\}, \tag{A.3d}$$

$$= \Big\{\sum_{k',\,k''}\{\epsilon_3(k',k) + \epsilon_3(k',k'+k'')\}\langle 1_{\mathtt{s}}|\,a_{k'+k''}^{\dagger\dagger}(\tau)\,a_{k'}(\tau)\,a_{k+k''}(\tau)$$
$$- \sum_{k'}\epsilon_2(k,\,k')\,\bar{n}(\epsilon_{k'})\langle 1_{\mathtt{s}}|\,a_k(\tau)\Big\}\exp\{(-\,i\,(\epsilon_k+\Phi_k'') - \Phi_k' - \Psi_k)(t-\tau)\}, \tag{A.3e}$$

$$= \Big\{\sum_{k',\,k''}\{\epsilon_3(k',k) + \epsilon_3(k',k'+k'')\}\,Z_{k'+k''}^{1/2}(\tau)\,Z_{k'}^{1/2}(\tau)\,Z_{k+k''}^{1/2}(\tau)$$
$$\times\,\langle 1_{\mathtt{s}}|\,\tilde{\alpha}_{k'+k''}(\tau)\,(\alpha_{k'}(\tau) + h_{k'}(\tau)\,\tilde{\alpha}_{k'}^\ddagger(\tau))\,(\alpha_{k+k''}(\tau) + h_{k+k''}(\tau)\,\tilde{\alpha}_{k+k''}^\ddagger(\tau))$$
$$- \sum_{k'}\epsilon_2(k,\,k')\,\bar{n}(\epsilon_{k'})\,Z_k^{1/2}(\tau)\langle 1_{\mathtt{s}}|\,\alpha_k(\tau)\Big\}\exp\{(-\,i\,(\epsilon_k+\Phi_k'') - \Phi_k' - \Psi_k)(t-\tau)\}, \tag{A.3f}$$

$$= \Big\{\sum_{k',\,k''}\{\epsilon_3(k',k) + \epsilon_3(k',k'+k'')\}\,Z_{k'}^{1/2}(\tau)\,Z_{k+k''}^{1/2}(\tau)\,Z_{k'+k''}^{1/2}(\tau)$$
$$\times\,\langle 1_{\mathtt{s}}|\big\{\alpha_{k'}(\tau)\,\alpha_{k+k''}(\tau)\,\tilde{\alpha}_{k'+k''}(\tau) + h_{k+k''}(\tau)\,\alpha_k(\tau)\,\delta_{k',\,k} + h_{k'}(\tau)\,\alpha_k(\tau)\,\delta_{k'',\,0}\big\}$$
$$- \sum_{k'}\epsilon_2(k,\,k')\,\bar{n}(\epsilon_{k'})\,Z_k^{1/2}(\tau)\langle 1_{\mathtt{s}}|\,\alpha_k(\tau)\Big\}\exp\{(-\,i\,(\epsilon_k+\Phi_k'') - \Phi_k' - \Psi_k)(t-\tau)\}, \tag{A.3g}$$

$$\langle 1_{\rm S}|\, a_k^{\dagger}\, U(t)\, \hat{\mathcal{H}}_{\rm S1}(\tau) = \langle 1_{\rm S}|\, a_k^{\dagger\dagger}(t)\, \hat{\mathcal{H}}_{\rm S1}(\tau) = Z_k^{1/2}(t)\, \langle 1_{\rm S}|\, \tilde{\alpha}_k(t)\, \hat{\mathcal{H}}_{\rm S1}(\tau), \tag{A.4a}$$

$$= Z_k^{1/2}(\tau)\, \langle 1_{\rm S}|\, \tilde{\alpha}_k(\tau)\, \hat{\mathcal{H}}_{\rm S1}(\tau) \exp\{(i\,(\epsilon_k + \Phi_k'') - \Phi_k' - \Psi_k)\,(t-\tau)\}, \tag{A.4b}$$

$$= Z_k(\tau)\, \langle 1_{\rm S}|\, [\, \tilde{a}_k(\tau) - h_k(\tau)\, a_k^{\dagger\dagger}(\tau)\, , \hat{\mathcal{H}}_{\rm S1}(\tau)\, ] \exp\{(i\,(\epsilon_k + \Phi_k'') - \Phi_k' - \Psi_k)\,(t-\tau)\}, \tag{A.4c}$$

$$= \Big\{ - \sum_{k',\, k''} \big\{ \epsilon_3(k,k') \langle 1_{\rm S}|\, a_{k'}^{\dagger\dagger}(\tau)\, a_{k+k''}^{\dagger\dagger}(\tau)\, a_{k'+k''}(\tau) + \epsilon_3(k',k'') \langle 1_{\rm S}|\, a_{k''}^{\dagger\dagger}(\tau)\, a_{k'+k-k''}^{\dagger\dagger}(\tau)\, a_{k'}(\tau) \big\}$$
$$+ \sum_{k'} \epsilon_2(k,\, k')\, \bar{n}(\epsilon_{k'}) \langle 1_{\rm S}|\, a_k^{\dagger\dagger}(\tau) \Big\} Z_k(\tau)(1 - h_k(\tau)) \exp\{(i\,(\epsilon_k + \Phi_k'') - \Phi_k' - \Psi_k)(t-\tau)\}, \tag{A.4d}$$

$$= \Big\{ - \sum_{k',\, k''} \{ \epsilon_3(k,k') + \epsilon_3(k'+k'',k') \} \langle 1_{\rm S}|\, a_{k'}^{\dagger\dagger}(\tau)\, a_{k+k''}^{\dagger\dagger}(\tau)\, a_{k'+k''}(\tau)$$
$$+ \sum_{k'} \epsilon_2(k,\, k')\, \bar{n}(\epsilon_{k'}) \langle 1_{\rm S}|\, a_k^{\dagger\dagger}(\tau) \Big\} \exp\{(i\,(\epsilon_k + \Phi_k'') - \Phi_k' - \Psi_k)(t-\tau)\}, \tag{A.4e}$$

$$= \Big\{ - \sum_{k',\, k''} \{ \epsilon_3(k,k') + \epsilon_3(k'+k'',k') \}\, Z_{k'}^{1/2}(\tau)\, Z_{k+k''}^{1/2}(\tau)\, Z_{k'+k''}^{1/2}(\tau)$$
$$\times \langle 1_{\rm S}|\, \tilde{\alpha}_{k'}(\tau)\, (\alpha_{k+k''}^{\ddagger}(\tau) + \tilde{\alpha}_{k+k''}(\tau))\, (\alpha_{k'+k''}(\tau) + h_{k'+k''}(\tau)\, \tilde{\alpha}_{k'+k''}^{\ddagger}(\tau))$$
$$+ \sum_{k'} \epsilon_2(k,\, k')\, \bar{n}(\epsilon_{k'})\, Z_k^{1/2}(\tau) \langle 1_{\rm S}|\, \tilde{\alpha}_k(\tau) \Big\} \exp\{(i\,(\epsilon_k + \Phi_k'') - \Phi_k' - \Psi_k)(t-\tau)\}, \tag{A.4f}$$

$$= \Big\{ - \sum_{k',\, k''} \{ \epsilon_3(k,k') + \epsilon_3(k'+k'',k') \}\, Z_{k'}^{1/2}(\tau)\, Z_{k+k''}^{1/2}(\tau)\, Z_{k'+k''}^{1/2}(\tau)$$
$$\times \langle 1_{\rm S}| \big\{ \tilde{\alpha}_{k'}(\tau)\, \tilde{\alpha}_{k+k''}(\tau)\, \alpha_{k'+k''}(\tau) + h_{k+k''}(\tau)\, \tilde{\alpha}_k(\tau)\, \delta_{k',\,k} + h_{k'}(\tau)\, \tilde{\alpha}_k(\tau)\, \delta_{k'',\,0} \big\},$$
$$+ \sum_{k'} \epsilon_2(k,\, k')\, \bar{n}(\epsilon_{k'})\, Z_k^{1/2}(\tau) \langle 1_{\rm S}|\, \tilde{\alpha}_k(\tau) \Big\} \exp\{(i\,(\epsilon_k + \Phi_k'') - \Phi_k' - \Psi_k)(t-\tau)\}. \tag{A.4g}$$

# B Derivation of the next higher-order parts $\chi^{(1)}_{S_k^+ S_k^-}(\omega)$

In this Appendix, we derive form of the next higher-order parts $\chi^{(1)}_{S_k^+ S_k^-}(\omega)$ given by (3.22) with (3.23) for the transverse magnetic susceptibility $\chi_{S_k^+ S_k^-}(\omega)$ in the spin-wave approximation, using the quasi-particle operators introduced in Ref. [9]. The first term of (3.22) with the spin-wave interaction $\mathcal{H}_{\rm S1}$ given by (3.23) can be calculated by using (A.3g)

and the form of $n_k(t)$ $[=\langle 1_{\rm S}|a_k^{\dagger\dagger}(t)a_k(t)|\rho_0\rangle]$ given in Refs. [9], as follows,

$$
\begin{aligned}
&\text{(first term of } \chi^{(1)}_{S_k^+ S_k^-}(\omega) \text{ [(3.22)])},\\
&= \frac{S\,\hbar\,\gamma^2}{2}\int_0^\infty dt\int_0^t d\tau\,\langle 1_{\rm S}|\,a_k(t)\,\hat{\mathcal{H}}_{\rm S1}(\tau)(a_k^\dagger-\tilde{a}_k)\,|\rho_0\rangle\{1-i\,X_k(\omega)\}\exp(i\,\omega\,t), &\text{(B.1a)}\\
&= \frac{S\,\hbar\,\gamma^2}{2}\int_0^\infty dt\int_0^t d\tau\Big\{\sum_{k',\,k''}\{\epsilon_3(k',k)+\epsilon_3(k',k'+k'')\}\,Z_{k'}^{1/2}(\tau)\,Z_{k+k''}^{1/2}(\tau)\,Z_{k'+k''}^{1/2}(\tau)\\
&\qquad\times\langle 1_{\rm S}|\big\{\alpha_{k'}(\tau)\,\alpha_{k+k''}(\tau)\,\tilde{\alpha}_{k'+k''}(\tau)+h_{k+k''}(\tau)\,\alpha_k(\tau)\,\delta_{k',\,k}+h_{k'}(\tau)\,\alpha_k(\tau)\,\delta_{k'',\,0}\big\}\\
&\qquad-\sum_{k'}\epsilon_2(k,\,k')\,\bar{n}(\epsilon_{k'})\,Z_k^{1/2}(\tau)\langle 1_{\rm S}|\,\alpha_k(\tau)\Big\}\,\alpha_k^\ddagger\,|\rho_0\rangle\,Z_k^{1/2}(0)(1-h_k(0))\,\{1-i\,X_k(\omega)\}\\
&\qquad\qquad\times\exp\{(-\,i\,(\epsilon_k+\Phi_k'')-\Phi_k'-\Psi_k)(t-\tau)+i\,\omega\,t\}, &\text{(B.1b)}\\
&= \frac{S\,\hbar\,\gamma^2}{2}\int_0^\infty dt\int_0^t d\tau\sum_{k'}\big\{(\epsilon_3(k,k)+\epsilon_3(k,k+k'))\,n_{k+k'}(\tau)+(\epsilon_3(k',k)+\epsilon_3(k',k'))\,n_{k'}(\tau)\\
&\qquad\qquad-\epsilon_2(k,\,k')\,\bar{n}(\epsilon_{k'})\big\}\{1-i\,X_k(\omega)\}\exp\{(i\,(\omega-\epsilon_k-\Phi_k'')\,t-(\Phi_k'+\Psi_k)\,t\}, &\text{(B.1c)}\\
&= \frac{S\,\hbar\,\gamma^2}{2}\int_0^\infty dt\int_0^t d\tau\sum_{k'}\big\{\{\epsilon_3(k,k)+\epsilon_3(k,k')+\epsilon_3(k',k)+\epsilon_3(k',k')\}\,n_{k'}(\tau)\\
&\qquad\qquad-\epsilon_2(k,\,k')\,\bar{n}(\epsilon_{k'})\big\}\{1-i\,X_k(\omega)\}\exp\{(i\,(\omega-\epsilon_k-\Phi_k'')\,t-(\Phi_k'+\Psi_k)\,t\}, &\text{(B.1d)}\\
&= \frac{S\,\hbar\,\gamma^2}{2}\int_0^\infty d\tau\int_\tau^\infty dt\sum_{k'}\big\{\epsilon_2(k,k')\{(n_{k'}-\bar{n}(\epsilon_{k'}))\exp(-2\,\Phi_{k'}'\tau)+\bar{n}(\epsilon_{k'})\}\\
&\qquad\qquad-\epsilon_2(k,\,k')\,\bar{n}(\epsilon_{k'})\big\}\{1-i\,X_k(\omega)\}\exp\{(i\,(\omega-\epsilon_k-\Phi_k'')\,t-(\Phi_k'+\Psi_k)\,t\}, &\text{(B.1e)}\\
&= \frac{S\,\hbar\,\gamma^2}{2}\int_0^\infty d\tau\sum_{k'}\epsilon_2(k,k')\,(n_{k'}-\bar{n}(\epsilon_{k'}))\{1-i\,X_k(\omega)\}\exp(-2\,\Phi_{k'}'\tau)\\
&\qquad\qquad\times\frac{\exp\{(i\,(\omega-\epsilon_k-\Phi_k'')\,\tau-(\Phi_k'+\Psi_k)\,\tau\}}{-\,i\,(\omega-\epsilon_k-\Phi_k'')+\Phi_k'+\Psi_k}, &\text{(B.1f)}\\
&= \frac{S\,\hbar\,\gamma^2}{2}\sum_{k'}\frac{\epsilon_2(k,k')\,(n_{k'}-\bar{n}(\epsilon_{k'}))\{1-i\,X_k(\omega)\}}{\{-\,i\,(\omega-\epsilon_k-\Phi_k'')+\Phi_k'+\Psi_k\}\{-\,i\,(\omega-\epsilon_k-\Phi_k'')+\Phi_k'+\Psi_k+2\,\Phi_{k'}'\}}, &\text{(B.1g)}
\end{aligned}
$$

where we have used that according to (2.9b), (2.10) and (2.14),

$$\epsilon_3(k,k)+\epsilon_3(k,k')+\epsilon_3(k',k)+\epsilon_3(k',k')=\epsilon_3(k,k)+2\,\epsilon_3(k,k')+\epsilon_3(k',k')=\epsilon_2(k,\,k'), \tag{B.2}$$

and have substituted the form of $n_k(t)$ $[=\langle 1_{\rm S}|a_k^{\dagger\dagger}(t)a_k(t)|\rho_0\rangle]$ given in Refs. [9]:

$$n_k(t)=\langle 1_{\rm S}|a_k^{\dagger\dagger}(t)a_k(t)|\rho_0\rangle=\{n_k-\bar{n}(\epsilon_k)\}\exp(-\,2\,\Phi_k'\,t))+\bar{n}(\epsilon_k), \tag{B.3}$$

with $n_k = n_k(0) = \langle 1_{\rm S}|a_k^\dagger a_k|\rho_0\rangle$. The second term of (3.22) can be calculated as follows,

$$
\begin{aligned}
&\text{(second term of } \chi^{(1)}_{S_k^+ S_k^-}(\omega) \text{ [(3.22)])} \\
&= -\frac{\hbar\,\gamma^2}{8\,N}\sum_{k',\,k''}\int_0^\infty dt\,\langle 1_{\rm S}|\,a^{\dagger\dagger}_{k'+k''-k}(t)\,a_{k'}(t)\,a_{k''}(t)\,(a_k^\dagger-\tilde a_k)\,|\rho_0\rangle\{i+X_k(\omega)\}\exp(i\,\omega\,t), && \text{(B.4a)}\\
&= -\frac{\hbar\,\gamma^2}{8\,N}\sum_{k',\,k''}\int_0^\infty dt\,Z^{1/2}_{k'+k''-k}(t)\,Z^{1/2}_{k'}(t)\,Z^{1/2}_{k''}(t)\,Z^{1/2}_{k}(0)\,(1-h_k(0))\,\{i+X_k(\omega)\}\exp(i\,\omega\,t) \\
&\qquad\times\langle 1_{\rm S}|\,\tilde\alpha_{k'+k''-k}(t)\,(\alpha_{k'}(t)+h_{k'}(t)\,\tilde\alpha^\ddagger_{k'}(t))\,(\alpha_{k''}(t)+h_{k''}(t)\,\tilde\alpha^\ddagger_{k''}(t))\,\alpha_k^\ddagger\,|\rho_0\rangle, && \text{(B.4b)}\\
&= -\frac{\hbar\,\gamma^2}{8\,N}\sum_{k',\,k''}\int_0^\infty dt\,Z^{1/2}_{k'+k''-k}(t)\,Z^{1/2}_{k'}(t)\,Z^{1/2}_{k''}(t)\,Z^{-1/2}_{k}(0)\,\{i+X_k(\omega)\}\exp(i\,\omega\,t) \\
&\qquad\times\langle 1_{\rm S}|\{\tilde\alpha_{k'+k''-k}(t)\,\alpha_{k'}(t)\,\alpha_{k''}(t)+h_{k''}(t)\,\alpha_k(t)\,\delta_{k',\,k}+h_{k'}(t)\,\alpha_k(t)\,\delta_{k'',\,k}\}\,\alpha_k^\ddagger\,|\rho_0\rangle, && \text{(B.4c)}\\
&= -\frac{\hbar\,\gamma^2}{8\,N}\sum_{k',\,k''}\int_0^\infty dt\,Z^{1/2}_{k'+k''-k}(t)\,Z^{1/2}_{k'}(t)\,Z^{1/2}_{k''}(t)\,Z^{-1/2}_{k}(t)\,\{i+X_k(\omega)\}\exp(i\,\omega\,t) \\
&\qquad\times(h_{k''}(t)\,\delta_{k',\,k}+h_{k'}(t)\,\delta_{k'',\,k})\exp\{-i\,(\epsilon_k+\Phi''_k)\,t-(\Phi'_k+\Psi_k)\,t\}, && \text{(B.4d)}\\
&= -\frac{\hbar\,\gamma^2}{4\,N}\sum_{k'}\int_0^\infty dt\,\{i+X_k(\omega)\}\,Z_{k'}(t)\,h_{k'}(t)\exp\{i\,(\omega-\epsilon_k-\Phi''_k)\,t-(\Phi'_k+\Psi_k)\,t\}, && \text{(B.4e)}\\
&= -\frac{\hbar\,\gamma^2}{4\,N}\sum_{k'}\int_0^\infty dt\,\{i+X_k(\omega)\}\,n_{k'}(t)\exp\{i\,(\omega-\epsilon_k-\Phi''_k)\,t-(\Phi'_k+\Psi_k)\,t\}, && \text{(B.4f)}\\
&= -\frac{\hbar\,\gamma^2}{4\,N}\sum_{k'}\Big\{\frac{(n_{k'}-\bar n(\epsilon_{k'}))\,\{i+X_k(\omega)\}}{-\,i\,(\omega-\epsilon_k-\Phi''_k)+\Phi'_k+\Psi_k+2\,\Phi'_{k'}}+\frac{\bar n(\epsilon_{k'})\,\{i+X_k(\omega)\}}{-\,i\,(\omega-\epsilon_k-\Phi''_k)+\Phi'_k+\Psi_k}\Big\}, && \text{(B.4g)}
\end{aligned}
$$

where we have substituted (B.3). The third term of (3.22) can be calculated as follows,

$$
\begin{aligned}
&\text{(third term of } \chi^{(1)}_{S_k^+ S_k^-}(\omega) \text{ [(3.22)])} \\
&= -\,i\,\frac{\hbar\,\gamma^2}{8\,N}\sum_{k_1,\,k_2}\int_0^\infty dt\,\langle 1_{\rm S}|\,a_k U(t)(a^\dagger_{k_1}a^\dagger_{k_2}a_{k_1+k_2-k}-\tilde a^\dagger_{k_1+k_2-k}\tilde a_{k_1}\tilde a_{k_2})\,|\rho_0\rangle\exp(i\,\omega\,t), \\
&= -\,i\,\frac{\hbar\,\gamma^2}{8\,N}\sum_{k',\,k''}\int_0^\infty dt\,\langle 1_{\rm S}|\,a_k(t)\,(a^\dagger_{k'}\,a^\dagger_{k''}\,a_{k'+k''-k}-\tilde a^\dagger_{k'+k''-k}\,\tilde a_{k'}\,\tilde a_{k''})\,|\rho_0\rangle\exp(i\,\omega\,t), && \text{(B.5a)}\\
&= -\,i\,\frac{\hbar\,\gamma^2}{8\,N}\sum_{k',\,k''}\int_0^\infty dt\,Z^{1/2}_k(t)\,\langle 1_{\rm S}|\,\alpha_k(t)\,(a^\dagger_{k'}\,a^\dagger_{k''}\,a_{k'+k''-k}-\tilde a^\dagger_{k'+k''-k}\,\tilde a_{k'}\,\tilde a_{k''})\,|\rho_0\rangle\exp(i\,\omega\,t), && \text{(B.5b)}\\
&= -\,i\,\frac{\hbar\,\gamma^2}{8\,N}\sum_{k',\,k''}\int_0^\infty dt\,Z^{1/2}_k(0)Z^{1/2}_{k'}(0)Z^{1/2}_{k''}(0)Z^{1/2}_{k'+k''-k}(0)\exp\{-\,i\,(\epsilon_k+\Phi''_k)\,t-(\Phi'_k+\Psi_k)\,t\} \\
&\qquad\times\langle 1_{\rm S}|\,\alpha_k\,\{(\alpha^\ddagger_{k'}+\tilde\alpha_{k'})(\alpha^\ddagger_{k''}+\tilde\alpha_{k''})\,h_{k'+k''-k}(0)\,\tilde\alpha^\ddagger_{k'+k''-k} \\
&\qquad\qquad-(\tilde\alpha^\ddagger_{k'+k''-k}+\alpha_{k'+k''-k})(\tilde\alpha_{k'}+h_{k'}(0)\,\alpha^\ddagger_{k'})\,h_{k''}(0)\,\alpha^\ddagger_{k''}\}|\rho_0\rangle\exp(i\,\omega\,t), && \text{(B.5c)}\\
&= -\,i\,\frac{\hbar\,\gamma^2}{8\,N}\sum_{k',\,k''}\int_0^\infty dt\,Z^{1/2}_k(0)Z^{1/2}_{k'}(0)Z^{1/2}_{k''}(0)Z^{1/2}_{k'+k''-k}(0)\exp\{i\,(\omega-\epsilon_k-\Phi''_k)\,t-(\Phi'_k+\Psi_k)\,t\} \\
&\qquad\times\{h_{k''}(0)\,\delta_{k,\,k'}+h_{k'}(0)\,\delta_{k,\,k''}-h_k(0)\,h_{k''}(0)\,\delta_{k,\,k'}-h_k(0)\,h_{k'}(0)\,\delta_{k,\,k''}\}, && \text{(B.5d)}\\
&= -\,i\,\frac{\hbar\,\gamma^2}{4\,N}\sum_{k'}\int_0^\infty dt\,Z_k(0)(1-h_k(0))\,Z_{k'}(0)h_{k'}(0)\exp\{i\,(\omega-\epsilon_k-\Phi''_k)\,t-(\Phi'_k+\Psi_k)\,t\}, && \text{(B.5e)}\\
&= -\,i\,\frac{\hbar\,\gamma^2}{4\,N}\sum_{k'}\frac{n_{k'}}{-\,i\,(\omega-\epsilon_k-\Phi''_k)+\Phi'_k+\Psi_k}, && \text{(B.5f)}
\end{aligned}
$$

where $Z_k(0)(1-h_k(0))=1$ and $Z_k(0)h_k(0)=n_k(0)=n_k$. Thus, we obtain the form (3.24) of the next higher-order parts $\chi^{(1)}_{S_k^+ S_k^-}(\omega)$ of the transverse magnetic susceptibility $\chi_{S_k^+ S_k^-}(\omega)$.

# C Calculation of corresponding interference terms $X_k(\omega)$

In this Appendix, we derive the concrete forms of the the real part $X'_k(\omega)$ and the imaginary part $X''_k(\omega)$ of the corresponding interference terms $X_k(\omega)$ given by (3.16) or (3.20). In order to deal with the fractions in the calculations

of the corresponding interference terms $X_k(\omega)$ given by (3.16) or (3.20), we use the following form for $\Phi_k(\epsilon)$ defined by (3.18) with the phonon correlation functions given by (4.1a) and (4.1b) :

$$\Phi_k(\epsilon) = \frac{S}{2}\int_0^\infty d\tau \sum_\alpha |g_{1\alpha}|^2 \langle 1_{\rm R}|[B_{k\alpha}(\tau), B_{k\alpha}^\dagger]|\rho_{\rm R}\rangle \exp(i\,\epsilon\,\tau) = \frac{g_1^2\,S/2}{-\,i\,(\epsilon-\omega_{{\rm R}k})+\gamma_{{\rm R}k}}. \tag{C.1}$$

Then, the corresponding interference terms $X_k(\omega)$ can be calculated using (C.1) and (4.6) as follows,

$$\begin{aligned} X_k(\omega) &= \frac{\Phi_k(\omega)-\Phi_k(\epsilon_k)}{\omega-\epsilon_k} + \frac{\Psi_k(\omega-\epsilon_k)-\Psi_k}{\omega-\epsilon_k}, \\ &= \Big\{\frac{g_1^2\,S/2}{-\,i\,(\omega-\omega_{{\rm R}k})+\gamma_{{\rm R}k}} - \frac{g_1^2\,S/2}{-\,i\,(\epsilon_k-\omega_{{\rm R}k})+\gamma_{{\rm R}k}}\Big\}/(\omega-\epsilon_k) \\ &\quad + \Big\{\frac{g_2^2\,\bar n(\omega_{{\rm R}k})\{\bar n(\omega_{{\rm R}k})+1\}}{-\,i\,(\omega-\epsilon_k)+2\,\gamma_{{\rm R}k}} - \frac{g_2^2\,\bar n(\omega_{{\rm R}k})\{\bar n(\omega_{{\rm R}k})+1\}}{2\,\gamma_{{\rm R}k}}\Big\}/(\omega-\epsilon_k), \\ &= \frac{i\,g_1^2\,S/2}{\{-\,i\,(\omega-\omega_{{\rm R}k})+\gamma_{{\rm R}k}\}\{-\,i\,(\epsilon_k-\omega_{{\rm R}k})+\gamma_{{\rm R}k}\}} + \frac{i\,g_2^2\,\bar n(\omega_{{\rm R}k})\{\bar n(\omega_{{\rm R}k})+1\}}{2\,\gamma_{{\rm R}k}\{-\,i\,(\omega-\epsilon_k)+2\,\gamma_{{\rm R}k}\}}, \end{aligned} \tag{C.2}$$

which leads to the real part $X_k'(\omega)$ and the imaginary part $X_k''(\omega)$ as

$$X_k'(\omega) = \frac{-\,g_1^2\,(S/2)\,\gamma_{{\rm R}k}\,(\omega+\epsilon_k-2\,\omega_{{\rm R}k})}{\{(\omega-\omega_{{\rm R}k})^2+(\gamma_{{\rm R}k})^2\}\{(\epsilon_k-\omega_{{\rm R}k})^2+(\gamma_{{\rm R}k})^2\}} - \frac{g_2^2\,\bar n(\omega_{{\rm R}k})\{\bar n(\omega_{{\rm R}k})+1\}(\omega-\epsilon_k)}{2\,\gamma_{{\rm R}k}\{(\omega-\epsilon_k)^2+4\,(\gamma_{{\rm R}k})^2\}}, \tag{C.3a}$$

$$X_k''(\omega) = \frac{g_1^2\,(S/2)\{(\gamma_{{\rm R}k})^2-(\omega-\omega_{{\rm R}k})(\epsilon_k-\omega_{{\rm R}k})\}}{\{(\omega-\omega_{{\rm R}k})^2+(\gamma_{{\rm R}k})^2\}\{(\epsilon_k-\omega_{{\rm R}k})^2+(\gamma_{{\rm R}k})^2\}} + \frac{g_2^2\,\bar n(\omega_{{\rm R}k})\{\bar n(\omega_{{\rm R}k})+1\}}{\{(\omega-\epsilon_k)^2+4\,(\gamma_{{\rm R}k}))^2\}}. \tag{C.3b}$$

# D Derivation of the equilibrium number $n_k$ of the spin deviation

In this Appendix, we derive the form of the equilibrium number $n_k$ $[=\langle 1_{\rm S}|a_k^\dagger a_k|\rho_0\rangle]$ of the spin deviation up to the second order in powers of the spin-phonon interaction. The ket-vector $|\rho_0\rangle$ $[=\langle 1_{\rm R}|\rho_{\rm TE}\rangle]$ can be expanded in powers of the spin-phonon interaction as [24]

$$|\rho_0\rangle = |\rho_{\rm S}\rangle + |\rho_0^{(2)}\rangle + \cdots, \tag{D.1}$$

where the second-order part $|\rho_0^{(2)}\rangle$ of $|\rho_0\rangle$ in powers of the spin-phonon interaction $\mathcal{H}_{\rm SR}$, is given by [24]

$$|\rho_0^{(2)}\rangle = \int_0^\beta d\beta_1 \int_0^{\beta_1} d\beta_2 \langle 1_{\rm R}\big|\big\{\mathcal{H}_{\rm SR}(-i\hbar\beta_1)\mathcal{H}_{\rm SR}(-i\hbar\beta_2) - \langle 1_{\rm SR}|\mathcal{H}_{\rm SR}(-i\hbar\beta_1)\mathcal{H}_{\rm SR}(-i\hbar\beta_2)|\rho_{\rm R}\rangle|\rho_{\rm S}\rangle\big\}\big|\rho_{\rm R}\big\rangle\big|\rho_{\rm S}\big\rangle, \tag{D.2}$$

with notation $\langle 1_{\rm SR}| = \langle 1_{\rm S}|\langle 1_{\rm R}|$. Here, $\rho_{\rm S}$ is given by

$$\rho_{\rm S} = \exp(-\beta\,\mathcal{H}_{\rm S})/\langle 1_{\rm S}|\exp(-\beta\,\mathcal{H}_{\rm S})\rangle = \exp(-\beta\,\mathcal{H}_{\rm S})/{\rm tr}_{\rm S}\exp(-\beta\,\mathcal{H}_{\rm S}), \tag{D.3}$$

which is the normalized, time-independent density operator for the spin system at temperature $T=(k_{\rm B}\beta)^{-1}$. As done in Ref. [24], the second-order part $|\rho_0^{(2)}\rangle$ can be expressed with time-integrals alone by transforming inverse-temperature-integrals into time-integrals as

$$|\rho_0^{(2)}\rangle = -\int_0^\infty d\tau_1 \int_0^{\tau_1} d\tau_2\, \langle 1_{\rm R}|\,\hat{\mathcal{H}}_{\rm SR}(-\tau_2)\,\hat{\mathcal{H}}_{\rm SR}(-\tau_1)\,|\rho_{\rm R}\rangle|\rho_{\rm S}\rangle\exp(-\mu\,\tau_1)\big|_{\mu\to+0}\,. \tag{D.4}$$

In Eqs. (D.2) and (D.4), $\mathcal{H}_{\rm SR}(t)$ and $\hat{\mathcal{H}}_{\rm SR}(t)$ are defined by $\mathcal{H}_{\rm SR}(t)=\exp\{i\,(\mathcal{H}_{\rm S}+\mathcal{H}_{\rm R})\,t/\hbar\}\mathcal{H}_{\rm SR}\exp\{-\,i\,(\mathcal{H}_{\rm S}+\mathcal{H}_{\rm R})\,t/\hbar\}$ and $\hat{\mathcal{H}}_{\rm SR}(t)=\exp\{i\,(\hat{\mathcal{H}}_{\rm S}+\hat{\mathcal{H}}_{\rm R})\,t\}\hat{\mathcal{H}}_{\rm SR}\exp\{-\,i\,(\hat{\mathcal{H}}_{\rm S}+\hat{\mathcal{H}}_{\rm R})\,t\}$. By substituting (2.22) into (D.4), the second-order part

$|\rho_0^{(2)}\rangle$ can be written as

$$
\begin{aligned}
|\rho_0^{(2)}\rangle = &-\frac{S}{2}\int_0^\infty d\tau_1 \int_0^{\tau_1} d\tau_2 \sum_{k,\,\alpha} |\, g_{1\alpha}\,|^2 \exp(-\mu\,\tau_1)\,|_{\mu\to+0} \\
&\times \big\{(a_k-\tilde{a}_k^\dagger)\{a_k^\dagger\langle 1_{\rm R}|B_{k\alpha}^\dagger(\tau_1-\tau_2)B_{k\alpha}|\rho_{\rm R}\rangle - \tilde{a}_k\langle 1_{\rm R}|B_{k\alpha}B_{k\alpha}^\dagger(\tau_1-\tau_2)|\rho_{\rm R}\rangle\}|\rho_{\rm S}\rangle \exp\{-i\,\epsilon_k(\tau_1-\tau_2)\} \\
&\quad + (a_k^\dagger-\tilde{a}_k)\{a_k\langle 1_{\rm R}|B_{k\alpha}(\tau_1-\tau_2)B_{k\alpha}^\dagger|\rho_{\rm R}\rangle - \tilde{a}_k^\dagger\langle 1_{\rm R}|B_{k\alpha}^\dagger B_{k\alpha}(\tau_1-\tau_2)|\rho_{\rm R}\rangle\}|\rho_{\rm S}\rangle \exp\{i\,\epsilon_k(\tau_1-\tau_2)\}\big\} \\
&-\int_0^\infty d\tau_1 \int_0^{\tau_1} d\tau_2 \sum_{k_1,\,k_2}\sum_{\alpha} g_{2\alpha}^2\,\{(S-a_{k_1}^\dagger a_{k_1})-(S-\tilde{a}_{k_1}^\dagger\tilde{a}_{k_1})\}\exp(-\mu\,\tau_1)\,|_{\mu\to+0} \\
&\quad\times\big\{(S-a_{k_2}^\dagger a_{k_2})\langle 1_{\rm R}|\Delta(B_{k_1\alpha}^\dagger(\tau_1-\tau_2)B_{k_1\alpha}(\tau_1-\tau_2))\Delta(B_{k_2\alpha}^\dagger B_{k_2\alpha})|\rho_{\rm R}\rangle|\rho_{\rm S}\rangle \\
&\qquad-(S-\tilde{a}_{k_2}^\dagger\tilde{a}_{k_2})\langle 1_{\rm R}|\Delta(B_{k_2\alpha}^\dagger B_{k_2\alpha})\Delta(B_{k_1\alpha}^\dagger(\tau_1-\tau_2)B_{k_1\alpha}(\tau_1-\tau_2))|\rho_{\rm R}\rangle|\rho_{\rm S}\rangle\big\}, \qquad \text{(D.5a)} \\
= &-\frac{S}{2}\int_0^\infty d\tau_1 \int_0^{\tau_1} d\tau \sum_{k,\,\alpha} |\, g_{1\alpha}\,|^2 \exp(-\mu\,\tau_1)\,|_{\mu\to+0} \\
&\times \big\{(a_k-\tilde{a}_k^\dagger)\{a_k^\dagger\langle 1_{\rm R}|B_{k\alpha}^\dagger(\tau)B_{k\alpha}|\rho_{\rm R}\rangle - \tilde{a}_k\langle 1_{\rm R}|B_{k\alpha}B_{k\alpha}^\dagger(\tau)|\rho_{\rm R}\rangle\}|\rho_{\rm S}\rangle \exp(-i\,\epsilon_k\,\tau) \\
&\quad + (a_k^\dagger-\tilde{a}_k)\{a_k\langle 1_{\rm R}|B_{k\alpha}(\tau)B_{k\alpha}^\dagger|\rho_{\rm R}\rangle - \tilde{a}_k^\dagger\langle 1_{\rm R}|B_{k\alpha}^\dagger B_{k\alpha}(\tau)|\rho_{\rm R}\rangle\}|\rho_{\rm S}\rangle \exp(i\,\epsilon_k\,\tau)\big\} \\
&-\int_0^\infty d\tau_1 \int_0^{\tau_1} d\tau \sum_{k_1,\,k_2}\sum_{\alpha} g_{2\alpha}^2\,\{(S-a_{k_1}^\dagger a_{k_1})-(S-\tilde{a}_{k_1}^\dagger\tilde{a}_{k_1})\}\exp(-\mu\,\tau_1)\,|_{\mu\to+0} \\
&\quad\times\big\{(S-a_{k_2}^\dagger a_{k_2})\langle 1_{\rm R}|\Delta(B_{k_1\alpha}^\dagger(\tau)B_{k_1\alpha}(\tau))\Delta(B_{k_2\alpha}^\dagger B_{k_2\alpha})|\rho_{\rm R}\rangle \\
&\qquad-(S-\tilde{a}_{k_2}^\dagger\tilde{a}_{k_2})\langle 1_{\rm R}|\Delta(B_{k_2\alpha}^\dagger B_{k_2\alpha})\Delta(B_{k_1\alpha}^\dagger(\tau)B_{k_1\alpha}(\tau))|\rho_{\rm R}\rangle\big\}|\rho_{\rm S}\rangle, \qquad \text{(D.5b)}
\end{aligned}
$$

with the notation $\Delta(B_{k\alpha}^\dagger(\tau)B_{k\alpha}(\tau)) = B_{k\alpha}^\dagger(\tau)B_{k\alpha}(\tau) - \langle 1_{\rm R}|B_{k\alpha}^\dagger B_{k\alpha}|\rho_{\rm R}\rangle$, where $B_{k\alpha}(\tau)$ and $B_{k\alpha}^\dagger(\tau)$ are the Heisenberg operators $B_{k\alpha}(\tau) = \exp(i\mathcal{H}_{\rm R}\tau/\hbar)B_{k\alpha}\exp(-i\mathcal{H}_{\rm R}\tau/\hbar)$ and $B_{k\alpha}^\dagger(\tau) = \exp(i\mathcal{H}_{\rm R}\tau/\hbar)B_{k\alpha}^\dagger\exp(-i\mathcal{H}_{\rm R}\tau/\hbar)$ of the phonon reservoir. Here, we have ignored the higher-order parts in the spin-wave approximation. Then, $\langle 1_{\rm S}|a_k^\dagger a_k|\rho_0^{(2)}\rangle$ can be calculated by using the phonon correlation functions (4.1a) and (4.1b) as follows,

$$
\begin{aligned}
\langle 1_{\rm S}|\,a_k^\dagger a_k\,|\rho_0^{(2)}\rangle = &-\frac{S}{2}\sum_{\alpha}|\,g_{1\alpha}\,|^2\int_0^\infty d\tau\int_\tau^\infty d\tau_1\exp(-\mu\,\tau_1)\,|_{\mu\to+0} \\
&\times\big\{\{\langle 1_{\rm S}|a_k^\dagger a_k|\rho_{\rm S}\rangle\langle 1_{\rm R}|B_{k\alpha}(\tau)B_{k\alpha}^\dagger|\rho_{\rm R}\rangle - \langle 1_{\rm S}|a_k a_k^\dagger|\rho_{\rm S}\rangle\langle 1_{\rm R}|B_{k\alpha}^\dagger B_{k\alpha}(\tau)|\rho_{\rm R}\rangle\}\exp(i\,\epsilon_k\,\tau) \\
&\quad+\{\langle 1_{\rm S}|a_k^\dagger a_k|\rho_{\rm S}\rangle\langle 1_{\rm R}|B_{k\alpha}B_{k\alpha}^\dagger(\tau)|\rho_{\rm R}\rangle - \langle 1_{\rm S}|a_k a_k^\dagger|\rho_{\rm S}\rangle\langle 1_{\rm R}|B_{k\alpha}^\dagger(\tau)B_{k\alpha}|\rho_{\rm R}\rangle\}\exp(-i\,\epsilon_k\,\tau)\big\}, \qquad \text{(D.6a)} \\
= &\,S\int_0^\infty d\tau\cdot\tau\,{\rm Re}\sum_{\alpha}|\,g_{1\alpha}\,|^2\,\{\bar{n}(\epsilon_k)\langle 1_{\rm R}|B_{k\alpha}(\tau)B_{k\alpha}^\dagger|\rho_{\rm R}\rangle\exp(i\,\epsilon_k\,\tau) \\
&\qquad-\{\bar{n}(\epsilon_k)+1\}\langle 1_{\rm R}|B_{k\alpha}^\dagger(\tau)B_{k\alpha}|\rho_{\rm R}\rangle\exp(-i\,\epsilon_k\,\tau)\big\}, \qquad \text{(D.6b)} \\
= &-{\rm Re}\,S\,\frac{\partial}{\partial\,\gamma_{{\rm R}k}}\int_0^\infty d\tau\big\{\bar{n}(\epsilon_k)\,g_1^2\,\{\bar{n}(\omega_{{\rm R}k})+1\}\exp(-i\,\omega_{{\rm R}k}\,\tau-\gamma_{{\rm R}k}\,\tau+i\,\epsilon_k\,\tau) \\
&\qquad-\{\bar{n}(\epsilon_k)+1\}\,g_1^2\,\bar{n}(\omega_{{\rm R}k})\exp(i\,\omega_{{\rm R}k}\,\tau-\gamma_{{\rm R}k}\,\tau-i\,\epsilon_k\,\tau)\big\}, \qquad \text{(D.6c)} \\
= &\,S\,g_1^2\,\frac{\partial}{\partial\,\gamma_{{\rm R}k}}\,{\rm Re}\Big\{\frac{\{\bar{n}(\epsilon_k)+1\}\,\bar{n}(\omega_{{\rm R}k})}{i\,(\epsilon_k-\omega_{{\rm R}k})+\gamma_{{\rm R}k}} - \frac{\bar{n}(\epsilon_k)\{\bar{n}(\omega_{{\rm R}k})+1\}}{-i\,(\epsilon_k-\omega_{{\rm R}k})+\gamma_{{\rm R}k}}\Big\}, \qquad \text{(D.6d)} \\
= &\,S\,g_1^2\,\frac{\partial}{\partial\,\gamma_{{\rm R}k}}\,\gamma_{{\rm R}k}\,\frac{\{\bar{n}(\epsilon_k)+1\}\,\bar{n}(\omega_{{\rm R}k})-\bar{n}(\epsilon_k)\{\bar{n}(\omega_{{\rm R}k})+1\}}{(\epsilon_k-\omega_{{\rm R}k})^2+(\gamma_{{\rm R}k})^2} = S\,g_1^2\,\frac{\partial}{\partial\,\gamma_{{\rm R}k}}\,\gamma_{{\rm R}k}\,\frac{\bar{n}(\omega_{{\rm R}k})-\bar{n}(\epsilon_k)}{(\epsilon_k-\omega_{{\rm R}k})^2+(\gamma_{{\rm R}k})^2}, \qquad \text{(D.6e)} \\
= &\,S\,g_1^2\,\{\bar{n}(\omega_{{\rm R}k})-\bar{n}(\epsilon_k)\}\Big\{\frac{1}{(\epsilon_k-\omega_{{\rm R}k})^2+(\gamma_{{\rm R}k})^2} - \frac{2\,(\gamma_{{\rm R}k})^2}{\{(\epsilon_k-\omega_{{\rm R}k})^2+(\gamma_{{\rm R}k})^2\}^2}\Big\}, \qquad \text{(D.6f)}
\end{aligned}
$$

which gives the equilibrium number $n_k$ $[=\langle 1_{\rm S}|a_k^\dagger a_k|\rho_0\rangle]$ of the spin deviation as

$$
\begin{aligned}
n_k &= \langle 1_{\rm S}|\,a_k^\dagger\,a_k\,|\rho_0\rangle = \langle 1_{\rm S}|\,a_k^\dagger\,a_k\,|\rho_{\rm S}\rangle + \langle 1_{\rm S}|\,a_k^\dagger\,a_k\,|\rho_0^{(2)}\rangle, \\
&= \bar{n}(\epsilon_k) + S\,g_1^2\,\{\bar{n}(\omega_{{\rm R}k})-\bar{n}(\epsilon_k)\}\,\frac{(\epsilon_k-\omega_{{\rm R}k})^2-(\gamma_{{\rm R}k})^2}{\{(\epsilon_k-\omega_{{\rm R}k})^2+(\gamma_{{\rm R}k})^2\}^2}, \qquad \text{(D.7)}
\end{aligned}
$$

with $\bar{n}(\epsilon_k)$ given by (2.15).

# E Investigation of the region valid for the low spin-wave approximation

In this Appendix, we investigate numerically the region valid for the low spin-wave approximation, which includes the dominant parts of the higher-order parts in the spin-wave approximation [5] and is referred as "the low spin

wave approximation", in the ferromagnetic system of one-dimensional infinite spins. When the expectation value $n/(4S)$ $[=\langle n_j\rangle/(4S)=\langle a_j^\dagger a_j\rangle/(4S)]$ of the second term in the expansion (2.2) is smaller than about 0.01, the low spin-wave approximation is considered to become valid. In order to investigate the region valid for the low spin-wave approximation, we consider the expectation value $n(t)$ of number $a_j^\dagger a_j$ $[=n_j]$ of the spin deviation, which is referred to as "the spin-deviation number". The expectation value $n(t)$ is defined in the low spin-wave approximation by

$$n(t)=\frac{1}{N}\sum_j\langle 1_{\rm S}|\, a_j^\dagger a_j\, U(t)|\rho_0\rangle=\frac{1}{N}\sum_k\langle 1_{\rm S}|\, a_k^\dagger a_k\, U(t)|\rho_0\rangle=\frac{1}{N}\sum_k n_k(t), \tag{E.1}$$

with $|\rho_0\rangle=\langle 1_{\rm R}|\rho_{\rm TE}\rangle$, where $n_k(t)$ is defined in Ref. [9] and takes the form given by (B.3) [9]. Here, we have performed the Fourier transformation (2.6) and their Hermite conjugates. The spin-deviation number $n(t)$ can be calculated by substituting $n_k$ $[=n_k(0)]$ given by (4.8) into (B.3), by replacing the wave-number summation with the numerical integration (4.13) and by using the approximate form (4.14b) of $\epsilon_k$. We perform the numerical calculation for the case that $g_1/\omega_z=g_2/\omega_z=0.25$ for the coupling constants $g_1$ and $g_2$ between the spin and phonon, and that $\zeta\,[=J_2/J_1]=1.0$ and $J_1/\omega_z=1.0$, i.e., $J_1=J_2=J=\omega_z$. We consider the case that $V_{\rm R}/\omega_z=0.5$, $\omega_{\rm R0}/\omega_z=0.5$ and $\gamma_{{\rm R}k}/\omega_z=0.5$. In Fig. 26, the spin-deviation number $n(t)$ given by (E.1) is displayed varying the time $t$ scaled by $1/\omega_z$ from 0 to 500 for the cases of the spin-magnitudes $S=1$, 3/2, 2, 5/2, and for the temperature $T$ given by $k_{\rm B}T/(\hbar\omega_z)=1.0$ and the anisotropy energy $\hbar K$ given by $K/\omega_z=1.0$. Figure 26 shows that as the time $t$ becomes large, the spin-deviation number $n(t)$ decreases and approach to the finite value, and that as the the spin-magnitude $S$ becomes large, $n(t)$ decreases. Thus, the spin-deviation number $n(t)$ is the decrease function of the time $t$ and spin-magnitude $S$, and approaches the finite value $n(\infty)$ in the infinite time limit $(t\to\infty)$. In order to confirm the region valid for the low

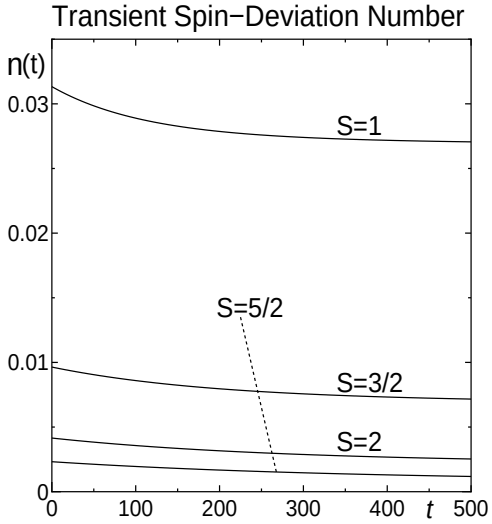


Figure 26: The spin-deviation number $n(t)$ given by (E.1) is displayed varying the time $t$ scaled by $1/\omega_z$ from 0 to 500 for the cases of the spin-magnitudes $S=1$, 3/2, 2, 5/2, and for the temperature $T$ given by $k_{\rm B}T/(\hbar\omega_z)=1.0$ and the anisotropy energy $\hbar K$ given by $K/\omega_z=1.0$. As the time $t$ becomes large, the spin-deviation number $n(t)$ decreases and approach to the finite value. As the spin-magnitude $S$ becomes large, $n(t)$ decreases.

spin-wave approximation, we investigate numerically the spin-deviation numbers $n(0)$ and $n(\infty)$ at the initial time $(t=0)$ and in the infinite time limit $(t\to\infty)$, which are given by

$$n(0)=\frac{1}{N}\sum_k n_k, \qquad\qquad n(\infty)=\frac{1}{N}\sum_k \bar{n}(\epsilon_k). \tag{E.2}$$

In Fig. 27, the spin-deviation numbers $n(0)$ and $n(\infty)$ are displayed varying the temperature $T$ scaled by $\hbar\omega_z/k_{\rm B}$ from 0 to 1.5 for the cases of the spin-magnitudes $S=1$, 3/2, 2, and for the anisotropy energy $\hbar K$ given by $K/\omega_z=1.0$. The spin-deviation number $n(0)$ at the initial time $(t=0)$ is displayed by the solid lines, and the spin-deviation number $n(\infty)$ in the infinite time limit $(t\to\infty)$ is displayed by the short dash lines. Figure 27 shows that as the temperature $T$ becomes high, the spin-deviation numbers $n(0)$ and $n(\infty)$ increase. In Fig. 28, the spin-deviation numbers $n(0)$ and $n(\infty)$ are displayed varying the anisotropy energy $\hbar K$ scaled by $\hbar\omega_z$ from 0 to 5.0 for the cases of the spin-magnitudes $S=1$, 3/2, 2, and for the temperature $T$ given by $k_{\rm B}T/(\hbar\omega_z)=1.5$. The spin-deviation number $n(0)$ at the initial time $(t=0)$ is displayed by the solid lines, and the spin-deviation number $n(\infty)$ in the infinite time limit $(t\to\infty)$ is displayed by the short dash lines. The anisotropy energy is denoted as "$A$" $[=K/\omega_z]$ in the figures. Figure 28 shows that as the anisotropy energy $\hbar K$ increases, the spin-deviation numbers $n(0)$ and $n(\infty)$ decrease. Figures $26-28$ show that when the spin-magnitudes $S=1$, the expectation values $n(0)$ and $n(\infty)$ of the spin-deviation numbers are smaller than about 0.04 in the regions of the temperature $T$ and anisotropy energy $\hbar K$ given by $k_{\rm B}T/(\hbar\omega_z)\le 1.1$ and $K/\omega_z\ge 1.0$, or by $k_{\rm B}T/(\hbar\omega_z)\le 1.5$ and $K/\omega_z\ge 2.0$. In these regions, the expectation value $n/(4S)$ $[=\langle n_j\rangle/(4S)=\langle a_j^\dagger a_j\rangle/(4S)]$ of the second term in the expansion (2.2) is smaller than about 0.01 for the spin-magnitudes $S=1$. Therefore, when the spin-magnitudes $S=1$, the low spin-wave approximation is valid in the regions of the temperature $T$ and anisotropy energy $\hbar K$ given by $k_{\rm B}T/(\hbar\omega_z)\le 1.1$ and $K/\omega_z\ge 1.0$, or $k_{\rm B}T/(\hbar\omega_z)\le 1.5$ and $K/\omega_z\ge 2.0$. When the spin-magnitudes $S$ is larger than 1, the region valid for the low spin-wave approximation become wider than those regions.

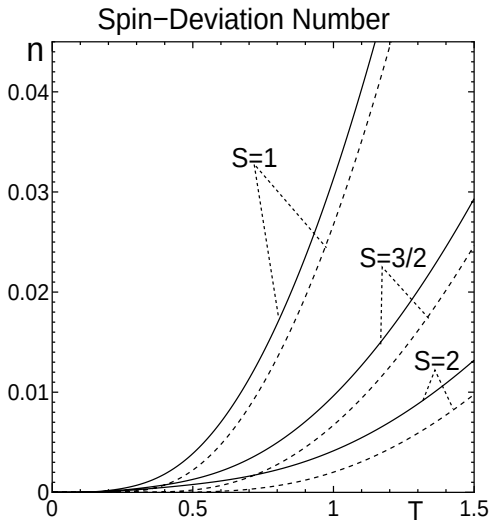


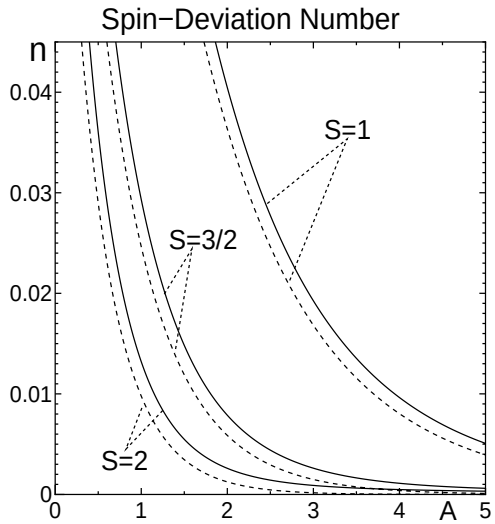


Figure 27: The spin-deviation numbers $n(0)$ and $n(\infty)$ are displayed varying the temperature $T$ scaled by $\hbar\omega_z/k_{\rm B}$ from 0 to 1.5 for the cases of the spin-magnitudes $S=1$, 3/2, 2, and for the anisotropy energy $\hbar K$ given by $K/\omega_z=1.0$. The spin-deviation number $n(0)$ at the initial time ($t=0$) is displayed by the solid lines, and the spin-deviation number $n(\infty)$ in the infinite time limit ($t\to\infty$) is displayed by the short dash lines. As the temperature $T$ becomes high, the spin-deviation numbers $n(0)$ and $n(\infty)$ increase.

Figure 28: The spin-deviation numbers $n(0)$ and $n(\infty)$ are displayed varying the anisotropy energy $\hbar K$ scaled by $\hbar\omega_z$ from 0 to 5.0 for the cases of the spin-magnitudes $S=1$, 3/2, 2, and for the temperature $T$ given by $k_{\rm B}T/(\hbar\omega_z)=1.5$. The spin-deviation number $n(0)$ at the initial time ($t=0$) is displayed by the solid lines, and the spin-deviation number $n(\infty)$ in the infinite time limit ($t\to\infty$) is displayed by the short dash lines. As the anisotropy energy $\hbar K$ increases, the spin-deviation numbers $n(0)$ and $n(\infty)$ decrease. The anisotropy energy is denoted as "$A$" [$=K/\omega_z$] in the figures.

# References


[1] C. Kittel, Phys. Rev. **73**, 155 (1948).

[2] J. H. Van Vleck, Phys. Rev. **78**, 266 (1950).

[3] A. I. Akhiezer, V. G. Bar'yakhtar and M. I. Kaganov, Sov. Phys. Usp. **3**, 567 (1961).

[4] A. I. Akhiezer, V. G. Bar'yakhtar and M. I. Kaganov, Sov. Phys. Usp. **3**, 661 (1961).

[5] T. Oguchi and A. Honma, J. Phys. Soc. Jpn. **16**, 79 (1961).

[6] T. Holstein and H. Primakoff, Phys. Rev. **58**, 1908 (1940).

[7] H. Mori and K. Kawasaki, Progr. Theor. Phys. **27**, 529 (1962).

[8] R. Kubo, J. Phys. Soc. Jpn. **12**, 570 (1957).

[9] M. Saeki, Physica A **390**, 1884 (2011).

[10] M. Saeki, Progr. Theor. Phys. **67**, 1313 (1982).

[11] M. Saeki, J. Phys. Soc. Jpn. **55**, 1846 (1986).

[12] M. Saeki, Progr. Theor. Phys. **79**, 396 (1988).

[13] M. Saeki, Progr. Theor. Phys. **89**, 607 (1993).

[14] M. Saeki, J. Phys. Soc. Jpn. **68**, 3831 (1999).

[15] M. Saeki, *Recent Research Developments in Physics* (Transworld Research Network, India, 2003), Vol. **4**, pp. 73-96.

[16] M. Saeki, Progr. Theor. Phys. **114**, 907 (2005).

[17] M. Saeki, Physica A **387**, 1827 (2008).

[18] T. Arimitsu and H. Umezawa, Progr. Theor. Phys. **74**, 429 (1985).

[19] T. Arimitsu and H. Umezawa, Progr. Theor. Phys. **77**, 32 (1987).

[20] T. Arimitsu and H. Umezawa, Progr. Theor. Phys. **77**, 53 (1987).

[21] M. Saeki, Prog. Theor. Phys. **124**, 95 (2010).

[22] M. Saeki, Physica A **389**, 3720 (2010).

[23] M. Saeki, Progr. Theor. Phys. **121**, 165 (2009).

[24] M. Saeki, C. Uchiyama, T. Mori and S. Miyashita, Phys. Rev. E **81**, 031131 (2010).

[25] M. Saeki, Progr. Theor. Phys. **98**, 1025 (1997).

[26] M. Saeki, J. Phys. Soc. Japan **69**, 1327 (2000).

[27] L. van Hove, Physica **23**, 441 (1957).

[28] R. Kubo, in *Tokei Butsurigaku*, eds. M. Toda and R. Kubo (Iwanami, Tokyo, 1978), 2nd ed., (Chapter 6) [in Japanese]; trans. *Statistical Physics II*, eds. R. Kubo, M. Toda and N. Hashitsume (Springer-Verlag, Berlin, 1978).

[29] M. Saeki and S. Miyashita, Physica A **446**, 272 (2016).

[30] M. Saeki, Prog. Theor. Exp. Phys. **2021**, 113I01 (2021).

[31] F. Shibata, J. Phys. Soc. Jpn. **49**, 15 (1980).

[32] M. Asou and F. Shibata, J. Phys. Soc. Jpn. **50**, 1846 (1981).

[33] M. Asou and F. Shibata, J. Phys. Soc. Jpn. **50**, 2481 (1981).